Resource Allocation in Energy Cooperation Enabled 5G Cellular Networks

by

Bingyu Xu

A thesis submitted to the University of London for the degree of Doctor of Philosophy

School of Electronic Engineering and Computer Science
Queen Mary University of London
United Kingdom

June 2018

TO MY FAMILY

Abstract

In fifth generation (5G) networks, more base stations (BSs) and antennas have been deployed to meet the high data rate and spectrum efficiency requirements. Heterogeneous and ultra dense networks not only pose substantial challenges to the resource allocation design, but also lead to unprecedented surge in energy consumption. Supplying BSs with renewable energy by utilising energy harvesting technology has became a favourable solution for cellular network operators to reduce the grid energy consumption. However, the harvested renewable energy is fluctuating in both time and space domains. The available energy for a particular BS at a particular time might be insufficient to meet the traffic demand which will lead to renewable energy waste or increased outage probability. To solve this problem, the concept of energy cooperation was introduced by Sennur Ulukus in 2012 as a means for transferring and sharing energy between the transmitter and the receiver. Nevertheless, resource allocation in energy cooperation enabled cellular networks is not fully investigated. This thesis investigates resource allocation schemes and resource allocation optimisation in energy cooperation enabled cellular networks that employed advanced 5G techniques, aiming at maximising the energy efficiency of the cellular network while ensuring the network performance.

First, a power control algorithm is proposed for energy cooperation enabled millimetre wave (mmWave) HetNets. The aim is to maximise the time average network data rate while keeping the network stable such that the network backlog is bounded and the required battery capacity is finite. Simulation results show that the proposed power control scheme can reduce the required battery capacity and improve the network throughput.

Second, resource allocation in energy cooperation enabled heterogeneous networks (HetNets) is investigated. User association and power control schemes are proposed to max-

imise the energy efficiency of the whole network respectively. The simulation results reveal that the implementation of energy cooperation in HetNets can improve the energy efficiency and the improvement is apparent when the energy transfer efficiency is high.

Following on that, a novel resource allocation for energy cooperation enabled non-orthogonal multiple access (NOMA) HetNets is presented. Two user association schemes which have different complexities and performances are proposed and compared. Following on that, a joint user association and power control algorithm is proposed to maximise the energy efficiency of the network. It is confirmed from the simulation results that the proposed resource allocation schemes efficiently coordinate the intra-cell and inter-cell interference in NOMA HetNets with energy cooperation while exploiting the multiuser diversity and BS densification.

Last but not least, a joint user association and power control scheme that considers the different content requirements of users is proposed for energy cooperation enabled caching HetNets. It shows that the proposed scheme significantly enhances the energy efficiency performance of caching HetNets.

Acknowledgments

Firstly, I would like to express my deepest appreciation to my principle supervisor Prof. Yue Chen, the most influential people in my Ph.D study process. Not only she has guided me in the research work, she has also given me the much-needed suggestions for daily lives with patient and immense knowledge. Without her ongoing support, I could not have finished my research.

I would like to thank the rest of my committee: Dr. Jesús Requena-Carrión and Dr. Kok Keong Chai, for their insightful comments and encouragement, also for the hard question which incented me to widen my research from various perspectives.

And also, I would like to express my thanks to Prof. Tiankui Zhang (Beijing University of Posts and Telecommunications), Prof. Shuguang Cui (University of California at Davis), Prof. Qiang Ni (Lancaster University), Dr. Jonathan Loo (Middlesex University), Prof. Alexey Vinel (Halmstad University) and Kai-Kit Wong (University College London), for their valuable comments and advices on my research work.

I would also like to express my gratitude towards my family for the encouragement which helped me in completion of my research. Without their love and support over the years none of this would have been possible.

Last but not the least, I would like to thank all my colleagues and friends: Dr. Dan Zhao, Dr. Dantong Liu, Dr. Anqi He, Dr. Lexi Xu, Dr. Yuanwei Liu, Dr. Yansha Deng, Dr. Xingyu Han, Dr. Yun Li, Dr. Xinyue Wang, Dr. Zhijin Qin, Dr. Liumeng Song, Dr. Shenglan Huang, Dr. Jingjing Zhao, Dr. Yuan Ma, Dr. Luwei Yang, Dr. Yanru Wang, Yuting Fang, Xingjian Zhang, Lingyun Zhao, Beici Liang, Qianyun Zhang, Yuhang Dai, Bizhu Wang, among others, for the stimulating discussions and for all the fun we have had in the last four years.

Table of Contents

List of Figures

List of Tables

List of Abbreviations

5G	The Fifth Generation
AWGN	Additive White Gaussian Noise
BS	Base Station
Capex	Capital Expenditure
CINR	Channel to Inter-cell Interference Plus Noise Ratios
CoMP	Coordinated Multi-point Transmission and Reception
CO2	Carbon Dioxide
CSI	Channel State Information
C-RAN	Cloud Radio Access Network
DL	Downlink
D2D	Device to Device
EE	Energy Efficiency
EH	Energy Harvesting
FDMA	Frequency Division Multiple Access
FTPA	Fractional Transmission Power Allocation
GA	Genetic Algorithm
GSMA	Global System of Mobile Communications Association
GRA	Gradient Descent Method
H2H	Human to Human

HetNet	Heterogeneous Network
HomoNet	Homogeneous Network
ICT	Information and Communication Technology
IEEE	Institute of Electrical and Electronics Engineers
IoT	Internet of Things
KKT	Karush-Kuhn-Tucker
LOS	Line-of-Sight
LP	Linear Programming
LPN	Low Power Nodes
LTE	Long Term Evolution
M2M	Machine to Machine
MAC	Multiple Access Channel
MBS	Macro Base Station
MIMO	Multiple-Input Multiple-Output
MILP	Mixed Integer Linear Programming
MINLP	Mixed Integer Non-linear Programming
mmWave	Millimeter Wave
NLOS	Non-Line-of-Sight
NOMA	Non-orthogonal Multiple Access
NP	Non-deterministic Polynomial
OFDM	Orthogonal Frequency Division Multiplexing
OMA	Orthogonal Multiple Access
OPEX	Operating Expense
PBS	Pico Base Station
PDF	Probability Density Function
PPP	Poisson Point Process
QoS	Quality of Service
RAN	Radio Access Network

RES Renewable Energy Sources

RRH Remote Radio Head

RSRP Reference Signal Received Power

SE Spectrum Efficiency

SIC Successive Interference Cancelation

SINR Signal to Interference Plus Noise Ratio

TDMA Time Division Multiple Access

UA User Association

UE User Equipment

Chapter 1

Introduction

1.1 Background

During the last decade, the cellular networks market has grown tremendously and the traffic demand has climbed rapidly. By 2020, there will be 50 billion connected devices based on the white paper published by CISCO[Eva11]. From 2014 to 2019, the global mobile data traffic will increase nearly tenfold. Such vast level of connectivity will lead to an unprecedented surge in global energy consumption without effective energy management. According to the latest data, Information and Communications Technology (ICT) accounts for about 10% of the world's energy consumption [JZLS16]. Wireless access networks account for about 60% to 80% of the telecom's energy consumption [HHA$^+$11]. The amount of energy consumption leads to high greenhouse gas emission. Based on the data from Institute of Electrical and Electronics Engineers (IEEE) Green ICT in 2015, ICT industry needs to responsible for approximately 2 percent of global carbon dioxide (CO2) emissions. The data is anticipated to grow over 4 percent in 5 years [Elm]. In addition to the carbon emission, the energy cost also plays a significant part of network performances, especially on operating expense (OPEX). The base stations (BSs) connected to the electrical grid may cost approximately 3000$ per year to operate and the

BSs in remote areas which generally run on diesel power generators may cost ten times more [HBB11].

Meanwhile, in fifth generation (5G) networks, more advanced technologies and architectures have been prevalently implemented such as millimeter wave (mmWave) and heterogeneous networks (HetNets) to meet escalating data demands. Under this architecture, the density of networks is much higher compared with previous generations [ABC+14]. Large number of antennas and small cells in the same area as conventional networks make the energy consumption problem more serious. This trend stimulates more emerging technologies to be proposed to meet the energy saving targets and reduce the energy cost of BSs.

Energy harvesting technology is an appealing solution to reduce energy costs as the energy can be harvested from ambiance such as solar panels and wind turbines. According to [TGH+16], the largest part of energy consumption (about 60%) in mobile networks is contributed by BSs. The harvested energy can be used as a supplement of the energy from the power grid to support BSs, especially in places where power grids are hard to be laid. By this way, the cost of grid energy is reduced and the network is more energy efficient. Base on the data from Global System of Mobile Communications Association (GSMA), there are 320100 off-grid (without any grid connectivity) BSs in the world [CS16], the data are predicted to grow by 22% by 2020. From 2003, Huawei started to help the largest communications operator Safaricom in Kenya to deploy BSs which are jointly powered by wind energy, solar energy and diesel. With the novel power supply plan, the diesel engine only works 1.32 hours per day and the diesel oil consumption reduced about 95%. In 2009, Ericsson and Orange decided to deploy more than 100 BSs which are solely powered by solar energy in Guinea, Africa. It aims to reduce more than 20% of CO2 emission by 2020 [Nys].

1.2 Research Motivation

Although energy harvesting is a promising solution for reducing energy consumption of cellular networks, it also brings challenges to resource allocation and wireless network design. First, due to the fluctuating nature of the harvested energy, the energy harvested at BSs may not be sufficient to meet their load conditions. Generally, each BS manages its own harvested energy. Some BSs have abundant energy and these energy may be wasted because the capacity of the battery is limited, while the energy harvested by some BSs is insufficient. Conventional resource allocation scheme utilises traffic offloading to ensure user equipments (UEs) can be served by the BS with sufficient energy. Traffic offloading due to energy availability will lead to high signalling costs in the frequently handover process among cells. Moreover, the traffic offloading can reduce the signal to interference plus noise ratio (SINR). That's because the UE cannot connect with the closest BS which will lead to higher co-channel interference.

To compensate the fluctuating energy and utilise the renewable energy more efficiently, the concept of energy cooperation was proposed in wireless networks so that extra energy can be transferred between BSs [GOYU13c]. In this way, UEs could be still associated with the BS which can provide highest service while the associated BS can obtain energy from adjacent BSs. Figure 1.1 shows a model of energy cooperation enabled green networks.

Until now, energy cooperation is still not fully studied in literatures. It's important to investigate the implications of energy cooperation and quantify its benefits. Compared with conventional renewable energy powered networks, in energy cooperation enabled networks, how much energy should be transferred and the tradeoff between UEs' offloading and energy transfer are new problems. In addition, there is a transmission loss associated with transferring energy among BSs, hence, it is important to quantify the tradeoff between the energy efficiency gain and energy transfer loss. Therefore, the resource allocation schemes for grid or conventional renewable energy powered wireless

networks without energy cooperation are no longer effective for the energy cooperation enabled networks and it is critical to explore new resource allocation schemes for this new scenario.

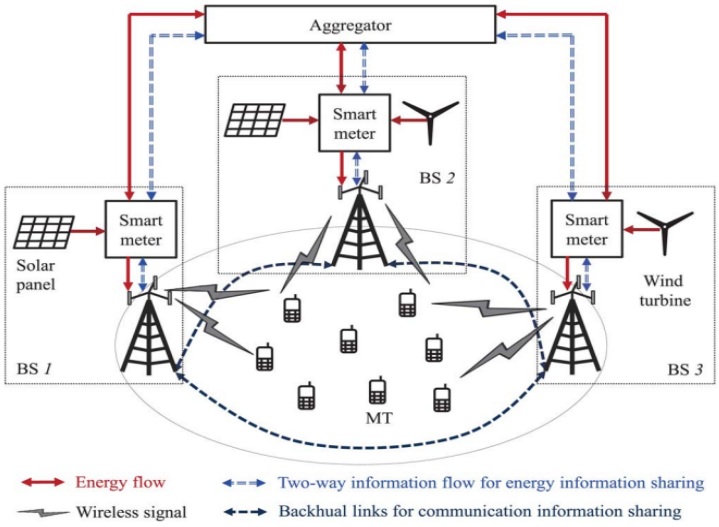

Figure 1.1: The system model for energy cooperation enabled green networks [XZ15a]

1.3 Research Contributions

Motivated by the critical technical issues aforementioned, in this thesis, new resource allocation schemes for renewable energy powered cellular networks with energy cooperation are proposed and investigated, in order to enhance the energy efficiency of the whole network while ensuring the quality of service of UEs, in the 5G context, where advanced technologies are applied such as HetNets and mmWave. The network performance is enhanced via applying mathematical tools such as convex optimisation and stochastic optimisation in resource allocation design. Simulation results can provide a guidance to deploy energy cooperation in cellular networks. Specifically, the contributions of the thesis are summarised as follows.

- A power control algorithm is proposed based on Lyapunov optimisation in energy

cooperation aided mmWave cellular networks. The aim is maximising the time average network throughput while keeping the network stable, where the network backlog is bounded and the required battery capacity is finite. The impacts of BS numbers, energy transfer efficiency and a control variable used for Lyapunov optimisation are investigated.

- Resource allocation policies in energy cooperation enabled HetNets are investigated. First, a novel user association is proposed based on the primal-dual interior point method, which aims to maximise the number of accepted UEs and minimise the energy transfer loss between BSs. Then, power control is optimised to maximise the energy efficiency of the whole network. The impact of energy transfer efficiency, user number and small cell number for both resource allocation policies are evaluated.

- Downlink transmission in non-orthogonal multiple access (NOMA) HetNets is evaluated. A joint user association and power control algorithm is developed to maximise the energy efficiency of the whole network. The proposed algorithm is compared with orthogonal multiple access (OMA) networks and conventional resource allocation schemes such as reference signal received power (RSRP) based user association to confirm the capability in enhancing the energy efficiency of the overall network.

- A joint user association and power control problem is investigated in cache-enabled energy-cooperative HetNets. A resource allocation algorithm is developed to achieve the tradeoff between the network throughput and the total grid energy consumption. The convergence analysis is given to ensure that the proposed algorithm converges. The impact of the cache size and content popularity are evaluated.

1.4 Publications List

Journal Paper

1. **Bingyu Xu**, Yue Chen and Jesús Requena-Carrión,"Power Control in Ultra-dense mmWave Backhaul with Hybrid Energy Supplies", submitted to *IEEE Transactions on Vehicular Technology.*

2. **Bingyu Xu**, Yue Chen, Jesús Requena-Carrión and Tiankui Zhang, "Resource Allocation in Energy-Cooperation Enabled Two-tier NOMA HetNets Towards Green 5G", *IEEE Journal on Selected Areas in Communications*, vol. 35, no. 12, pp. 2758-2770, July 2017.

3. **Bingyu Xu**, Yue Chen, Jesús Requena-Carrión, Jonathan Loo and Alexey Vinel, "Energy-aware Power Control in Energy Cooperation Aided Millimeter Wave Cellular Networks with Renewable Energy Resources", *IEEE Access*, vol. 5, pp. 432-442, Dec. 2016.

Conference Paper

1. **Bingyu Xu**, Yue Chen, Jesús Requena-Carrión and Tiankui Zhang, "Resource Allocation in Cache-enabled Energy-cooperative HetNets", *IEEE Wireless Communications and Networking Conference (WCNC)*,2018.

2. **Bingyu Xu**, Yue Chen, Jesús Requena-Carrión, Qiang Ni and Tiankui Zhang, "Energy-Aware User Association in Energy-Cooperation Enabled HetNets", *IEEE Wireless Communications and Networking Conference Workshops (WCNCW)*, pp. 1-6, Mar. 2017.

3. **Bingyu Xu**, Yue Chen and Jesús Requena-Carrión, "Energy-aware Power Control in Energy-Cooperation Enabled HetNets with Hybrid Energy Supplies", *IEEE Global Communications Conference (GLOBECOM)*, pp. 1-6, Dec. 2016.

4. **Bingyu Xu**, Yue Chen, Maged Elkashlan, Tiankui Zhang and Kai-Kit Wong, "User Association in Massive MIMO and mmWave Enabled HetNets Powered by Renewable Energy", *IEEE Wireless Communications and Networking Conference (WCNC)*, pp. 1-6, Apr. 2016.

5. **Bingyu Xu**, Dantong Liu, Yue Chen and Jesús Requena-Carrión, "User Association in Energy Cooperation Enabled HetNets with Renewable Energy Powered Base Stations", *10th International Conference on Communications and Networking in China (Chinacom)*, pp. 801-806, Aug. 2015.

1.5 Thesis Outline

Chapter 2 presents the concepts of several candidate architectures and technologies for enabling 5G networks. The fundamental concept and the state-of-the-art of resource allocation in 5G cellular networks are introduced under different scenarios, including power grid supplied networks, renewable energy supplied networks and hybrid energy supplied networks. Then a detailed overview about energy cooperation is presented and followed by an introduction in convex optimisation.

Chapter 3 explores power control in energy cooperation enabled mmWave networks. The downlink optimisation problem for optimising harvested energy, transmit powers and transferred energy is formulated, which aims to maximise the network throughput while keeping the network stable. An online algorithm is proposed based on the Lyapunov optimisation technique which can let the data queue and the required energy storage capacity keep in a low level.

Chapter 4 formulates user association in energy cooperation enabled HetNets and maximises the number of accepted UEs while minimising the transferred energy loss. The problem is solved based on the primal-dual interior point method and simplified by predictor-corrector technique. Then power control in energy cooperation enabled

HetNets is conducted. An optimisation problem for maximising energy efficiency is formulated as a non-linear fractional programming problem, which is solved with the help of maximum interference temperature. The impact of energy transfer efficiency, number of picocells and number of UEs are investigated.

Chapter 5 studies joint user association and power control in a energy cooperation enabled two-tier NOMA HetNet. It aims to maximise the energy efficiency of the overall network while ensuring the data rates of UEs. Two user association schemes under fixed transmit powers are proposed and compared, which use Lagrangian dual and the genetic algorithm respectively. Then, a joint user association and power control algorithm is proposed to further maximise the energy efficiency compared with conventional fractional transmission power allocation scheme. The energy efficiency performance of NOMA and OMA are also evaluated and compared.

Chapter 6 addresses the joint user association and power control problem in energy cooperation enabled caching HetNets. The formulated problem aims at maximising the network throughput while minimising the conventional grid energy consumption. A decomposition approach is adopted to optimise the user association and power control alternately. The impact of the cache size is analysed.

Chapter 7 presents the conclusions of the thesis and some potential directions for future work.

Chapter 2

Fundamental Concepts and State-of-the-Art

2.1 Overview

This chapter first presents the key technologies for enabling fifth generation (5G) networks. The investigation of the resource allocation in wireless networks under different scenarios including grid energy supplied networks, renewable energy supplied networks and hybrid energy supplied networks is included in the following section. Followed on that, the review of energy cooperation is also included. At last, convex optimisation is explained.

2.2 Key Technologies in 5G Wireless Networks

5G wireless networks will be designed for the provision of the anticipated 1000x data increase [5GP]. To achieve this target, several advanced techniques such as dense heterogeneous networks (HetNets) and millimeter wave (mmWave) are developed [ABC+14, HH15]. Meanwhile, new multiple access technologies such as non-orthogonal multiple

access (NOMA) are also investigated for 5G networks.

2.2.1 Heterogeneous networks

One of the effective methods to increase the network throughput is to add more cells and allow user equipments (UEs) be closer to their associated base stations (BSs). Heterogeneous network deployment has already been commercialised to enhance the throughput for the next generation wireless network. A HetNet, is a new network deployment consisting of several kinds of low power nodes (LPN) (transmit power: 100mW−2W) such as picocells and femtocells within the coverage of normal macro BSs (transmit power: 5W−40W), to provide extra throughput. Table 2-A shows the parameters of the macrocell and smallcells such as femtocell and remote radio head (RRH). Macrocell is used to provide open public access for all UEs and ensure the coverage of the cell. Each small cell has an omnidirectional or directional antenna and is always located in the indoor environment or outdoor hotspots area.

Table 2-A: The parameters of macrocells and small cells

Node Type	**Transmit Power**	**Coverage Area**	**Backhaul**
Macrocell	46 dBm	Several km	S1
Picocell	24-30 dBm	<300m	X2
Femtocell	< 23dBm	< 50m	Internet IP
Relay	30 dBm	300m	Wireless
RRH	46 dBm	Few km	Fiber

The main benefit of HetNets is the reuse of spectrum in a geographical area. UEs can be offloaded to adjacent small BSs who use same spectrum. By this way, the resource scarcity of macrocells can be alleviated and the quality of service (QoS) requirements of UEs can be satisfied. In this thesis, if there is no special circumstance, QoS represents data rates' requirement of UEs. Even in ultra dense networks, each BS can nearly serve only one UE [ABC+14]. Second, in the hotpot area or the area where large cells are hard to be established (e.g., rural area), small cells are good choices. In addition, compared with the traditional homogeneous network (HomoNet), HetNet offers an economically

viable approach to meet the data rate needs of UEs. The transmit powers of small cells are very small so that they can be fully sustained by energy harvesters. This can make the network more sustainable and green.

However, HetNets also bring many challenges for resource allocation. First, the transmit powers are different between small cells and macrocells in HetNets. It means that the coverage of the macrocell is very large and only few UEs are offloaded to small cells. Second, compared with the conventional HomoNet, the smaller coverage of cells lead to frequently handovers. This will impact the instant achievable data rate of UEs and result in high handover latency. The characteristics of HetNets impose substantial challenges to resource allocation including user association, power control and mobility management.

2.2.2 Millimeter Wave

Generally, wireless systems' microwave frequencies are confined to the limit from hundred MHz to a few GHz. The correspondent wavelengths are in the range of a few centimeters up to about a meter. Due to the high data rate requirement, much more bandwidth is needed [ABC+14]. Fortunately, huge amount of spectrum is idle in 30-300 GHz, which called mmWave range. Also, several GHz in the 20-30 GHz range is idle.

In the last century, mmWave was seen as unsuitable for mobile communications due to the poor propagation qualities, including strong pathloss, atmospheric and rain absorption, low diffraction around obstacles and penetration through objects. However, in the last few years, thanks to the development of semiconductors and an accurate understanding of signal propagation and channel characteristics, both indoor and outdoor mmWave channels have been extensively studied [ABC+14].

Generally, based on the Friis equation ${\lambda^2}_c = (c/f_c)^2$, where λ^2 is the carrier wavelength, c is the light speed and f_c is the carrier frequency, the effective antenna area is ${\lambda^2}_c/4\pi$. For mmWave BS which has really high carrier frequency, the antenna has a

very small effective area and most energy is lost in spreading process. This leads to high susceptibility of mmWave to pathloss, blocking and other obstacles. This problem brings new challenges for mmWave design compared with the network without mmWave.

Compared with conventional network systems, mmWave has two fundamental physical differences: due to the strong pathloss, blocking, atmospheric and rain absorption, signals are vulnerable to propagation; need for significant directionality at the transmitter and/or receiver, which is achieved through the use of large antenna arrays of small individual elements. Such that, the small effective area problem can be solved by a moderately sized two dimentional array of small antenna elements[ABK$^+$17].

Along with the strong required directionality, mmWave cellular's susceptibility to blocking required important changes to the cellular network architecture and deployment, including blocking models, spatial channel modelling and beamforming. Usually, in mmWave networks, for line-of-sight (LOS) and non-line-of-sight (NLOS) links, the path loss exponents are different due to the impact of blocks and attenuation. Meanwhile, large amount of antenna arrays at the BS is another key feature of mmWave cellular networks. In mmWave networks, analog beamforming is applied at both BSs and UEs [ABC$^+$14]. The coverage of mmWave cell is very small due to the high sensitive to the environment, and the density of the mmWave would be large. Hence, the beam alighment and resource allocation such as use association is significant for mmWave enabled networks.

2.2.3 Non-Orthogonal Multiple Access

Multiple access in wireless networks is a technique that allows multiple UEs to share available resources such as time and spectrum based on a specific scheme [JWY05]. System performance can be improved by selecting the multiple access technology appropriately. In general, there are two types of multiple access schemes, namely orthogonal multiple access (OMA) and NOMA [IADK17]. In OMA systems such as time division multiple

access (TDMA), and orthogonal frequency-division multiple access (OFDMA), time and spectrum resources are allocated orthogonally so as to eliminate the interference among UEs. Ideally, by using OMA, the intra-cell interference can be omitted. However, to ensure the orthogonal performance, the number of UEs and resources for each UE is limited.

Recently, NOMA has received much attention. The rationale of NOMA is to exploit the power or code domain in order to save time and frequency resources [SKB+13, DWY+15, DAP16, IADK17]. Compared to OMA, with the help of successive interference cancellation (SIC), NOMA allows BSs to serve multiple UEs simultaneously in the same frequency band and can substantially enhance the spectral efficiency and faireless. In [CLD+17] and [ZLC+17], NOMA has been considered to be used with mmWave and HetNets respectively.

The basic idea of NOMA is to implement multiple access in the power domain. Generally, in order to ensure the performance of cell edge UEs, the transmit power required by these UEs are larger and UEs' signals are stronger than the cell center UEs. SIC is employed to cancel the intra-cell interference from the stronger UEs' signals. Figure 2.1 illustrates the scenario of downlink NOMA with two UEs. Compared with conventional OMA networks, there are two main advantages. First, NOMA can improve spectrum efficiency by accepting massive connectivity which increase overall throughput of networks. Second, NOMA doesn't need precise synchronisation.

The achievable NOMA gain is mainly due to the different transmit power among UEs, resource allocation for NOMA is different and more complex, especially for power allocation and how to select UEs.

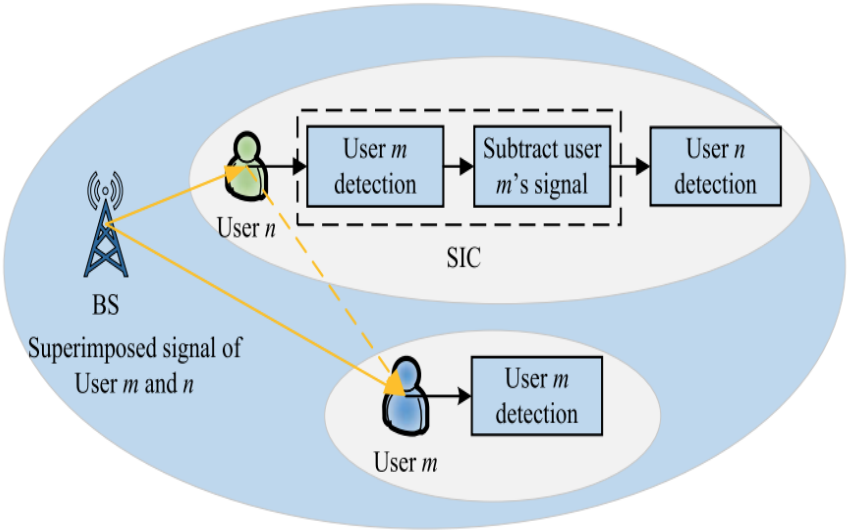

Figure 2.1: Downlink NOMA architecture with two UEs [LQE+17]

2.3 Resource Allocation in 5G cellular Networks

Resource allocation in wireless networks is a process of allocating available resources to BSs and UEs which is an essential part of network design. It is a key technique to improve the system performance while guaranteeing the UEs' QoS. Meanwhile, delay and data rate requirements of UEs are varied which makes the resource allocation more complex. Basically, there are several parts of resource allocation, including user association, resource block allocation, spectrum allocation, power control and sleep mode. User association is also cited as cell selection and determines which BS and UE should be associated with. Spectrum assignment is the process of regulating the use of radio frequencies to promote efficient use, and power control can decide the transmit power of the BS to achieve good performance such as higher data rate or lower energy consumption. The sleep mode means that each BS needs to make decision whether it should be on or off. The most prevalent objectives to evaluate the performance of resource allocation includes throughput, data quality, energy efficiency, energy consumption and delay. Meanwhile, except consider one objective solely, many works jointly consider several of objectives and the tradeoff among them are also investigated.

2.3.1 Resource Allocation in Grid Energy Powered 5G cellular networks

There has been many studies for resource allocation in conventional grid energy powered networks where all BSs are powered by constant energy supply. Till now, many works have been done for resource allocation in this scenario which aim to improve the performance of the whole networks or UEs. In the following part, the existing research results on resource allocation in grid energy powered networks are categorised according to different performance objectives, including energy efficiency, throughput and others such as fairness and delay.

The skyrocketing increase of throughput inevitably triggers a tremendous escalation of energy consumption in wireless networks. How to reduce energy consumption and how to use less energy to transmit the same amount of data become surge problems for 5G networks. Energy efficiency becomes a crucial concerns of future networks. Recent years, the literature is rich in dealing with the design of resource allocation strategies aiming at the optimisation of system's energy efficiency. For downlink, the user association and resource block allocation problem in a single cell OFDMA network is investigated to maximise the energy efficiency of the whole cell. In [LKM$^+$16], the power control and spectrum assignment problem is considered in a cellular network to maximise the energy efficiency. A distributed power control algorithm for energy efficiency maximisation in an uplink cellular network is proposed in [ZSD16] which uses a non-cooperative game theoretic approach to solve the problem. Meanwhile, many works study resource allocation in networks with 5G "big three" techniques including HetNets, massive multiple-input multiple-output (MIMO) and mmWave. Authors of [YWWZ17] optimise user association and the density of small BSs in HetNets. Both high-data requirement and low-data requirement are considered. The problem of on-off switching, user association and power control in multicell HetNets with massive MIMO is investigated in [FMJ17]. The resource allocation problem in mmWave HetNets is studied in [MHP$^+$16], where the working spectrum of each femtocell access point and user association are optimised

in a uplink single cell. In addition to fronthaul networks, there are also works for backhaul networks [NGL+17, MZK17], which consider power control and user association respectively.

Data rate is another significant indicator for networks. Reference [LH12] presents a resource block allocation algorithm which tries to maximise the system throughput with QoS support for real-time traffic flows in a single-cell OFDMA-based system. A power control scheme in HetNets aiming at maximising the worst UEs's throughput is proposed in [AH13]. Authors of [BBPC16] consider the optimal user association problem for massive MIMO HetNets while authors of [CK17] propose an algorithm to maximise the network multicast throughput via power control and backhaul resource allocation in a downlink cloud radio access network (C-RAN). In [PDDLN16], a joint BS assignment, sub-carrier and power allocation algorithm is proposed to maximise the network throughput. It considers the downlink dynamic resource allocation in multi-cell virtualised wireless networks to support the UEs of different service providers in OFDMA cellular networks.

Except energy efficiency and data rate, fairness and spectrum efficiency are also key indicators in cellular networks. The balance between energy efficiency and spectrum efficiency, the tradeoff between fairness and energy efficiency/spectrum efficiency are investigated in [WFGW14] for a single-cell OFDMA network. In [LCC+14], the human-to-human(H2H) traffic and machine-to-machine (M2M) traffic are defined as primary service and secondary service respectively. An user association optimisation problem is formulated to support fair resource allocation for M2M traffic without jeopardising data rate of H2H traffic.

2.3.2 Resource Allocation in Renewable Energy Powered 5G cellular Networks

Recent developments in energy harvesting technology have enabled many general wireless networks to power their devices by harvesting energy from the surrounding environment (e.g., wind turbines and solar panels). By this way, the energy demand of the power grid can be reduced which can support the wireless networks with potentially infinite lifetime. It is envisioned that energy harvester powered devices will play an important role in future wireless networks, especially in places where power grids are hard to be laid.

Along with the benefits, the fluctuating nature of renewable energy sources also brings challenges to resource allocation and wireless network design. The conventional resource allocation schemes for grid powered wireless networks are not adequate anymore. Hence it is critical to explore new resource allocation schemes for renewable energy supported networks, which need to jointly consider the traffic profile, QoS requirement and the renewable energy statistics [GTZN14].

Generally, based on the source of energy, research in renewable energy powered networks are separated into two parts, solely renewable energy powered networks and hybrid energy powered networks. Until now, considerable research efforts have been devoted to study solely renewable energy enabled cellular networks for sustainable operation.

2.3.2.1 Resource Allocation in Solely Renewable Energy Powered 5G cellular Networks

In the last decade, many works have been done to investigate the resource allocation problem in 5G cellular networks which solely powered by renewable energy. The deployment of relays with energy harvesting capabilities has attracted attention recently. In [JZLL15], user association is considered in a cooperative network where UEs are associ-

ated with energy-harvesting relays, and user association decision is made to improve the achievable rate. By using the conventional reference signal received power (RSRP)-based user association, the fundamental limits of HetNets with renewable energy harvesting are analysed in [DLN+14]. In [ZXL+15], a user association problem for maximising the data rate proportional fairness is formulated by considering the energy-load tradeoff in HetNets with renewable energy sources, and a topology potential based user association algorithm is proposed to solve this problem.

Besides user association in cellular networks, many other resource allocation problems are studied. Authors of [LHSX17] study spectrum and energy allocation problem in device-to-device (D2D) cellular networks. A sum rate maximisation problem of the whole cellular network is formulated under the constraint of minimum data rate requirement. The joint sub-carriers allocation, RRHs distribution and data scheduling problem in renewable energy powered C-RAN is investigated in [ZCC+16]. It considers the UEs data rates and stability of RRHs' data and energy queues, where the network backlog is bounded and the required battery capacity is finite.

2.3.2.2 Resource Allocation in Hybrid Energy Powered 5G cellular Networks

Although renewable energy is promising for green 5G networks, there are additional constraints in resource allocation for solely renewable energy enabled networks. Generally, in solely renewable energy enabled networks, power allocation is constrained by the stochasticity of the renewable energy arrival rate. It is hard to fulfill the QoS performance of UEs. Hence, let renewable energy be the supplement of the grid energy is more practical for the real networks [NLS13].

Authors of [HA13a] propose a distributed user association scheme called Green-energy Aware and Latency Aware (GALA) in HetNets, which can decrease the on-grid energy consumption and the average traffic delivery latency. The work of [LCC+15] studies

the joint user association and green energy allocation for two-tier HetNets, where user association is optimised in space dimension and green energy allocation is optimised in time dimension. In [HYM+17], user association is extended to K-tier HetNets, where BSs are powered by the power grid, renewable energy sources or both, and a distributed user association algorithm is developed to maximise the network throughput in an online way. The joint user association, power control and dynamic cell activation optimisation problem in two-tier HetNets is studied in [ZZZ+16] for minimising the on-grid energy consumption. The outage probability is obtained by stochastic geometry and energy consumption is analysed using M/D/1 queue. M/D/1 queue represents a queue in a system with a single server, where arrivals are determined by a poisson process and job service times are fixed.

A two-timescale delay optimal transmission control and user association problem for downlink coordinated MIMO systems is proposed in [CLW12], where an optimisation problem is formulated as a partially observed Markov decision problem and a delay-aware distributed solution is obtained to reduce the complexity of the system.

In [NLS13], a sub-carrier and power allocation scheme in downlink OFDMA networks is proposed to maximise the energy efficiency of the network. The storage of each BS is finite, and both the offline and online designs are developed based on the availability of non-causal/causal knowledge of channel state information and energy arrivals. In order to minimise the grid energy consumption, [HA13b] considers a green energy optimisation problem with multi-stage energy allocation and multi-BSs energy balancing. In this work, green energy allocation is optimised in time dimension and energy consumption among BSs is balanced in space dimension.

In [GTZN14], the average grid energy consumption minimisation problem is formulated by optimising the BS sleeping policy, subcarriers allocation and renewable energy allocation. The formulated problem in [GTZN14] is solved by a two-stage dynamic programming algorithm.

Generally, in renewable energy sources powered cellular networks, each BS manages its own energy consumption. When a particular BS does not have enough energy to support the traffic demand, some UEs of it which are originally connected to this BS will have to be offloaded to neighbour BSs. This process introduces two problems. First, the signalling cost for facilitating the handover process will be enormous especially when the number of UEs is huge nowadays. Second, the QoS of UEs will be affected by enforcing them to associated with the second best serving cell. To solve this problem, the concept of energy cooperation was proposed [GOYU13a].

2.4 Energy Cooperation

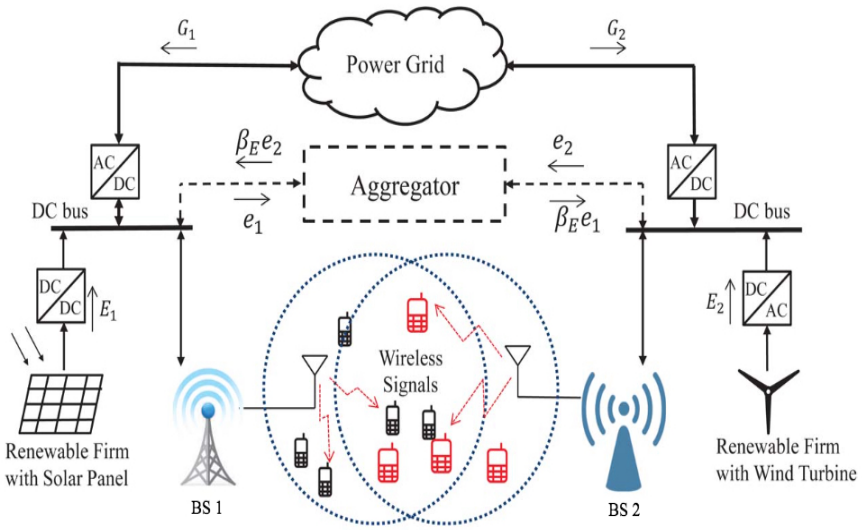

Figure 2.2: An example of energy cooperation between two BSs [GXDZ14]

Thanks to the development of the smart grid, which enables both two-way information and energy flows, the energy cooperation concept was introduced in [GOYU13a] which allows energy transferred between BSs. The energy is transferred through the existing power grid or the latest smart grid. Figure 2.2 is an example of a two BSs' cellular network with energy cooperation. Here, E_1 and G_1 are the energy obtained from the solar panel and the power grid by BS 1 respectively. e_1 and $\beta_{\mathcal{E}} e_2$ are the cooperated energy of

BS 1 transferred to/from the aggregator respectively. BS 2 is in the same manner. The BSs use wind turbines or solar panels as the complementary of the traditional power grid. The energy is transferred with the help of an aggregator. One BS injects the extra energy to the aggregator while the other BSs who need energy could draw from the aggregator at the same time. With the help of energy cooperation, when the BS 1's renewable energy is not enough, it doesn't need to switch off which will deteriorate the QoS of UEs. The extra energies of BS 2 will be transferred to BS 1 with some energy cost. By this way, the renewable energy can be utilised more effectively.

Energy cooperation in the multiple access transmission context have been studied in [GOYU13a, GOYU12, GOYU13b, TY13b, TY13a, HZZN13, WRW+14]. Reference [GOYU13a] is the first paper which considers energy cooperation in the wireless network. It considers a simple multi-hop wireless communication system which includes a transmitter, a receiver and a relay. The energy is allowed to be transferred between the transmitter and the relay. It addresses the throughput maximisation problem by optimising the energy management policies. Meanwhile, the achievable rates regions of the Gaussian two-way channel and the multiple access channel are studied in [GOYU12] with one-way energy transfer. Reference [GOYU13b] extends the two-way channel in [GOYU12] by formulating a throughput maximisation problem of the whole system with energy cooperation. Reference [TY13b] jointly optimises the transmit power allocation and energy cooperation in order to maximise the throughput of the multiple access and two-way channels. A multiple access relay communication network with energy cooperation is studied in [TY13a]. Energy is allowed to be transferred in bi-direction. Reference [HZZN13] proposes an Energy and Data Aware (EDA) algorithm for energy allocation and data admission to maximise the throughput of energy cooperation enabled networks. Reference [WRW+14] develops an energy cooperation scheme for cognitive networks which has two stages. In the first stage, primary systems harvest energy from the secondary systems' signals. In the second stage, primary systems transmit primary messages with the harvested energy and energy from the sustain power supply.

Meanwhile, there are also some studies about the energy cooperation in cellular networks. The first energy cooperation enabled cellular network is studied in [CSZ14b]. In [CSZ14b], two algorithms (offline and online) are proposed in order to minimise the conventional energy consumption in the case of two BSs when the energy cooperation between them is allowed. The energy cooperation problem of a two-cell system with different numbers of cell users is studied in [GLM13]. It formulates the problem for an frequency division multiple access (FDMA) system which is solved by a bisection search and water-filling to optimise the direction and quantum of energy to transfer. The joint energy cooperation and spectrum allocation scheme is studied in [GXDZ14]. It optimises the transferred energy and the spectrum allocation between two hybrid powered BSs which belong to two different cellular systems together aiming to minimise the weighted sum energy cost.

To further improve the performance of networks, more studies associate energy cooperation with other techniques, such as coordinated multipoint (CoMP) [XZ15a, XZ16], HetNets [RB16, RMSM$^+$17] and mmWave[XCC$^+$17]. The authors of [XZ15a, XZ16] investigate the performance of joint CoMP and energy cooperation enabled cellular networks, which consider one single coordinated multi-point cluster. Reference [XZ15a] aims to optimise the transmit power and the amount of transferred energy among BSs in order to maximise the sum rate of the whole system while [XZ16] optimise the purchased/sold energy from/to the grid to minimise the energy cost. Authors of [RB16] study power control and the discarded excess energy in a hybrid energy powered two-tier HetNet to maximise the energy efficiency. While [RB16] using convex optimisation, [RMSM$^+$17] uses game theory to minimise the grid energy consumption in a multi-tier HetNet. Power control in energy cooperation enabled mmWave networks is studied in [XCC$^+$17], which maximise the time average network throughput while keeping the network stable. In [VY16], an energy cooperation scheme is proposed to maximise the energy efficiency of each UE in a wireless Ad Hoc network. It formulates the problem as a matching game between transmitters and receivers. Reference [RCZ18] considers the energy cooperation

problem between two microgrids with individual energy storage. It optimises the grid energy consumption, transferred energy and the energy charged from the power grid to minimise the overall grid energy consumption.

So far, energy cooperation becomes more important to maximise the throughput of renewable energy enabled networks and reduce grid energy consumption. However, in energy cooperation enabled networks, besides the conventional parameters, grid energy consumption and transferred energy also need to be optimised, which make the conventional resource allocation schemes can not be used directly anymore. Resource allocation such as user association and power control are more complex and urgent for implementing energy cooperation.

2.5 Convex Optimisation

Design and optimisation of wireless networks rely heavily on mathematical modelling tools. Convex optimisation, is a widely used mathematical method to solve a special class of optimisation problems, such as least-squares and linear programming problems [LY06]. It can find the optimal solution for nonlinear problems over convex constraint sets. Convex optimisation is appealing since a local optimum is also a global optimum for a convex problem, which can reduce the required computation compared with other problems. Convex optimisation has been studied for about a century, some complex problems such as semidefinite programs and second-order cone programs can be solved as easily as linear programs [BV04]. Meanwhile, the exiting of softwares such as CVX and SeDuMi makes convex optimisation even more popular. When convex optimisation is used, the problem need to be formulated or transformed as a convex optimisation problem. Generally, a typical convex optimisation problem is one of the form

$$\underset{x}{\text{minimise}} \quad f_0(x) \tag{2.1}$$

$$\text{subject to} \quad f_i(x) \leq b_i, i = 1, ..., m, \tag{2.2}$$

where the functions $f_0, ..., f_m : R^n \to R$ are convex, *i.e.*, satisfy

$$f_i(\alpha x + \beta y) \leq \alpha f_i(x) + \beta f_i(y) \tag{2.3}$$

for all $x, y \in R^n$ and all $\alpha, \beta \in R$ with $\alpha + \beta = 1,\ \alpha \geq 0,\ \beta \geq 0$.

The (2.1) is the objective function of the problem where vector $x = (x_1, ..., x_n)$ is the optimisation variables of the problem. the functions $f_i : R^n \to R,\ i = 1, ..., m$ are the inequality constraint functions. The vector x^* is called optimal, if it has the smallest objective value among all vectors that satisfy the constraints. For a convex problem, the objective function and all constraints should be convex.

For resource allocation in wireless networks, the most common used method is Lagrange duality theory [YU12, SLW$^+$15, TGUBL13, RPI14, NLS13]. The original problem is named primal problem. This method is taking the constraints into account by augmenting the objective function with a weighted sum of the constraint functions by introducing nonnegative Lagrange multipliers, and the new objective function is called Lagrangian function. After that, a new problem which called dual problem is formulated. Lagrangian function is its objective function and variables are Lagrange multipliers. Then the solution of the dual problem provides a lower bound to the primal problem and the new problem is maximising the dual problem where the variable is Lagrange multiplier.

2.6 Summary

This chapter provides an overview of the advanced technologies such as HetNets and mmWave in 5G networks. As one of important parts of networks design, resource allocation problems have been extensively studied in grid powered 5G networks. Since harvested energy becomes a more promising solution to reduce grid energy consumption

which is one of key indicators for 5G networks, detailed review for resource allocation in renewable energy supplied 5G networks is also presented. To solve the fluctuating problem of renewable energy and use renewable energy more efficiently, energy cooperation becomes more important in the last few years and the extensive review for energy cooperation in both multiple access and cellular networks are given.

Due to the exist of the transferred energy in energy cooperation, there is a tradeoff between offloading and energy transfer between BSs. Conventional resource allocation schemes are not suitable anymore. More research is required to optimise resource allocation in energy cooperation enabled networks. Meanwhile, it is worth to investigate the performance of energy cooperation under 5G networks including other technologies rather than using it solely.

In the next four chapters, resource allocation in energy cooperation enabled networks under the scenarios with different 5G technologies are investigated. The optimisation method used in this thesis is convex optimisation, which is also presented briefly in this chapter.

Chapter 3

Resource Allocation in Energy Cooperation Enabled mmWave Networks

3.1 Overview

In this chapter, the energy management problem in energy cooperation enabled millimeter wave (mmWave) cellular networks is studied. By considering the stochastic traffic and energy arrivals, a stochastic optimisation problem is formulated to maximise the time average throughput of the whole network. Then an online algorithm based on Lyapunov optimisation is proposed. Finally, the performance of the proposed algorithm is investigated through simulations. The impacts of base staion (BS) numbers, energy transfer efficiency and a control variable used for Lyapunov optimisation are illustrated.

3.2 System Model and Problem Formulation

In this section, the system model of energy cooperation in mmWave networks is presented which has not been investigated before and the power control problem in energy cooperation enabled mmWave networks is formulated.

3.2.1 Network Downlink Model

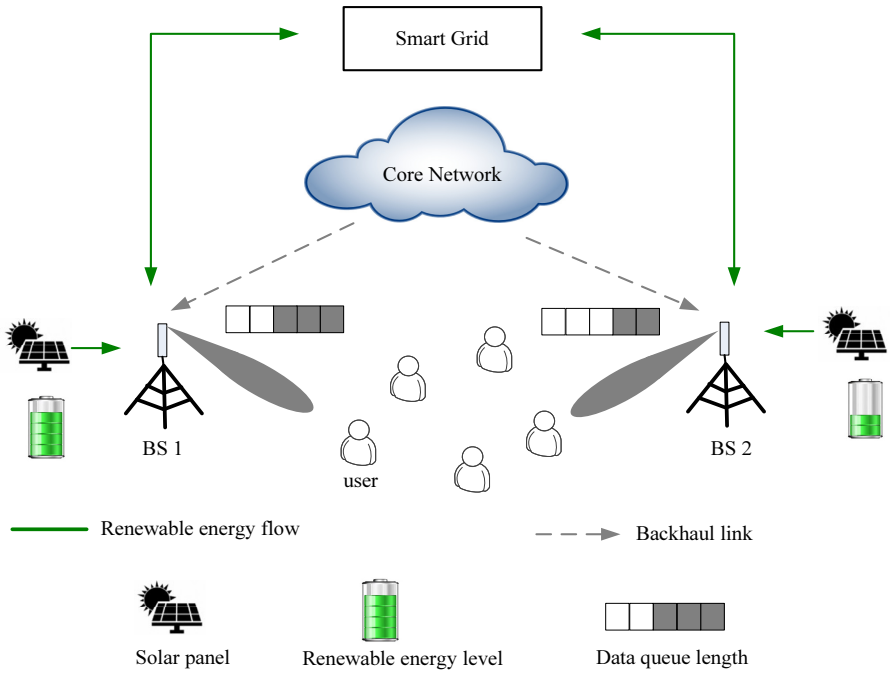

Figure 3.1: An example of an energy cooperation enabled mmWave cellular network powered by solar panels.

As shown in Figure 3.1, a downlink energy cooperation enabled mmWave cellular network is modelled, where BSs are solely powered by renewable energy sources, and energy can be shared between BSs through the smart grid. In this chapter, to focus on the power control and energy cooperation problem, there is no specific assumption of the types of renewable energy sources being used. In such a network, there are M mmWave BSs denoted as $BS_j, j \in \{1, 2, ..., M\}$ that share the same spectrum, and user equipments (UEs) are randomly located. User association is assumed to be already implemented before the power allocation, and there are N_j UEs denoted as UE_j^i $(i \in \{1, 2, ..., N_j\})$

served by BS_j. All BSs and UEs are equipped with directional antennas, and the antenna gains achieved by each BS and UEs are G_{b} and G_{u}, respectively.

Due to the use of higher frequencies and directional transmissions, mmWave cellular networks tend to be noise-limited [ABC+14, LSH16, ALS+14], which means that the interference between BSs can be negligible. Thus, under the framework of Shannon equation, the theoretical downlink data rate of UE i connected to the BS j at time slot t is given by

$$R_{ij}(t) = (N_j)^{-1}\log_2\left(1 + \frac{P_j(t)\, L_{ij}(d_{ij})\, G_{\mathrm{b}}G_{\mathrm{u}}}{\sigma_o^2}\right), \tag{3.1}$$

where $P_j(t)$ is the transmit power of BS j at time t, σ_o^2 is the noise power level. $L_{ij}(d_{ij})$ is the path loss between the UE i and its associated BS j with a distance d_{ij}. Each UE receives $(N_j)^{-1}$ of all the spectrum of BS j and the overall spectrum of BS j is normalised to 1. The channel is regarded as static and the data rate is considered as time-averaged. The path loss laws are different in line-of-sight (LOS) and non-line-of-sight (NLOS) conditions. In this chapter, the mmWave path loss model proposed in [ALS+14] is employed and each mmWave link can be in one of three conditions: LOS, NLOS or outage.

It should be mentioned that in the thesis, all data rates are calculated based on Shannon equation which is the theoretical rate or the upper bound of rate rather than the actual rate.

The unit size of time is "slots" and the amount of transmitted data between UE i and BS j in time slot t is $R_{ij}(t) \times (1 \text{ slot})$. Here, the implicit multiplication is omitted by 1 time slot when converting between the data rate and the amount of data that transmit from the queue per time slot as suggested in [HN13]. In the same manner, the unit of the $P_j(t)$ is joule when converting between power and energy. As such, the transmitted

data of the whole network at the time t is given by

$$U(t) = \sum_{j=1}^{M} \sum_{i=1}^{N_j} R_{ij}(t). \tag{3.2}$$

3.2.2 UE's Traffic and Data Queue Model

It is assumed that the data traffic required by the UE is stochastic. The amount of data traffic arrival for UE i served by BS j during time slot t is $D_{ij}(t)$. Let $D_{\max}$ denote the maximum allowable data traffic arrival rate per UE due to backhaul throughput constraint, then I have

$$0 \leq D_{ij}(t) \leq D_{\max}, \forall i, j, t. \tag{3.3}$$

Based on the downlink data rate and traffic arrival rate, the data queue length $Q_{ij}(t)$ for UE i served by BS j evolves as follows:

$$Q_{ij}(t+1) = [Q_{ij}(t) - R_{ij}(t)]^{+} + D_{ij}(t), \ \forall i \in \mathcal{U}, \ j \in \mathcal{B}, \tag{3.4}$$

where $[x]^{+} = \max\{0, x\}$. At the beginning, it is assumed that $Q_{ij}(0) = 0, \forall i, \ j$.

3.2.3 Energy Cooperation and Energy Queue Model

Each BS stores the energy harvested from renewable energy sources and transferred energy from other BSs in its battery. At time t, the available energy at BS j is $E_j(t)$, and the amount of BS j's energy harvested from renewable energy sources is $e_j(t)$. It is assumed that there exists the maximum value $e_{\max}$ for harvesting renewable energy during the day, i.e., $e_j(t) \leq e_{\max} < \infty, \forall j, t$. It is assumed that the energy can be exchanged among BSs through the smart grid. The transferred energy from BS j to BS $j^{'}$ is $\varepsilon_{jj'}(t)$. Since the capacity of energy storage at each BS is limited, the total transferred

energy from BS j to other BSs satisfies $\sum_{j'=1,j'\neq j}^{M} \varepsilon_{jj'}(t) \leq \varepsilon_{\max}^{(\text{out})} < \infty, \forall j, t$, and total transferred energy received at BS j satisfies $\sum_{j'=1,j'\neq j}^{M} \beta\varepsilon_{j'j}(t) \leq \varepsilon_{\max}^{(\text{in})} < \infty, \forall j, t$. $\varepsilon_{\max}^{(\text{in})}$ and $\varepsilon_{\max}^{(\text{out})}$ are the maximum energy that can be transferred from/to each BS respectively. Here, $\beta \in [0, 1]$ is the energy transfer efficiency between each two BSs. The larger this value, the smaller energy loss in the energy transfer process. Considering the fact that the total energy consumed by each BS should not exceed the total power supply including the harvested energy and the transferred energy, the following power consumption constraint at time t is obtained:

$$P_j(t) \leq E_j(t) + \sum_{j'=1,j'\neq j}^{M} \beta\varepsilon_{j'j}(t) - \sum_{j'=1,j'\neq j}^{M} \varepsilon_{jj'}(t), \forall t, \forall j \in \mathcal{B}. \tag{3.5}$$

The transmit power of BS j at time t is $P_j(t) \times (1 \text{ slot})$, and the implicit multiplication by 1 time slot of the $P_j(t)$ is omitted when converting between power and energy. Under this constraint, the energy queue length evolves as follows:

$$E_j(t+1) = E_j(t) - P_j(t) + e_j(t) + \sum_{j'=1,j'\neq j}^{M} \beta\varepsilon_{j'j}(t) - \sum_{j'=1,j'\neq j}^{M} \varepsilon_{jj'}(t). \tag{3.6}$$

3.2.4 Problem Formulation

An online algorithm is proposed to maximise the time average network throughput while keeping the network stable. Here, stable means that the network backlog is bounded and the required battery capacity is finite. The data rate of an UE i connected to the BS j is $R_{ij}(t)$. The optimised variables are transmit powers of BSs $P_j(t)$ and energy transferred between BSs $\varepsilon_{jj'}(t)$ at every time slot. Meanwhile, the real harvested energy $e_j(t)$ which lower than the available harvested energy is adjusted with the optimised variables. Then,

the problem is formulated as

$$\max \lim_{T\to\infty} \sup \frac{1}{T} \sum_{t=0}^{T-1} \mathbb{E}\left[U(t)\right], \tag{3.7}$$

$$\begin{aligned}
\text{s.t.C1}: & \lim_{T\to\infty} \sup \frac{1}{T} \sum_{t=0}^{T-1} \mathbb{E}\left[\sum_{j=1}^{M}\sum_{i=1}^{N_j} Q_{ij}\left(t\right)\right] < \infty, \\
\text{C2}: & \lim_{T\to\infty} \sup \frac{1}{T} \sum_{t=0}^{T-1} \mathbb{E}\left[\sum_{j=1}^{M} E_j\left(t\right)\right] < \infty, \\
\text{C3}: & P_j\left(t\right) \leq E_j\left(t\right) + \sum_{j'=1, j'\neq j}^{M} \beta\varepsilon_{j'j}\left(t\right) - \sum_{j'=1, j'\neq j}^{M} \varepsilon_{jj'}\left(t\right), \forall t, \forall j, \\
\text{C4}: & P_j\left(t\right) \leq P_{\max}, \forall t, \forall j, \\
\text{C5}: & e_j\left(t\right) \geq 0, P_j\left(t\right) \geq 0, \varepsilon_{j'j}\left(t\right) \geq 0, \forall t, \forall j, j^{'}, j \neq j^{'},
\end{aligned} \tag{3.8}$$

where $\mathbb{E}[\cdot]$ represents the expectation that is taken over the potential randomness of the channel and energy states and control decision at time t [Nee06]. Constraint C1 ensures that the length of data queue is bounded to avoid an intolerant delay. C2 ensures that the length of energy queue is bounded such that only finite battery capacity is needed. C3 is the energy consumption constraint, which means the energy of each BS obtained from renewable energy sources and other BSs should greater than the energy consumption of it. C4 is the maximum BS transmit power constraint, and C5 makes sure that powers are non-negative. In the next section, It will be shown that how the formulated stochastic problem is solved by Lyapunov optimisation technique.

3.3 Proposed Power Control Scheme Based on Lyapunov Optimisation

In this section, an online algorithm for solving the stochastic optimisation problem (3.8) is developed with the help of Lyapunov optimisation. Compared with the conventional

methods such as Markov decision processes and dynamic programming, Lyapunov optimisation only needs the knowledge of the traffic and energy arrivals of the current time slot, which is a useful method for solving stochastic optimisation problems [LQP14].

3.3.1 Lyapunov Optimisation

Firstly, the Lyapunov function is defined as

$$L\left(t\right)=\frac{1}{2}\sum_{j=1}^{M}\sum_{i=1}^{N_j}\left(Q_{ij}\left(t\right)\right)^2+\frac{1}{2}\sum_{j=1}^{M}\left(E_j\left(t\right)-\theta_j\right)^2, \tag{3.9}$$

where θ_j is a perturbation. By adding a perturbation, It can be ensured that there are always enough energy in the energy queue for transmission. The Lyapunov function is used to measure the data and energy flow in the system.

The Lyapunov drift is used to measure the expected difference for the Lyapunov function between the time slot t and $(t+1)$. Let $\mathbf{Z}\left(t\right)=[\mathbf{Q}(t),\mathbf{E}(t)]$ with $\mathbf{Q}(t)=[Q_{ij}\left(t\right)]$ and $\mathbf{E}(t)=[E_j\left(t\right)]$, the one-time conditional Lyapunov drift is given by

$$\Delta\left(t\right)=\mathbb{E}\Big[L\left(t+1\right)-L\left(t\right)|\mathbf{Z}\left(\mathbf{t}\right)\Big]. \tag{3.10}$$

In addition, considering the objective function of problem (3.8), the drift-plus-penalty is defined as

$$\Delta_V\left(t\right)=\Delta\left(t\right)\underbrace{-V\mathbb{E}\Big[\sum_{j=1}^{M}\sum_{i=1}^{N_j}R_{ij}\left(t\right)|\mathbf{Z}\left(\mathbf{t}\right)\Big]}_{\text{Penalty term}}. \tag{3.11}$$

In (3.11), V is a non-negative control variable which represents the relative importance of minimising the energy and data queue length to a lower level and maximising the sum rate of the whole network. The upper bound of the drift-plus-penalty is derived as follows.

Lemma 1. *For any feasible values of* $e_j\left(t\right)$, $P_j\left(t\right)$, $\varepsilon_{j'j}\left(t\right)$, V *and* $\mathbf{Z}\left(\mathbf{t}\right)$ *at time* t, *the*

drift-plus-penalty is upper bounded as

$$\begin{aligned}\Delta_V(t) \leq A &- \sum_{j=1}^{M}\sum_{i=1}^{N_j} Q_{ij}(t)\,\mathbb{E}\left[\left(R_{ij}(t) - D_{ij}(t)\right) \mid \mathbf{Z}(\mathbf{t})\right] \\ &- \sum_{j=1}^{M}\left(E_j(t) - \theta_j\right)\mathbb{E}\Big[P_j(t) - e_j(t) + \sum_{j'=1,j'\neq j}^{M} \varepsilon_{jj'}(t) - \\ &\sum_{j'=1,j'\neq j}^{M} \beta\varepsilon_{j'j}(t) \mid \mathbf{Z}(t)\Big] - V\mathbb{E}\Big[\sum_{j=1}^{M}\sum_{i=1}^{N_j} R_{ij}(t) \mid \mathbf{Z}(t)\Big],\end{aligned} \tag{3.12}$$

where A is a positive constant value satisfying

$$A \geq \frac{\sum_{j=1}^{M}\sum_{i=1}^{N_j} D_{\max}}{2} + \sum_{j=1}^{M}\sum_{i=1}^{N_j}\mathbb{E}\left[\frac{\left(R_{ij}(t)\right)^2}{2} \mid \mathbf{Z}(\mathbf{t})\right] + M\frac{\left(P_{\max} + \varepsilon_{\max}^{(\text{out})}\right)^2 + \left(e_{\max} + \varepsilon_{\max}^{(\text{in})}\right)^2}{2}. \tag{3.13}$$

Proof. To obtain the upper bound of the drift-plus-penalty $\Delta_V(t)$, first the difference for the Lyapunov function between the time slot t and $t+1$ need to be calculated, i.e.,

$$\begin{aligned}L(t+1) - L(t) = &\underbrace{\sum_{j=1}^{M}\sum_{i=1}^{N_j}\frac{\left(Q_{ij}(t+1)\right)^2 - \left(Q_{ij}(t)\right)^2}{2}}_{\Theta_1} \\ &+ \underbrace{\sum_{j=1}^{M}\frac{\left(E_j(t+1) - \theta_j\right)^2 - \left(E_j(t) - \theta_j\right)^2}{2}}_{\Theta_2}.\end{aligned} \tag{3.14}$$

Based on (3.4), the square of the data queue for UE i served by BS j at time $t+1$ is upper bounded as

$$\left(Q_{ij}(t+1)\right)^2 \leq \left(Q_{ij}(t)\right)^2 + \left(R_{ij}(t)\right)^2 + \left(D_{ij}(t)\right)^2 - 2Q_{ij}(t)\left(R_{ij}(t) - D_{ij}(t)\right). \tag{3.15}$$

By summing (3.15) over all i and j, I have

$$\begin{aligned}\Theta_1 &\leq \sum_{j=1}^{M}\sum_{i=1}^{N_j}\frac{\left(R_{ij}\left(t\right)\right)^2+\left(D_{ij}\left(t\right)\right)^2}{2}-\sum_{j=1}^{M}\sum_{i=1}^{N_j}Q_{ij}\left(t\right)\left(R_{ij}\left(t\right)-D_{ij}\left(t\right)\right)\\ &\overset{(a)}{\leq}\frac{\sum_{j=1}^{M}\sum_{i=1}^{N_j}D_{\max}}{2}+\sum_{j=1}^{M}\sum_{i=1}^{N_j}\frac{\left(R_{ij}\left(t\right)\right)^2}{2}-\sum_{j=1}^{M}\sum_{i=1}^{N_j}Q_{ij}\left(t\right)\left(R_{ij}\left(t\right)-D_{ij}\left(t\right)\right),\end{aligned}\tag{3.16}$$

where (a) is obtained by using the backhaul throughput constraint in (3.3). Then, considering energy queue given by (3.6), the square of the energy queue for UE i served by BS j at time $t+1$ is upper bounded as

$$\begin{aligned}&\left(E_j\left(t+1\right)-\theta_j\right)^2\leq\left(E_j\left(t\right)-\theta_j\right)^2+\Big(P_j\left(t\right)+\sum_{j'=1,j'\neq j}^{M}\varepsilon_{jj'}\left(t\right)\Big)^2\\ &+\Big(e_j\left(t\right)+\sum_{j'=1,j'\neq j}^{M}\beta\varepsilon_{j'j}\left(t\right)\Big)^2-2\left(E_j\left(t\right)-\theta_j\right)\left(P_j\left(t\right)-e_j\left(t\right)\right)\\ &-2\left(E_j\left(t\right)-\theta_j\right)\Big(\sum_{j'=1,j'\neq j}^{M}\varepsilon_{jj'}\left(t\right)-\sum_{j'=1,j'\neq j}^{M}\beta\varepsilon_{j'j}\left(t\right)\Big)\\ &\leq\left(E_j\left(t\right)-\theta_j\right)^2+\Big(P_{\max}+\varepsilon_{\max}^{(\text{out})}\Big)^2\\ &+\Big(e_{\max}+\varepsilon_{\max}^{(\text{in})}\Big)^2-2\left(E_j\left(t\right)-\theta_j\right)\left(P_j\left(t\right)-e_j\left(t\right)\right)\\ &-2\left(E_j\left(t\right)-\theta_j\right)\Big(\sum_{j'=1,j'\neq j}^{M}\varepsilon_{jj'}\left(t\right)-\sum_{j'=1,j'\neq j}^{M}\beta\varepsilon_{j'j}\left(t\right)\Big).\end{aligned}\tag{3.17}$$

By summing (3.17) over all j, I have

$$\begin{aligned}\Theta_2\leq M\frac{\Big(P_{\max}+\varepsilon_{\max}^{(\text{out})}\Big)^2+\Big(e_{\max}+\varepsilon_{\max}^{(\text{in})}\Big)^2}{2}-\sum_{j=1}^{M}\left(E_j\left(t\right)-\theta_j\right)\left(P_j\left(t\right)-e_j\left(t\right)\right)\\ -\sum_{j=1}^{M}\left(E_j\left(t\right)-\theta_j\right)\Big(\sum_{j'=1,j'\neq j}^{M}\varepsilon_{jj'}\left(t\right)-\sum_{j'=1,j'\neq j}^{M}\beta\varepsilon_{j'j}\left(t\right)\Big).\end{aligned}\tag{3.18}$$

Based on (3.16) and (3.18), the one-time conditional Lyapunov drift $\Delta\left(t\right)$ is upper

bounded as

$$\begin{aligned}\Delta(t) \leq A &- \sum_{j=1}^{M}\sum_{i=1}^{N_j} Q_{ij}(t)\,\mathbb{E}\left[\left(R_{ij}(t) - D_{ij}(t)\right) \mid \mathbf{Z}(\mathbf{t})\right] \\ &- \sum_{j=1}^{M}\left(E_j(t) - \theta_j\right)\mathbb{E}\Big[P_j(t) - e_j(t) + \sum_{j'=1,j'\neq j}^{M}\varepsilon_{jj'}(t) \\ &- \sum_{j'=1,j'\neq j}^{M}\beta\varepsilon_{j'j}(t) \mid \mathbf{Z}(\mathbf{t})\Big],\end{aligned} \tag{3.19}$$

where A satisfies

$$A \geq \frac{\sum_{j=1}^{M}\sum_{i=1}^{N_j} D_{\max}}{2} + \sum_{j=1}^{M}\sum_{i=1}^{N_j}\mathbb{E}\left[\frac{\left(R_{ij}(t)\right)^2}{2} \mid \mathbf{Z}(\mathbf{t})\right] + M\frac{\left(P_{\max} + \varepsilon_{\max}^{(\text{out})}\right)^2 + \left(e_{\max} + \varepsilon_{\max}^{(\text{in})}\right)^2}{2}. \tag{3.20}$$

Substituting (3.19) into (3.11), the upper bound of the drift-plus-penalty $\Delta_V(t)$ is obtained, and the proof is completed. □

Based on the stochastic optimisation introduced in [Nee10, Chapter 4], the control decision is made at every time t for minimising the upper bound of drift-plus-penalty given in the right-hand-side (RHS) of (3.12). Note that the penalty term $-V\mathbb{E}\Big[\sum_{j=1}^{M}\sum_{i=1}^{N_j} R_{ij}(t)|\mathbf{Z}(\mathbf{t})\Big]$ in (3.12) is used to seek balance between minimising queue length drift and maximising the network throughput, and larger V represents that increasing the throughput is more essential. Therefore, by removing the expectation operations and constant terms in the RHS of (3.12), an optimisation problem needs to

be solved at time t, which is as follows:

$$\max_{\mathbf{e}(t),\mathbf{P}(t),\boldsymbol{\varepsilon}(t)} \sum_{j=1}^{M}\sum_{i=1}^{N_j} Q_{ij}(t) R_{ij}(t) - \sum_{j=1}^{M} (E_j(t) - \theta_j) e_j(t) + \sum_{j=1}^{M} (E_j(t) - \theta_j) \Big(P_j(t) + \sum_{j'=1, j'\neq j}^{M} \varepsilon_{jj'}(t) - \sum_{j'=1, j'\neq j}^{M} \beta \varepsilon_{j'j}(t) \Big) + V \sum_{j=1}^{M}\sum_{i=1}^{N_j} R_{ij}(t). \tag{3.21}$$

$$\text{s.t.} \quad \text{C3, C4, C5.}$$

Since the objective is to maximise (3.21), there will be no energy harvested at BS j when $E_j(t) > \theta_j$, i.e. $e_j(t) = 0$. This also ensures that the energy storage of each BS is finite (more details will be illustrated in the following subsection). After the energy harvesting decision, the power allocation policy $(\mathbf{P}(t), \boldsymbol{\varepsilon}(t))$ at time t is given by solving the following problem:

$$\max_{\mathbf{P}(t),\boldsymbol{\varepsilon}(t)} \sum_{j=1}^{M}\sum_{i=1}^{N_j} Q_{ij}(t) R_{ij}(t) + \sum_{j=1}^{M} (E_j(t) - \theta_j) \Big(P_j(t) + \sum_{j'=1, j'\neq j}^{M} \varepsilon_{jj'}(t) - \sum_{j'=1, j'\neq j}^{M} \beta \varepsilon_{j'j}(t) \Big) + V \sum_{j=1}^{M}\sum_{i=1}^{N_j} R_{ij}(t), \tag{3.22}$$

$$\text{s.t.} \quad \text{C3, C4, C5.}$$

It can be seen that the objective function of problem (3.22) is concave and the constraint functions are affine, which means that the whole problem is convergent. Then the problem can be solved by existing convex optimisation softwares such as CVX [GB]. Base on the stochastic optimisation introduced in [Nee10], problem (3.22) is equivalent to (3.8) and the original problem is solved. Finally, the proposed dynamic energy-aware power allocation (DEPA) algorithm for solving our stochastic optimisation problem (3.8) is obtained, which is shown in Algorithm 1.

Algorithm 1 DEPA Algorithm

if $t = 0$, **then**
  Intialise the perturbation vector $\boldsymbol{\theta}$. Observe the data queue length $Q_{ij}(t)$ and the energy queue length $E_j(t)$, $\forall i, j$.
else
  repeat
    Energy harvesting decision:
      BS j harvests energy when $E_j(t) \leq \theta_j$, $\forall j$.
    Power control decision:
    Obtain $(\mathbf{P}(t), \boldsymbol{\varepsilon}(t))$ by solving (3.22) using CVX.
    $t = t + 1$.
    Update the data queue length based on (3.4), $\forall i, j$.
    Update the energy queue length based on (3.6), $\forall j$.
  Until $t = t_{\text{end}}$.
end if

3.3.2 Performance Analysis

In this subsection, the performance of the proposed DEPA algorithm is analysed, to show some important properties. When the channel state of each node is independent and identically distributed (i.i.d.), the following theorem can be obtained by using DEPA algorithm.

Theorem 1. *a) The average data queue length is upper bounded as*

$$\lim_{T\to\infty} \sup \frac{1}{T} \sum_{t=0}^{T-1} \mathbb{E}\left[\sum_{j=1}^{M}\sum_{i=1}^{N_j} Q_{ij}(t)\right] \leq \frac{\widetilde{A} + VR_{\max}}{\xi} \tag{3.23}$$

with

$$\widetilde{A} = A + \sum_{j=1}^{M} \theta_j \left(P_{\max} + \varepsilon_{\max}^{(\text{out})}\right) + \left(e_{\max} + \varepsilon_{\max}^{(\text{in})}\right) \sum_{j=1}^{M} \left(\theta_j + \varepsilon_{\max}^{(\text{in})} + e_{\max}\right),$$

where $R_{\max} \geq \mathbb{E}\Big[\sum_{j=1}^{M}\sum_{i=1}^{N_j} R_{ij}(t)\Big]$, *and* ξ *is a positive finite value.*

b) Let $E_{\max}$ *represent BS's maximum battery capacity of storing energy, by setting*

the perturbation θ_j *as*

$$\theta_j = \theta = E_{\max} - \varepsilon_{\max}^{(\text{in})} - e_{\max}, \forall j, \tag{3.24}$$

the energy queue length is bounded by $0 \leq E_j(t) \leq E_{\max}, \forall t, j$.

Proof. a): Let the network achievable rates region Λ denote the set of traffic arrival rate that can be supported stably. Assuming that the average arrival rate is strictly interior to Λ, then, there exists a stationary randomised algorithm to achieve [Nee10]

$$\mathbb{E}\left[R_{ij}^{\text{ALT}}(t)\right] \geq \mathbb{E}\left[D_{ij}(t)\right] + \xi, \tag{3.25}$$

where $R_{ij}^{\text{ALT}}(t)$ is the data rate under this algorithm, $\mathbb{E}\left[D_{ij}(t)\right] + \xi \in \Lambda$, and ξ is a positive finite value. Note that (3.25) is commonly used for examining the network stability [Nee10], which indicates that each UE's average data rate is larger than its average traffic arrival rate. Since the aim of DEPA algorithm is to minimise the RHS of (3.12) under constraints C3-C5, I first have

$$\begin{aligned}
\Delta_V(t) \leq A &- \sum_{j=1}^{M}\sum_{i=1}^{N_j} Q_{ij}(t)\,\mathbb{E}\left[\left(R_{ij}^{\text{ALT}}(t) - D_{ij}(t)\right) \mid \mathbf{Z}(\mathbf{t})\right] \\
&+ \sum_{j=1}^{M}\left(E_j(t) - \theta_j\right)\mathbb{E}\Big[e_j^{\text{ALT}}(t) \mid \mathbf{Z}(t)\Big] \\
&- \sum_{j=1}^{M}\left(E_j(t) - \theta_j\right)\mathbb{E}\Big[P_j^{\text{ALT}}(t) + \sum_{j'=1,j'\neq j}^{M}\varepsilon_{jj'}^{\text{ALT}}(t) \mid \mathbf{Z}(t)\Big] \\
&+ \sum_{j=1}^{M}\left(E_j(t) - \theta_j\right)\mathbb{E}\Big[\sum_{j'=1,j'\neq j}^{M}\beta\varepsilon_{j'j}^{\text{ALT}}(t) \mid \mathbf{Z}(t)\Big] \\
&- V\mathbb{E}\Big[\sum_{j=1}^{M}\sum_{i=1}^{N_j} R_{ij}^{\text{ALT}}(t) \mid \mathbf{Z}(t)\Big],
\end{aligned} \tag{3.26}$$

where $\mathbf{R}^{\text{ALT}}(t), \mathbf{J}^{\text{ALT}}(t), \mathbf{e}^{\text{ALT}}(t), \mathbf{P}^{\text{ALT}}(t), \boldsymbol{\varepsilon}^{\text{ALT}}(t)$ represent the control decisions under the alternative algorithm satisfying (3.25). In light of boundedness of parameters and

(3.25), $\Delta_V(t)$ satisfies

$$\Delta_V(t) \leq A - \xi \sum_{j=1}^{M}\sum_{i=1}^{N_j} Q_{ij}(t) + \left(e_{\max} + \varepsilon_{\max}^{(\text{in})}\right)\sum_{j=1}^{M} E_j(t) + \sum_{j=1}^{M}\theta_j\left(P_{\max} + \varepsilon_{\max}^{(\text{out})}\right) - V\mathbb{E}\Big[\sum_{j=1}^{M}\sum_{i=1}^{N_j} R_{ij}^{\text{ALT}}(t) \mid \mathbf{Z}(t)\Big]. \tag{3.27}$$

By taking expectations over $\mathbf{Z}(t)$ and using telescoping sums over $t = 0, \ldots, T-1$ with respect to (3.27), I have

$$\begin{aligned}
&\mathbb{E}\left[L(T) - L(0)\right] - V\sum_{t=0}^{T-1}\mathbb{E}\Big[\sum_{j=1}^{M}\sum_{i=1}^{N_j} R_{ij}(t)\Big] \\
&\leq T\Big(A + \sum_{j=1}^{M}\theta_j\left(P_{\max} + \varepsilon_{\max}^{(\text{out})}\right)\Big) - \xi\sum_{t=0}^{T-1}\mathbb{E}\Big[\sum_{j=1}^{M}\sum_{i=1}^{N_j} Q_{ij}(t)\Big] \\
&+ \left(e_{\max} + \varepsilon_{\max}^{(\text{in})}\right) \times \sum_{t=0}^{T-1}\mathbb{E}\Big[\sum_{j=1}^{M} E_j(t)\Big] - V\sum_{t=0}^{T-1}\mathbb{E}\Big[\sum_{j=1}^{M}\sum_{i=1}^{N_j} R_{ij}^{\text{ALT}}(t)\Big].
\end{aligned} \tag{3.28}$$

Based on the energy harvesting decision of the DEPA algorithm, BS j will not harvest renewable energy at time t, if $E_j(t) > \theta_j$. In this case, BS j may still seek to receive the transferred energy from other BSs, but the transferred energy will be completely consumed for increasing data rate at this time slot, to minimise the upper bound of the drift-plus-penalty. As such, $E_j(t) \leq \theta_j + \varepsilon_{\max}^{(\text{in})} + e_{\max}, \forall t, j$. Therefore, by considering (3.28) and $\mathbb{E}\left[L(t)\right] > 0$, I can further obtain

$$\begin{aligned}
\xi\sum_{t=0}^{T-1}\mathbb{E}\Big[\sum_{j=1}^{M}\sum_{i=1}^{N_j} Q_{ij}(t)\Big] \leq T\Big(A + \sum_{j=1}^{M}\theta_j\left(P_{\max} + \varepsilon_{\max}^{(\text{out})}\right)\Big) + \mathbb{E}\left[L(0)\right] + \\
\left(e_{\max} + \varepsilon_{\max}^{(\text{in})}\right)\sum_{t=0}^{T-1}\mathbb{E}\Big[\sum_{j=1}^{M} E_j(t)\Big] + V\sum_{t=0}^{T-1}\mathbb{E}\Big[\sum_{j=1}^{M}\sum_{i=1}^{N_j} R_{ij}(t)\Big].
\end{aligned} \tag{3.29}$$

By dividing both sides by ξT and taking a limit as $T \to \infty$, I obtain (3.23) and complete the proof.

b): Since $E_j(0) \geq 0$ at the beginning time, according to (3.5) and (3.6), I have $E_j(t+1) \geq e_j(t) \geq 0, \forall j$. Hence $E_j(t) \geq 0, \forall t, j$. From (a), I note that $E_j(t) \leq \theta_j + \varepsilon_{\max}^{(\text{in})} + e_{\max}, \forall t, j$, thus $E_j(t) \leq E_{\max}, \forall t, j$. This completes the proof.

□

From Theorem 1, it is shown that the proposed DEPA algorithm satisfies the network stability, and prevents the renewable energy overflow by selecting appropriate value of θ_j under BS's battery constraint.

3.4 Simulation Platform and Results

In this section, numerical results are presented to demonstrate the performance of the proposed DEPA algorithm in subsection 3.3.1. Also comparisons by considering the cases with/without energy cooperation are given. For the case without energy cooperation, each power control decision in the DEPA algorithm is obtained by using CVX [GB] to solve problem (3.22) with $\varepsilon_{jj'} = 0, \forall j, j^{'}$. Our theoretical analysis is independent of the specific spatial distributions of BSs and UEs. In the simulation, It is assumed that each UE's data arrival rate follows an independent homogeneous poisson point process $\mathscr{P}$ with the same mean value λ as $\lambda = 0.5$ bits/slot/Hz for the sake of simplicity. Note that our model and proposed algorithm are also applied to the scenario with heterogeneous data arrival rate distributions. The energy harvesting process E_j at BS j is modeled as a uniformly stochastic process with the probability density function $f_j(z_j) = 1/(b_j - a_j), \forall z_j \in [a_j, b_j]$ where a_j and b_j is the minimum and maximum harvested energy of BS j respectively [ZPSY13a]. The system-level channel model and basic parameters are illustrated in Table 3-A, and the number of BSs, energy transfer efficiency, and the selected perturbation will be detailed in the following simulation results. In addition, the Monte Carlo simulation for $T = 5000$ time slots is ran in the Matlab software environment.

Table 3-A: Simulation Parameters

Parameter	**Value**
BS layout	Hexagonally arranged cell sites
UE layout	Uniformly located in area with 3 active UEs per BS cell
Inter site distance	200 m
Log-normal shadowing fading	10 dB
Bandwidth B	1 GHz
Carrier frequency of mmWave small cell	28 GHz
Path loss of mmWave BS	$\alpha + 10\eta \log_{10} d(m) + \xi$ $\xi \sim \mathcal{N}(0, \sigma^2)$, LOS :$\alpha = 61.4, \eta = 2$, $\sigma = 5.8$ dB; NLOS :$\alpha = 72.0$, $\eta = 2.92, \sigma = 8.7$ dB [ALS+14]
Probability of Outage(O)-LOS-NLOS in mmWave small cell	O: $P_{\mathrm{o}}(d) = \max\{0, 1 - e^{-\frac{d}{30}+5.2}\}$; LOS: $p_{\mathrm{L}}(d) = (1 - P_{\mathrm{o}}(d))e^{-\frac{d}{67.1}}$; NLOS: $1 - P_{\mathrm{o}}(d) - p_{\mathrm{L}}(d)$ [ALS+14]
Thermal noise power σ_o^2	-174 dBm/Hz+10 $\log_{10}$ (B) +noise figure of 7 dB
Maximum transmit power of BS $P_{\max}$	40 dBm
Antenna gain of BS G_b	18 dB
Antenna gain of UE G_u	0 dB
Min harvested power a_j	$[0, 20]$ dBm
Max harvested power b_j	$[20, 40]$ dBm

Figure 3.2 shows the average network throughput and energy queue versus V values. Here, utility in the figure represents the throughput of the network. V is used in (3.11) which represents the relative importance of minimising the energy and data queue length to a lower level and maximising the sum rate of the whole network. The number of BSs is 7, $\beta = 0.9$, and $\theta = V$. It can be observed that both the average network throughput and the average energy queue length increase with V. By using the proposed DEPA algorithm, the average network throughput quickly approaches an optimal value. For the same V, the average network throughput under energy cooperation is much better than that without energy cooperation. More importantly, using energy cooperation, the amount of energy in the queue is much lower, which indicates that energy cooperation has the ability to relieve the demand for large battery capacity at the BSs. The reason is that without energy cooperation, each BS has to store more its harvested energy and

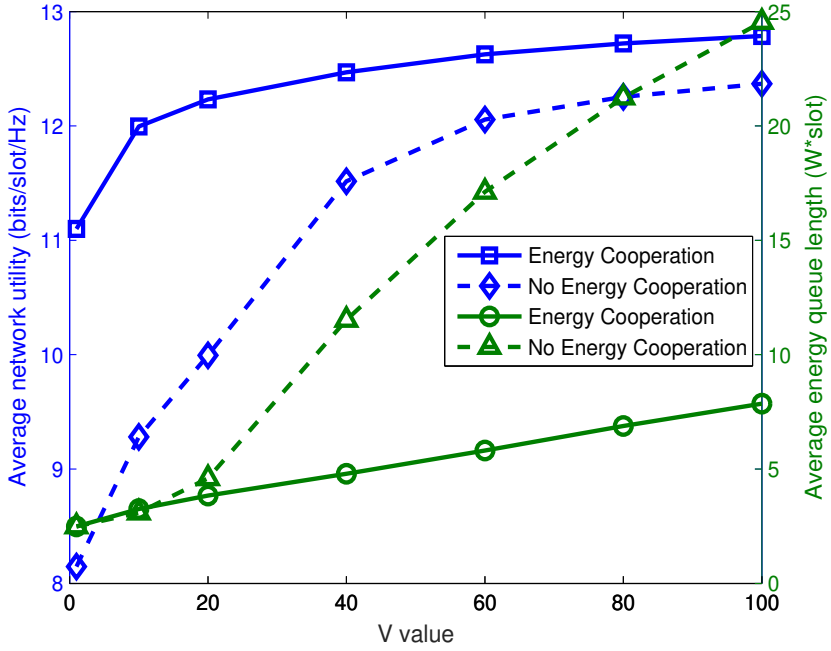

Figure 3.2: Average network data rate and energy queue length versus V value.

use it during the time slots when the harvested energy is insufficient, on the contrary, energy cooperation allows that BS can borrow energy from BSs with extra harvested energy at each time slot and BSs do not need to store large amount of harvested energy for supporting following transmissions.

Figure 3.3 shows the average data queue length versus V values. The number of BSs is 7, and $\theta = V$. It can be seen that when V is not large($V < 60$ in this figure), the size of average data queue under energy cooperation is much lower than that without energy cooperation, which indicates that the use of energy cooperation has the advantage of reducing delay. When V grows large, the average data queue length without energy cooperation is close to that under energy cooperation. The reason is that as shown in Figure 3.2, the average network throughput increases with V, which decreases the amount of waiting data. It is noted that in order to reduce the delay, large V is needed for no energy cooperation case, which results in the requirement of large battery capacity at BSs as seen in Figure 3.2. Meanwhile, when the energy transfer efficiency β is larger,

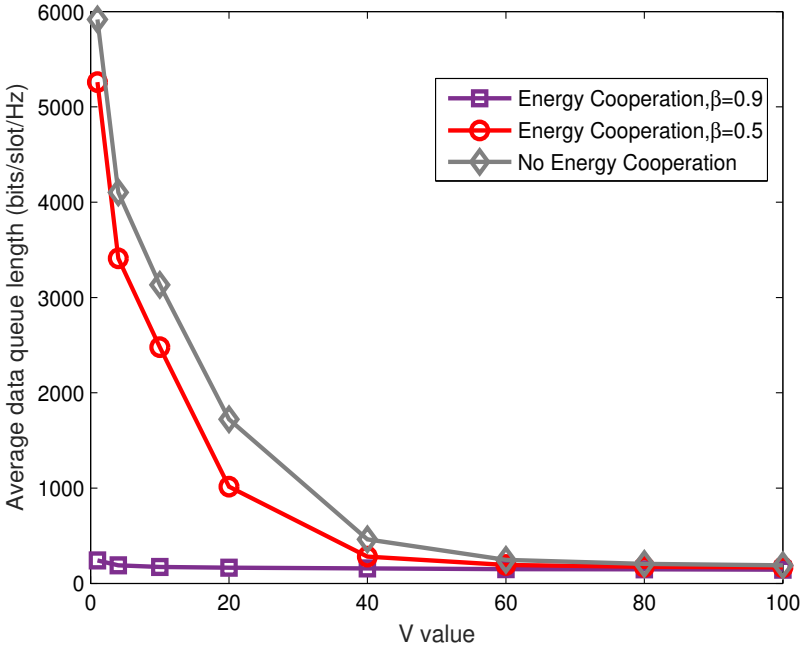

Figure 3.3: Average data queue length versus V value.

the average data queue of BSs is shorter, which means less data is blocked.

Figure 3.4 displays the average network throughput and energy queue length versus BS number. I choose $V = 100$, $\beta = 0.9$, and $\theta = 20$. It is observed that the average network throughput increases with the BS number. The throughput gap between with/without energy cooperation is expanded with increasing BS number. That's because when more BSs are deployed, more energy can be shared between BSs, which can support higher throughput and reduce the demand for large battery capacity. Meanwhile, as mentioned in Figure 3.2, the average energy queue length of the network with energy cooperation is lower than the network without energy cooperation.

Figure 3.5 illustrates the average data queue length versus the BS number with $V = 100$ and $\theta = 20$. It can be seen that the average data queue length increases with the BS number, due to more user services being provided. When adding more BSs, the length of the average data queue with energy cooperation increases much more slowly than the data queue without energy cooperation. This can be explained by the fact that

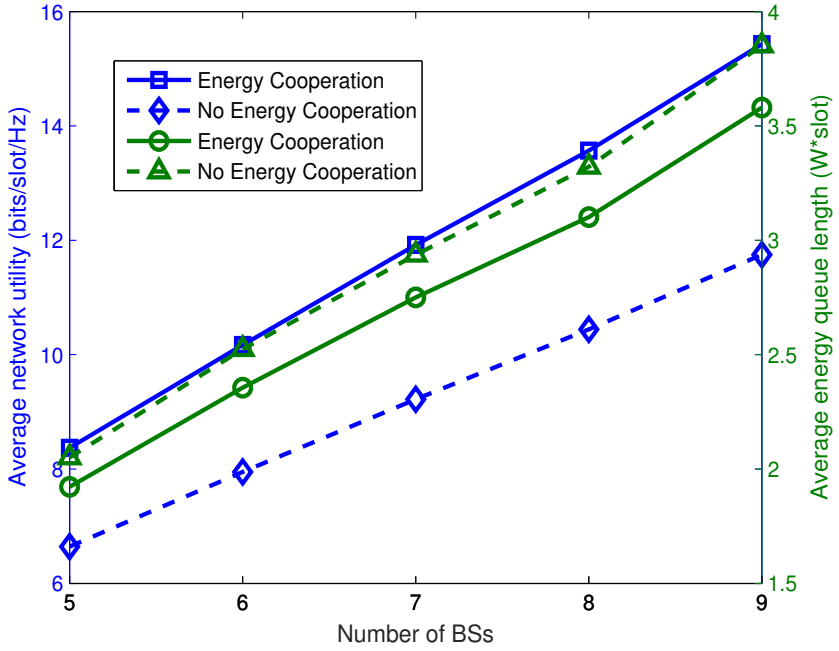

Figure 3.4: Average network throughput and energy queue length versus the number of BSs.

when the BS number is larger, under the same data traffic arrival rate, the increase of the network throughput with energy cooperation is much greater than the case of no energy cooperation, which in turn substantially reduce the growth rate of data queue length.

3.5 Summary

In this chapter, power control in energy cooperation enabled downlink mmWave cellular networks with renewable energy is studied. A stochastic optimisation problem is formulated, to maximise the time average network throughput and control the sizes of data queue and energy queue. Based on Lyapunov optimisation, an online algorithm called DEPA is developed to solved the formulated problem. It is confirmed that the proposed algorithm can ensure the stability of networks and prevent renewable energy overflow by selecting an appropriate value of perturbation used in the Lyapunov function. The

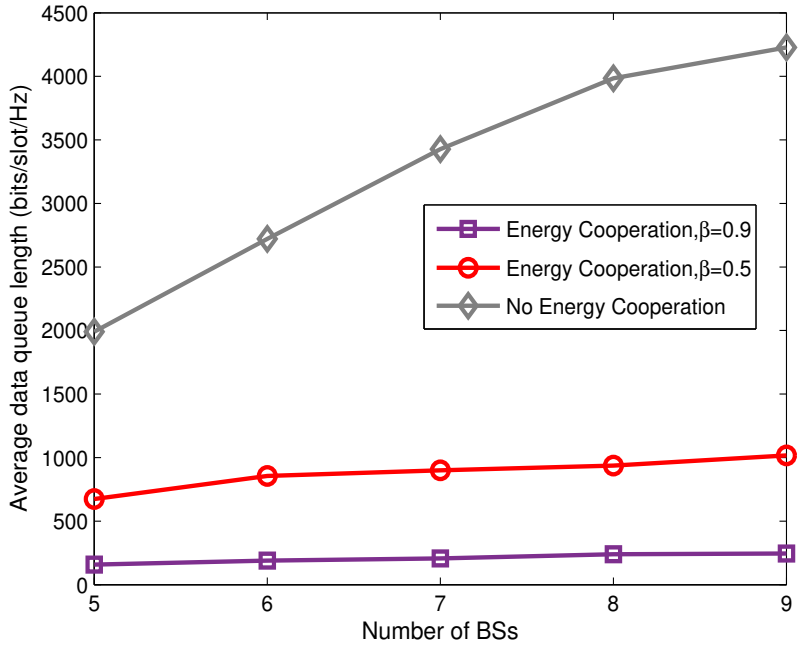

Figure 3.5: Average data queue length versus the number of BSs.

results show that compared with the system without energy cooperation, the proposed algorithm with energy cooperation can maximise the network throughput while keeping the data and energy queue lengths at a low level.

Chapter 4

Resource Allocation in Energy Cooperation Enabled HetNets

4.1 Overview

First, in this chapter, user association is formulated as an optimisation problem, aiming at maximising the number of accepted users by taking advantage of energy cooperation while minimising the energy transfer loss between base stations (BSs). An energy efficient user association algorithm is proposed based on the primal-dual interior point method. Simulation results show that the proposed algorithm can greatly increase the energy efficiency and the number of accepted users of the whole network. Then, power control in energy cooperation enabled heterogeneous networks (HetNets) is considered. Transmit power, grid energy consumption, and transferred energy are optimised for maximising the energy efficiency of the whole network. An energy efficient algorithm is proposed, in which the optimal resource allocation policy is obtained by using the lagrangian duality method. Simulation results demonstrate that energy efficiency is substantially improved by using the proposed power control algorithm with energy cooperation, compared with the cases where either power control or energy cooperation are considered.

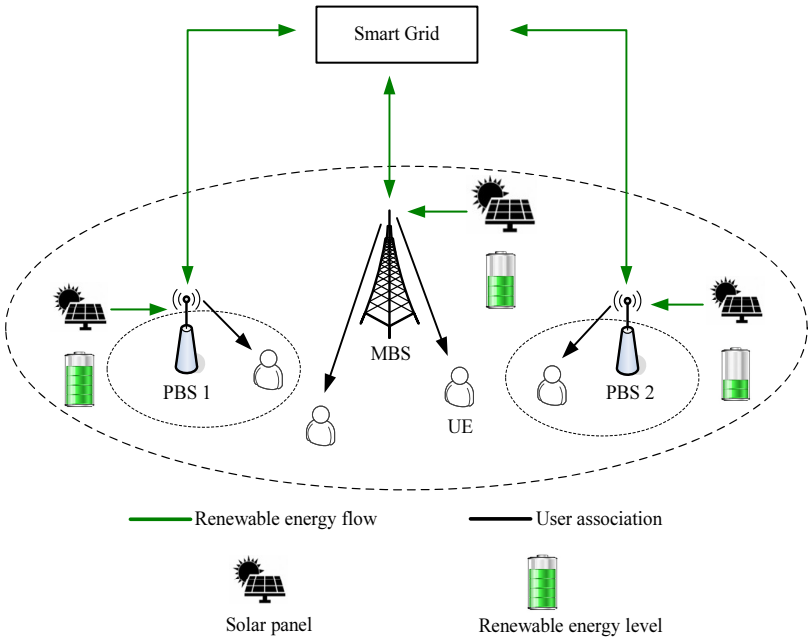

Figure 4.1: An illustration of an energy cooperation enabled two-tier HetNet with renewable energy sources.

4.2 System Model

As shown in Figure 4.1, a two-tier downlink HetNet consisting of K macrocell geographical areas is considered, where BSs can share the harvested renewable energy via smart grid. In each macrocell geographical area, there is one macro BS (MBS), denoted as BS_0^k, and M pico BSs (PBSs) denoted as BS_m^k, $m \in \{1, 2, ..., M\}$, $k \in \{1, 2, ..., K\}$. All BSs are assumed to share the same frequency band and each BS is solely powered by renewable energy sources. Different tiers are allowed to have different energy harvesting processes. There are N UEs denoted as UE_n^k ($n \in \{1, 2, ..., N\}$) in each macrocell geographical area. Each UE can only be associated with one BS for service at each time slot. It is assumed that all BSs have full buffers, and their transmit powers change slowly, so that the BS's transmit power is unaltered over one association time scale as mentioned in [YRC+13].

4.2.1 Energy Model

4.2.1.1 Renewable Energy

The harvested energy for BS_m^k is formulated as a uniform stochastic process E_m^k [ZPSY13a]. The rate of the renewable energy generation is assumed to be constant within each time slot and may change from one time slot to another [RCZ18].

4.2.1.2 Energy Cooperation

It is assumed that energy cooperation can only be implemented in the same macrocell geographical area. The energy transferred from BS_m^k to $BS_{m'}^k$ is denoted by $\mathcal{E}_{mm'}^k$. The energy transfer efficiency factor between two BSs is β $(0 < \beta < 1)$, which specifies how efficiently the harvested energy can be transferred. The energy transfer loss is $(1-\beta)\mathcal{E}_{mm'}^k$ and hence the higher β, the lower energy loss during the energy transfer process.

4.2.2 Downlink Transmission Model

The user association matrix $\mathbf{Y} = [y_{mn}^k]$ is defined as

$$y_{mn}^k = \begin{cases} 1, \text{ if } UE_n^k \text{ is associated with } BS_m^k \\ 0, \text{ otherwise} \end{cases} \tag{4.1}$$

If UE_n^k is associated with BS_m^k, the signal-to-interference-plus-noise ratio (SINR) is written as [LCC+15]

$$\gamma_{mn}^k = \frac{P_m^k h_{k,n}^{k,m}}{\sum\limits_{\substack{k'=1,\\ k'\neq k}}^{K} \sum\limits_{m'=0}^{M} P_{m'}^{k'} h_{k,n}^{k',m'} + \sum\limits_{\substack{m'=0,\\ m'\neq m}}^{M} P_{m'}^{k} h_{k,n}^{k,m'} + \sigma^2}, \tag{4.2}$$

where P_m^k is the transmit power of BS_m^k, $h_{k,n}^{k,m}$ is the average channel power gain between

UE_n^k and BS_m^k including pathloss and shadowing, and σ^2 is the noise power. Transmit power P_m^k should equal to or be lower than the maximum transmit power $P_{m,max}$. Note that the fast fading is averaged out in (4.2), since user association is carried out in a large time scale, and the low mobility environment is considered. The channel is regarded as static and the SINR is average over the association time [LCC+15].

To ensure that UEs can be served under the expected traffic amount, the required spectrum resource for UE_n^k when associated with BS_m^k is given by

$$\chi_{mn}^k = \frac{\tau_n^k}{\log(1+\gamma_{mn}^k)}, \tag{4.3}$$

where τ_n^k is the required data rate of UE_n^k. Accordingly, the normalised required spectrum resource ρ_m^k of BS_m^k is

$$\rho_m^k = \sum_{n=1}^{N} y_{mn}^k . \frac{\chi_{mn}^k}{\chi_{m,\max}^k}, \tag{4.4}$$

where $\chi_{m,\max}^k$ is the total bandwidth of BS_m^k.

4.2.3 Energy Consumption Model

Two types of energy consumptions at each BS are considered, namely static and adaptive. The adaptive energy consumption is dependent on the dynamic transmit power of BS, which is typically linear to the BS's load. Hence the linearly approximated BS energy consumption model is adopted [LCC+15, AGD+11], and the total energy consumption of BS_m^k can be expressed as[1]

$$\mathcal{J}_m^k = \Delta_m^k P_m^k \rho_m^k + \mathcal{J}_{m,\text{static}}^k, \tag{4.5}$$

where Δ_m^k is the slope of load-dependent energy consumption of BS_m^k, and $\mathcal{J}_{m,\text{static}}^k$ is the static energy consumption of BS_m^k consumed by the circuit and cooling systems.

[1]In this chapter, time is measured in unite size "slot", for simplicity, the multiplication by 1 slot is omitted when converting between power and energy.

4.2.4 Problem Formulation

The user association problem of our design is to determine the user association matrix $\mathbf{Y}$ and the energy transferred between BSs $\mathcal{E}^k_{mm'}$. The objective function expresses the goal of maximising the number of accepted UEs while minimising the energy loss during the energy transfer process, and is given by

$$\textbf{P1:} \quad \max_{\mathbf{Y},\mathcal{E}} \sum_{k=1}^{K}\sum_{m=0}^{M}\sum_{n=1}^{N} y^k_{mn} - \alpha \sum_{k=1}^{K}\sum_{m=0}^{M}\sum_{m'=0}^{M} (1-\beta)\mathcal{E}^k_{mm'}, \tag{4.6}$$

s.t.

$$\text{C1}: \mathcal{J}^k_m + \sum_{m'=0}^{M} \mathcal{E}^k_{mm'} - \beta \sum_{m'=0}^{M} \mathcal{E}^k_{m'm} \leq E^k_m, \ \forall m, k,$$

$$\text{C2}: \sum_{n=1}^{N} \chi^k_{mn} y^k_{mn} \leq \chi^k_{m,\max}, \ \forall k, m,$$

$$\text{C3}: \sum_{m=0}^{M} y^k_{mn} \leq 1, \ \forall k, n,$$

$$\text{C4}: y^k_{mn} \in \{0, 1\}, \ \forall k, m, n,$$

where α specifies the relative importance between the number of accepted UEs and the transferred energy loss. Here, $\alpha = 0$ represents that there is no concern about the transferred energy loss, and $\alpha > 0$ means that the transferred energy loss is controlled and energy cooperation will not operate when the transferred energy efficiency is low. Constraint C1 ensures that the total energy consumed by each BS should not exceed the total power supply including the harvested energy and the transferred energy. Constraint C2 indicates that the number of UEs associated with one BS is restricted by the total bandwidth of this BS. Finally, constraints C3 and C4 ensure that one UE can only be associated with one BS at any time.

4.3 Proposed User Association Method

The optimisation problem **P1** is a mixed integer linear programming (MILP) problem, which is a non-deterministic polynomial (NP)-hard problem. To solve it, the user association indicator y_{mn}^k is relaxed and the original problem is transformed to a convex problem. Then, an efficient user association algorithm is proposed based on the primal-dual interior point method. In addition, a predictor-corrector approach is used for computational efficiency.

4.3.1 Primal-Dual Interior Point Method

First $y_{mn}^k \in \{0,1\}$ is relaxed to $0 \leq y_{mn}^k \leq 1$ which represents the probability of the association between UE_n^k and BS_m^k. The linearised problem corresponding to one macrocell geographical area in Section 4.2.4 can be written as

$$\textbf{P1-a:} \max_{y,\mathcal{E}} \quad G_1^T y - \alpha(1-\beta) G_2^T \mathcal{E} \tag{4.7}$$

s.t.

$$\begin{aligned} \text{C1} - \text{a} &: G_3^T y + \mathcal{J}_{\text{static}} + G_4^T \mathcal{E} - \beta G_5^T \mathcal{E} + d = E, \\ \text{C2} - \text{a} &: G_6^T y + b = \chi_{\max}, \\ \text{C3} - \text{a} &: G_7^T y + a = e_1, \\ \text{C4} - \text{a} &: y + s = e_2, \\ \text{C5} - \text{a} &: y, \mathcal{E}, s, a, b, d \geq 0, \end{aligned}$$

where y, G_1, $s \in \mathcal{R}^{(M+1)N \times 1}$; $\mathcal{E}, G_2 \in \mathcal{R}^{(M+1)(M+1)\times 1}$; $\mathcal{J}_{\text{static}}$, E, $\chi_{\max}$, d, $b \in \mathcal{R}^{(M+1)\times 1}$; G_4, $G_5 \in \mathcal{R}^{(M+1)(M+1)\times(M+1)}$; G_3, $G_6 \in \mathcal{R}^{(M+1)N\times(M+1)}$; $a \in \mathcal{R}^{N\times 1}$; $G_7 \in \mathcal{R}^{(M+1)N\times N}$, and e_1, e_2 are vectors of all ones. Vectors G_1, G_2, G_6 and G_7 in P1-a, C2-a, C3-a, C4-a can be obtained from the objective function of **P1**, C2, C3, and C4, respectively. Substituting (4.4) and (4.5) into constraint C1, G_3, G_4, and C_5 can be obtained in

constraint C1.

Based on (4.7), the Lagrangian function can be written as

$$\begin{aligned} &L(y,\mathcal{E},s,a,b,d,\lambda_1,\lambda_2,\lambda_3,\lambda_4) = G_1^T y - \alpha(1-\beta)G_2^T\mathcal{E} + \\ &\lambda_1^T(G_3^T y + \mathcal{J}_{\text{static}} + G_4^T\mathcal{E} - \beta G_5^T\mathcal{E} + d - E) + \lambda_2^T \times \\ &(G_6^T y + b - \chi_{\max}) + \lambda_3^T(G_7^T y + a - e_1) + \lambda_4^T(y + s - e_2), \end{aligned} \tag{4.8}$$

where $\lambda_1, \lambda_2, \lambda_3, \lambda_4$ are Lagrange multipliers. With the help of (4.8), the dual problem of the primal problem (4.7) is derived as

$$\text{P2}: \min_{\lambda_1,\lambda_2,\lambda_3,\lambda_4} \quad (E - \mathcal{J}_{\text{static}})^T\lambda_1 + \chi_{\max}^T\lambda_2 + e_1^T\lambda_3 + e_2^T\lambda_4, \tag{4.9}$$

s.t.

$$\text{C1} - \text{b}: G_3\lambda_1 + G_6\lambda_2 + G_7\lambda_3 + \lambda_4 - w = G_1,$$

$$\text{C2} - \text{b}: G_4\lambda_1 - \beta G_5\lambda_1 - u = -\alpha(1-\beta)G_2,$$

$$\text{C3} - \text{b}: \lambda_1, \lambda_2, \lambda_3, \lambda_4, w, u \geq 0,$$

where $w \in R^{(M+1)N\times 1}$ and $u \in R^{(M+1)(M+1)\times 1}$. After obtaining the constraints of dual problem (4.9), the logarithmic barrier function can be defined by considering the objective function of the primal problem (4.7) and introducing the logarithmic penalty term, which is written as

$$\begin{aligned} B(y,\mathcal{E},s,a,b,d,\phi) &= G_1^T y - G_2^T\alpha(1-\beta)\mathcal{E} \\ &- \phi\sum_{i=1}^{(M+1)N}\ln y_i - \phi\sum_{i=1}^{(M+1)(M+1)}\ln\mathcal{E}_i - \phi\sum_{i=1}^{(M+1)N}\ln s_i \\ &- \phi\sum_{i=1}^{N}\ln a_i - \phi\sum_{i=1}^{M+1}\ln b_i - \phi\sum_{i=1}^{M+1}\ln d_i, \end{aligned} \tag{4.10}$$

where $\phi > 0$ is the barrier parameter. When ϕ approaches to zero, the solution of maximising the logarithmic barrier function (4.10) converges to the optimal solution of the primal problem (4.7) [Van14]. Hence first the Karush-Kuhn-Tucker (KKT) optimality

conditions need to be derived for (4.10) as

$$\begin{aligned}
&G_3^T y + \mathcal{J}_{\text{static}} + G_4^T \mathcal{E} - \beta G_5^T \mathcal{E} + d = E, \\
&G_6^T y + b = \chi_{\max}, \quad G_7^T y + a = e_1, \quad y + s = e_2, \\
&G_3 \lambda_1 + G_6 \lambda_2 + G_7 \lambda_3 + \lambda_4 - w = G_1, \\
&G_4 \lambda_1 - \beta G_5 \lambda_1 - u = -\alpha(1-\beta) G_2, \\
&WYe_3 = \phi e_3, \quad U\Omega e_4 = \phi e_4, \quad \Lambda_4 S e_3 = \phi e_3, \\
&\Lambda_1 D e_5 = \phi e_5, \quad \Lambda_2 B e_5 = \phi e_5, \quad \Lambda_3 A e_6 = \phi e_6,
\end{aligned} \tag{4.11}$$

where $W, Y, U, \Omega, S, D, B, A, \Lambda_1, \Lambda_2, \Lambda_3, \Lambda_4$ denote the diagonal matrix whose diagonal entries are the components of $w, y, u, \mathcal{E}, s, d, b, a, \lambda_1, \lambda_2, \lambda_3, \lambda_4$, and, e_3, e_4, e_5, e_6 are vectors of all ones. In (4.11), the first six equations are linear primal and dual feasibility constraints of the optimal solutions. The rest of equations are non-linear, which depend on the barrier parameter ϕ. Specifically, when $\phi = 0$, they become the usual complementarity constraints that need to be satisfied for optimality.

Based on KKT conditions in (4.11), the Newton's direction Δ can be obtained by solving the system of linear equations, which is

$$\mathrm{Q}\Delta = \begin{bmatrix}
-G_3^T y - \mathcal{J}_{\text{static}} - G_4^T \mathcal{E} + \beta G_5^T \mathcal{E} - d + E \\
-G_6^T y - b + \chi_{\max} \\
-G_7^T y - a + e_1 \\
-y - s + e_2 \\
G_1 + w - G_3 \lambda_1 - G_6 \lambda_2 - G_7 \lambda_3 - \lambda_4 \\
u - \alpha(1-\beta) G_2 - G_4 \lambda_1 + \beta G_5 \lambda_1 \\
\Theta
\end{bmatrix}, \tag{4.12}$$

where the Jacobian matrix Q can be obtained from (4.11), accordingly. In (4.12), $\Delta = (\Delta y, \Delta \mathcal{E}, \Delta s, \Delta a, \Delta b, \Delta d, \Delta \lambda_1, \Delta \lambda_2, \Delta \lambda_3, \Delta \lambda_4, \Delta w, \Delta u)^T$ and $\Theta = (\phi e_3 - WYe_3, \phi e_4 - U\Omega e_4, \phi e_3 - \Lambda_4 S e_3, \phi e_5 - \Lambda_1 D e_5, \phi e_5 - \Lambda_2 B e_5, \phi e_6 - \Lambda_3 A e_6)^T$.

The barrier parameter ϕ depends on the solution $(w, y, u, \mathcal{E}, s, d, b, a, \lambda_1, \lambda_2, \lambda_3, \lambda_4)$ in

each iteration and a desired reduction parameter δ, which is calculated as [Van14]

$$\phi = \delta \frac{w^T y + u^T \mathcal{E} + \lambda_4^T s + \lambda_1^T d + \lambda_2^T b + \lambda_3^T a}{2(M+1)N + (M+1)^2 + 2(M+1) + N}, \tag{4.13}$$

where $0 < \delta < 1$.

4.3.2 Predictor-Corrector Technique

In order to reduce the number of iterations, The Mehrotra's second order predictor-corrector technique is used to simplify the calculation of Newton's direction, and the efficiency of it has been proved [Ter13]. The predictor-corrector technique divides the Newton's direction into two parts:

$$\Delta = \Delta_1 + \Delta_2, \tag{4.14}$$

where Δ_1 is the affine-scaling component and Δ_2 is the centering component. Direction Δ_1 is the solution of (4.12) with $\phi = 0$, and Δ_2 is obtained by solving the following equation:

$$Q\Delta_2 = (0, 0, 0, 0, 0, 0, \Theta^T)^T. \tag{4.15}$$

4.3.3 User Association Algorithm

In this subsection, a user association algorithm with energy cooperation is proposed based on the previous analysis in Section 4.3.1 and 4.3.2, which is detailed in Algorithm 2. In this design, barrier parameter ϕ is updated based on the primal and dual parameters in each iteration. Moreover, a max-probability association approach is presented that each UE is only associated with the BS who has the largest association probability y. It can achieve a pseudo optimal solution which is located at the boundary of the feasible

Algorithm 2 Proposed User Association Algorithm

1: **if** $t = 0$, **then**
2: Initialise $y(t)$, $\mathcal{E}(t)$, $s(t)$, $a(t)$, $b(t)$, $d(t)$, $\lambda_1(t)$, $\lambda_2(t)$, $\lambda_3(t)$, $\lambda_4(t)$, $w(t)$, $u(t)$, which are feasible for both the primal problem and the dual.
3: Calculate the barrier parameter $\phi(t)$ according to (4.13).
4: **else**
5: Calculate the Newton's direction based on (4.14).
6: Update $y(t+1)$ via $y(t+1) = y(t) + \eta\Delta y$, where η is chosen so that the non-negativity of y is maintained, and update $\mathcal{E}(t+1)$, $s(t+1)$, $a(t+1)$, $b(t+1)$, $d(t+1)$, $\lambda_1(t+1)$, $\lambda_2(t+1)$, $\lambda_3(t+1)$, $\lambda_4(t+1)$, $w(t+1)$, $u(t+1)$ in the same way.
7: **if** convergence
8: Set the maximum value of association probability y_{mn}^k to 1, and then transmit it to the corresponding BS.
9: **else**
10: Update $\phi(t)$ via (4.13).
11: $t \leftarrow t + 1$.
12: **end if**
13: **for** $i = 1 : \text{length}(y(t))$
14: **if** $y(t)(i) \geq 0.5$
15: $y(t)(i) = 1$
16: **else**
17: $y(t)(i) = 0$
18: **end**
19: **end if**

region of the global optimal solution. Note that the proposed algorithm is applied to solve the relaxed problem 4.7, which is not the same as solving the original primal combinatorial problem **P1**. Nevertheless, the relaxation of the original problem is a commonly-used approach to solve **P1** [LCC+15]. After relaxation, the value of user association indicators are converted back to value 1 or 0 as step 13-18 in Algorithm 2. In the following simulation results of Section 4.4, the effectiveness of the proposed algorithm will be further illustrated.

4.4 Simulation Results

In our simulations, PBSs and UEs are generated randomly following uniform distributions. The energy harvesting process E_m^k at BS_m^k is modeled as a stationary stochastic process with pdf $f_m^k(z_m^k) = 1/(H_m^k - L_m^k), \forall z_m^k \in [L_m^k, H_m^k]$ where L_m^k and H_m^k are the minimum and maximum harvested energy respectively, as suggested in [ZPSY13a]. Note that our analysis and proposed algorithm are independent of the specific renewable energy distribution. The path loss between MBS and UE, PBS and UE is $128.1 + 37.6\log_{10}D(\text{km})$, and $140.7 + 36.7\log_{10}D(\text{km})$, respectively where $D(\text{km})$ is the distance between the UE and BS in kilometers. The basic simulation parameters are shown in Table 4-A.

Table 4-A: Simulation Parameters

Parameter	**Value**
Inter site distance	500m
Number of MBSs K	7
Static power consumption of MBS $\mathcal{J}_{0,\text{static}}^k$	780W
Number of PBSs per macro M	3
Static power consumption of PBS $\mathcal{J}_{m,\text{static}}^k$	13.6W
load-dependent cost slope of MBS Δ_0^k	4.7
Bandwidth $\chi_{m,\max}^k$	20 MHz
load-dependent cost slope of PBS Δ_m^k	4.0
Noise power density σ^2	-174 dBm/Hz
Max MBS harvested energy H_0^k	1600 W
MBS max transmit power $P_{0,\max}$	46 dBm
Max PBS harvested energy H_m^k	120 W
PBS max transmit power $P_{m,\max}$	30 dBm
Min MBS harvested energy L_0^k	350 W
Min PBS harvested energy L_m^k	20 W

The proposed user association algorithm with and without energy cooperation is simulated and evaluate the performance by two matrices. The first is the energy efficiency of the whole system calculated as $\text{EE} = \frac{\text{accepted UE number}}{\text{energy consumption}}\tau$ where τ is the required data rate of each UE. The second performance matrix is the ratio of the accepted UEs.

Figure 4.2 shows the energy efficiency versus energy transfer efficiency for different numbers of UEs. The number of PBSs in each macro cell is set as 3, the required data

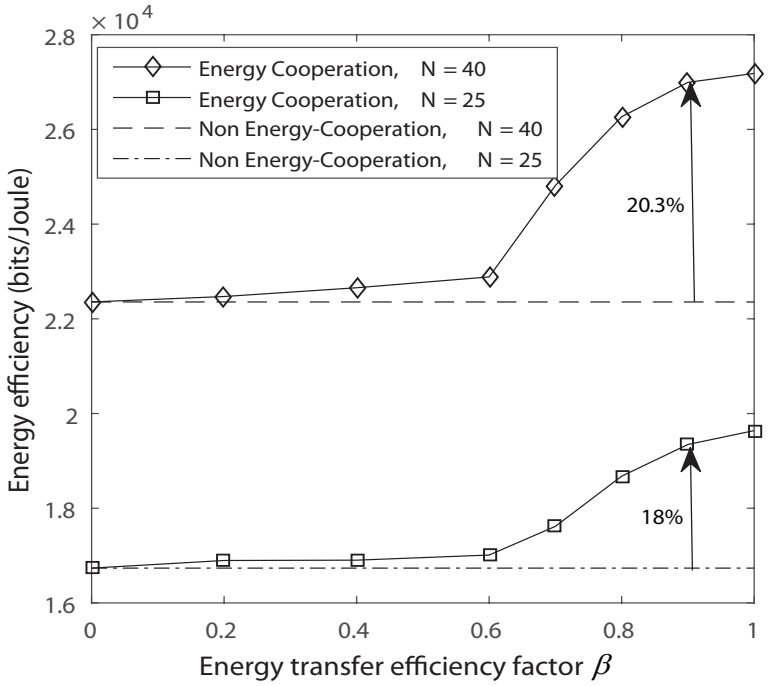

Figure 4.2: Energy efficiency versus energy transfer efficiency for different requested numbers of UEs N with/without energy cooperation.

rate for each UE is $\tau = 8 \times 10^5$ bits/s, and $\alpha = 0.3$. It is observed that when the energy transfer efficiency is low, the function of energy cooperation is limited, due to large energy loss. When the energy transfer efficiency improves beyond a critical value (0.6 in this figure), energy efficiency increases significantly by using the proposed user association algorithm with energy cooperation. Moreover, the performance gap between energy cooperation and non energy cooperation is expanded when there are more requested UEs. The reason is that under energy cooperation, more renewable energy is transferred between BSs to support more load of BSs, in contrast to the non energy cooperation case. Meanwhile, when there are more UEs in the network, energy efficiency is higher due to the multiuser diversity (i.e., different UE experiences different path loss, and more UEs with lower path loss help enhance energy efficiency.) [TV05].

Figure 4.3 shows the ratio of accepted UEs versus the requested numbers of UEs with/without energy cooperation. The number of PBSs in each macrocell is set as 3, $\beta = 0.8$, and $\alpha = 0.1$. The required data rate for each UE in Figure 4.3 and the following

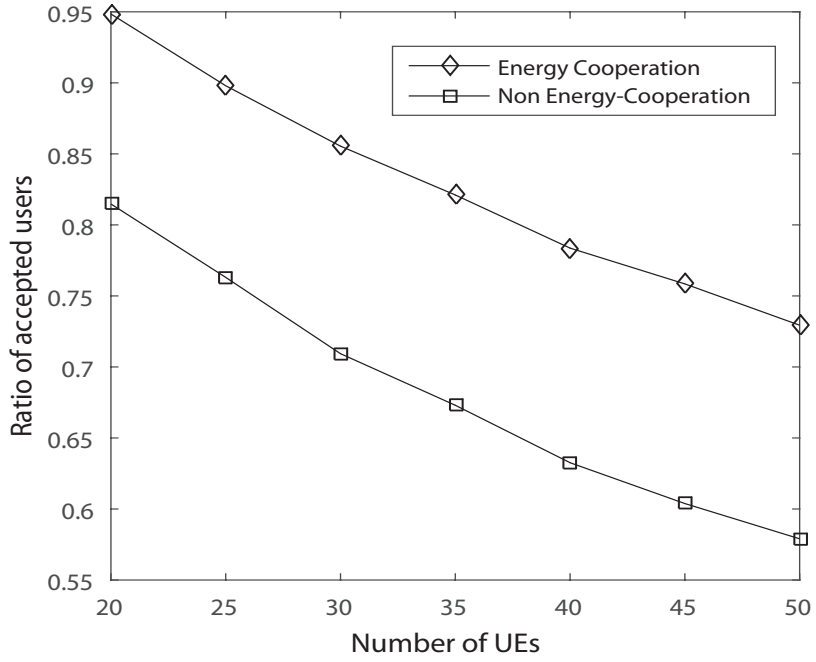

Figure 4.3: Ratio of accepted UEs versus the requested number of UEs with/without energy cooperation.

Figure 4.4 is $\tau = 5 \times 10^5$ bits/s. It can be found that the proposed algorithm with energy cooperation can accept more UEs than the scenario without energy cooperation. When more UEs demand services, the advantage of using proposed algorithm with energy cooperation becomes more significant, due to the fact that the proposed algorithm is capable of exploiting the multiuser diversity (i.e., different UEs experience different path loss, and more UEs with lower path loss help enhance spectrum efficiency.).

Figure 4.4 shows the throughput of the whole system versus the number of PBSs for different energy transferred efficiencies. The number of requested UEs in each macrocell is set as 30 and $\alpha = 0.1$. It can be observed that in the HetNets, deploying more PBSs can provide higher throughput. Under scenario with energy cooperation, high energy transfer efficiency allows more UEs to be accepted and achieves higher throughput of the network. When increasing the number of PBSs, the proposed algorithm with high energy transfer efficiency performs much better than the other cases.

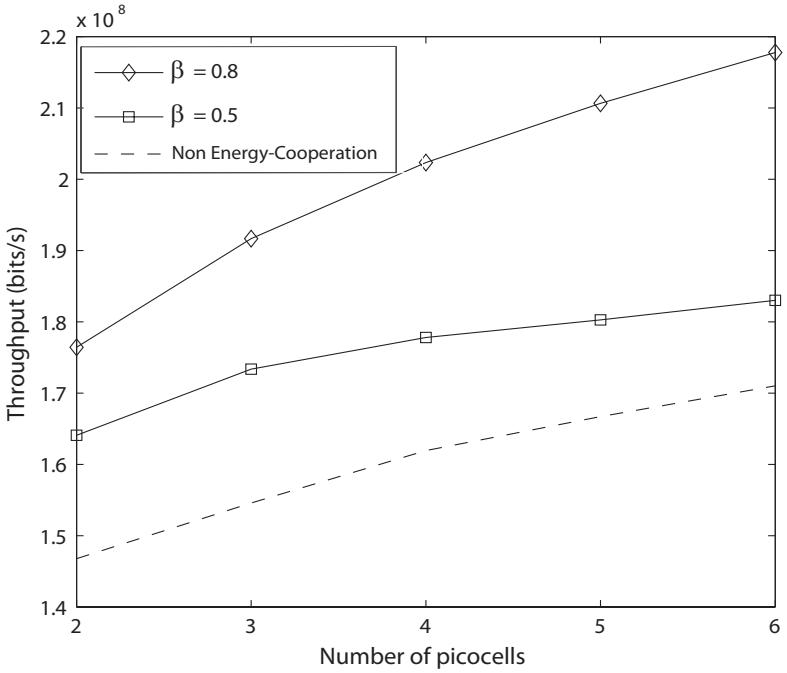

Figure 4.4: Throughput versus the number of PBSs for different energy transfer efficiencies β.

4.5 Power Control in Energy Cooperation Enabled HetNets

4.6 System Model and Problem Formulation

A two-tier downlink HetNet consisting of one MBS is considered, denoted as BS_0 and M PBSs denoted as $BS_i, i \in \{1, 2, ..., M\}$. The overall number of UEs in the network is $\mathrm{UE}_{\mathrm{num}}$. There are N_i UEs denoted as UE_j^i ($j \in \{1, 2, ..., N_i\}$) served by $BS_i, i \in \{0, 1, 2, ..., M\}$ and $\mathrm{UE}_{\mathrm{num}} = \sum_{i=0}^{M} N_i$. Each UE is associated with only one BS. In this network, all BSs are assumed to share the same frequency band, and are powered by both renewable energy sources and the power grid. Furthermore, different BSs have different energy harvesting rates.

4.6.1 Downlink Transmission Model

When UE_j^i is connected to BS_i, its downlink data rate R_j^i is given by

$$R_j^i = \frac{W}{N_i} \log_2 \left(1 + \gamma_j^i\right), \tag{4.16}$$

where W is the system bandwidth, and the SINR γ_j^i is

$$\gamma_j^i = \frac{P_i h_j^i}{\sum\limits_{i'=0, i' \neq i}^{M} P_{i'} h_{i,j}^{i'} + \sigma^2}. \tag{4.17}$$

In (5.5), P_i is the transmit power of BS_i, h_j^i is the channel power gain between UE_j^i and BS_i, $h_{i,j}^{i'}$ is the interfering channel power gain between UE_j^i and $BS_{i'}$, and σ^2 is the noise power.

4.6.2 Energy Cooperation Model

Each BS is powered by both the power grid and renewable energy sources. The energy drawn by BS_i from the grid is denoted as G_i. The energy harvested by BS_i from renewable energy sources is denoted as E_i, which is a constant in each time slot and may change from one time slot to another.

The energy transferred from BS_i to $BS_{i'}$ is denoted as $\mathcal{E}_{ii'} (\forall i, i' \in \{0, 1, 2..., M\})$, and the energy transfer efficiency factor between two BSs is denoted as $\beta_{\mathcal{E}}$. Hence $(1 - \beta_{\mathcal{E}})$ specifies the energy loss during the energy transmission process. In this chapter, It is assumed that there is no battery, and the energy cooperation problem in each time slot is independent.

The total power consumption of BS_i is modelled as

$$\mathcal{J}_i = \frac{P_i}{\rho_i} + \mathcal{J}_{i,o}, \forall i, \tag{4.18}$$

where ρ_i is the efficiency of the power amplifier, and $\mathcal{J}_{i,o}$ is the static power consumption.

4.6.3 Problem Formulation

Our objective is to maximise the energy efficiency via power control in energy cooperation enabled HetNets. Energy efficiency η is defined as the ratio of the overall network throughput to the overall grid energy consumption. Hence the optimisation problem is formulated as

$$\mathbf{P1}: \quad \max_{\mathbf{P},\mathcal{E},\mathbf{G}} \eta = \frac{\sum_{i=0}^{M}\sum_{j=1}^{N_i} R_j^i}{\sum_{i=0}^{M} G_i}, \tag{4.19}$$

$$\text{s.t.} \quad \text{C1}: \gamma_j^i > \Gamma_j^i, \ \forall i, \forall j \in \{1, 2..., N_i\},$$

$$\text{C2}: \mathcal{J}_i + \sum_{i'=0, i' \neq i}^{M} \mathcal{E}_{ii'} \leq G_i + E_i + \beta_{\mathcal{E}} \sum_{i'=0, i' \neq i}^{M} \mathcal{E}_{i'i}, \ \forall i,$$

$$\text{C3}: 0 \leq P_i \leq P_i^{\max}, \ \forall i,$$

$$\text{C4}: G_i \geq 0, \ \forall i,$$

$$\text{C5}: \mathcal{E}_{ii'} \geq 0, \ \forall i, i^{'}, i^{'} \neq i,$$

where Γ_j^i denotes the minimum SINR requirement of UE_j^i and $P_i^{\max}$ is the maximum transmit power of BS_i. C1 represents the SINR constraint; C2 means that the total power supply of BS_i including the grid energy, harvested energy and the transferred energy should be no less than the energy consumption of it [CSZ14a]; C3 ensures that the transmit power of BS_i should be smaller than the maximum transmit power; C4 and C5 are the boundary constraints for the grid energy and transferred energy, respectively.

4.7 Problem Transformation and Proposed Algorithm

4.7.1 Problem Transformation

The optimisation problem **P1** is a non-linear fractional problem. Following [Din67], the objective function of **P1** is reformulated using the Dinkelbach's method. The new problem **P2** can be written as

$$\mathbf{P2}: \max_{\mathbf{P},\mathcal{E},\mathbf{G}} z(\eta) = \sum_{i=0}^{M}\sum_{j=1}^{N_i} R_j^i - \eta \sum_{i=0}^{M} G_i, \tag{4.20}$$

$$\text{s.t.} \quad \text{C1}, \text{C2}, \text{C3}, \text{C4}.$$

The optimal solution set $(\mathbf{P}^*, \mathcal{E}^*, \mathbf{G}^*)$ of **P1** is the same as that of **P2** for $\eta = \eta^*$ [Din67], where η^* is the maximum energy efficiency given by

$$\eta^* = \frac{\sum_{i=0}^{M}\sum_{j=1}^{N_i} R_j^i(\mathbf{P}^*, \mathcal{E}^*, \mathbf{G}^*)}{\sum_{i=0}^{M} G_i(\mathbf{P}^*, \mathcal{E}^*, \mathbf{G}^*)}. \tag{4.21}$$

Problem **P1** is solved in an iterative manner as shown in Algorithm 3. First the interior problem **P2** for a given η is solved, and the optimal values of $\mathbf{P}^*, \mathcal{E}^*$ and $\mathbf{G}^*$ is obtained by using Algorithm 4. Then, the optimal η^* is determined as (4.21).

The interior optimisation problem **P2** is still a NP-hard problem. Inspired by [NLS12], **P2** can be efficiently solved by introducing an additional constraint as follows.

$$\text{C6}: \sum_{i'=0, i'\neq i}^{M} P_{i'} h_{i,j}^{i'} \leq \mathcal{I}, \tag{4.22}$$

where the bound $\mathcal{I}$ is called the maximum interference temperature.[2] Then, the data

[2]In the considered problem, $\mathcal{I}$ is not an optimisation variable but it can be properly found via simulation in an off-line manner [NLS12].

Algorithm 3 Dinkelbach's method to determine optimal η^*

if $t = 0$**, then**
  Intialize $\eta = 0$.
else
  Determine the optimal resource allocation policy $(\mathbf{P}^*, \mathcal{E}^*, \mathbf{G}^*)$ based on the η and Algorithm 4.
  if $\sum_{i=0}^{M} \sum_{j=1}^{N_i} R_j^i(\mathbf{P}^*, \mathcal{E}^*, \mathbf{G}^*) - \eta \sum_{i=0}^{M} G_i(\mathbf{P}^*, \mathcal{E}^*, \mathbf{G}^*) < \varepsilon$
    $\eta^* = \frac{\sum_{i=0}^{M} \sum_{j=1}^{N_i} R_j^i(\mathbf{P}^*, \mathcal{E}^*, \mathbf{G}^*)}{\sum_{i=0}^{M} G_i(\mathbf{P}^*, \mathcal{E}^*, \mathbf{G}^*)}$.
    break
  else
    Update $\eta = \frac{\sum_{i=0}^{M} \sum_{j=1}^{N_i} R_j^i(\mathbf{P}^*, \mathcal{E}^*, \mathbf{G}^*)}{\sum_{i=0}^{M} G_i(\mathbf{P}^*, \mathcal{E}^*, \mathbf{G}^*)}$.
    $t \leftarrow t + 1$.
  end if
end if

rate between UE_j^i and BS_i is lower bounded as

$$\bar{R}_j^i = \frac{W}{N_i} \log_2 \left(1 + \bar{\gamma}_j^i\right), \tag{4.23}$$

where $\bar{\gamma}_j^i = \frac{P_i h_j^i}{\mathcal{I} + \sigma^2 W}$. By substituting (4.23) into **P2**, the problem can be rewrote as

$$\begin{aligned} \mathbf{P3}: \max_{\mathbf{P}, \mathcal{E}, \mathbf{G}} & \sum_{i=0}^{M} \sum_{j=1}^{N_i} \bar{R}_j^i - \eta \sum_{i=0}^{M} G_i, \\ \text{s.t.} \quad & \text{C1}, \text{C2}, \text{C3}, \text{C4}, \text{C5}, \text{C6}. \end{aligned} \tag{4.24}$$

4.7.2 Lagrangian Dual

The transformed problem **P3** is concave and the constraints of it are linear inequalities, thus the Slater's condition is satisfied and the strong duality is held. Hence the Lagrangian duality method can be adopted to solve **P3**. First the following Lagrangian

function is presented,

$$\begin{aligned}
\mathcal{L}\left(\mathbf{P},\mathcal{E},\mathbf{G},\boldsymbol{\mu},\boldsymbol{\nu},\boldsymbol{\theta}\right) &= \sum_{i=0}^{M}\sum_{j=1}^{N_i}\bar{R}_j^i - \eta\sum_{i=0}^{M}G_i \\
&- \sum_{i=0}^{M}\sum_{j=1}^{N_i}\mu_j^i\left(\Gamma_j^i-\bar{\gamma}_j^i\right) - \sum_{i=0}^{M}\nu_i\Big(\mathcal{J}_i + \sum_{i'=0,i'\neq i}^{M}\mathcal{E}_{ii'} - G_i \\
&- E_i - \beta_{\mathcal{E}}\sum_{i'=0,i'\neq i}^{M}\mathcal{E}_{i'i}\Big) - \sum_{i=0}^{M}\sum_{j=1}^{N_i}\theta_j^i\Big(\sum_{i'=0,i'\neq i}^{M}P_{i'}h_{i,j}^{i'} - \mathcal{I}\Big) \\
&= \sum_{i=0}^{M}\Big(\sum_{j=1}^{N_i}\left(\bar{R}_j^i+\mu_j^i\bar{\gamma}_j^i\right) - \nu_i\frac{P_i}{\rho_i} - P_i\sum_{i'=0,i'\neq i}^{M}\sum_{j'=1}^{N_{i'}}\theta_{j'}^{i'}h_{i',j'}^{i}\Big) \\
&+ \sum_{i=0}^{M}\left(\nu_i-\eta\right)G_i + \sum_{i=0}^{M}\sum_{i'=0,i'\neq i}^{M}\left(\beta_{\mathcal{E}}\nu_{i'}-\nu_i\right)\mathcal{E}_{ii'} \\
&- \sum_{i=0}^{M}\sum_{j=1}^{N_i}\mu_j^i\Gamma_j^i + \sum_{i=0}^{M}\nu_i\Big(E_i-\mathcal{J}_{i,o}\Big) + \sum_{i=0}^{M}\sum_{j=1}^{N_i}\theta_j^i\mathcal{I},
\end{aligned} \tag{4.25}$$

where μ_j^i, ν_i, and θ_j^i are the non-negative Lagrange multipliers.

Based on (4.25), the dual function is given by

$$g(\boldsymbol{\mu},\boldsymbol{\nu},\boldsymbol{\theta}) = \begin{cases} \max\limits_{\mathbf{P},\mathcal{E},\mathbf{G}} \mathcal{L}\left(\mathbf{P},\mathcal{E},\mathbf{G},\boldsymbol{\mu},\boldsymbol{\nu},\boldsymbol{\theta}\right) \\ \text{s.t. } 0\leq P_i\leq P_i^{\max}, G_i\geq 0, \mathcal{E}_{ii'}\geq 0,\ \forall i,i^{'}. \end{cases} \tag{4.26}$$

Then, the dual problem of **P3** is defined as

$$\mathbf{P3-D}: \min_{\boldsymbol{\mu}\geq 0,\boldsymbol{\nu}\geq 0,\boldsymbol{\theta}\geq 0} g(\boldsymbol{\mu},\boldsymbol{\nu},\boldsymbol{\theta}). \tag{4.27}$$

To let $g(\boldsymbol{\mu},\boldsymbol{\nu},\boldsymbol{\theta})$ be bounded, the following lemma can be obtained:

Lemma 2. *The dual function is bounded by satisfying*

1. $\nu_i \leq \eta,\ \forall i.$

2. $\beta_{\mathcal{E}}\nu_{i'} \leq \nu_i,\ \forall i, i^{'}, i^{'}\neq i.$

Proof. Contradiction is used to prove the lemma. First, It is supposed that there exists a ν_i satisfying $\nu_i > \eta$. It can be seen that the objective value of (4.26) goes to infinity as $G_i \to \infty$. The dual function becomes unbounded. Hence, to ensure the bounded dual function, $\nu_i \leq \eta$, $\forall i$ must hold. Using the similar method, the second part of the Lemma 2 can be proved. □

Given the dual variables μ_j^i, ν_i and θ_j^i, the problem in (4.26) can be decomposed into $(1+M)^2+(1+M)$ subproblems by removing the constant terms of the Lagrangian function, which are as follows:

$$\max_{0\leq P_i\leq P_i^{\max}} \sum_{j=1}^{N_i} \left(\bar{R}_j^i + \mu_j^i \bar{\gamma}_j^i\right) - \nu_i \frac{P_i}{\rho_i} - P_i \sum_{i'=0, i'\neq i}^{M} \sum_{j'=1}^{N_{i'}} \theta_{j'}^{i'} h_{i',j'}^{i}, \forall i, \tag{4.28}$$

$$\max_{G_i\geq 0} \left(\nu_i - \eta\right) G_i, \forall i, \tag{4.29}$$

$$\max_{\mathcal{E}_{ii'}\geq 0} \left(\beta_{\mathcal{E}} \nu_{i'} - \nu_i\right) \mathcal{E}_{ii'} \forall i, i', i \neq i'. \tag{4.30}$$

Since the subproblems in (4.28) are concave, some commonly-used descent methods such as Newton's method can efficiently solve it [BV04]. Let $f(P_i)$ be the objective function of (4.28), first the first-order and the second-order partial derivatives of $f(P_i)$ with respect to P_i is calculated as

$$\frac{\partial f(P_i)}{\partial P_i} = \sum_{j=1}^{N_i} \left(\frac{W}{N_i \ln 2} \frac{\bar{\gamma}_j^i}{1+\bar{\gamma}_j^i} \frac{1}{P_i} + \mu_j^i \frac{\bar{\gamma}_j^i}{P_i}\right) - \nu_i \frac{1}{\rho_i} - \sum_{i'=0, i'\neq i}^{M} \sum_{j'=1}^{N_{i'}} \theta_{j'}^{i'} h_{i',j'}^{i}, \tag{4.31}$$

and

$$\frac{\partial^2 f(P_i)}{\partial P_i^2} = -\frac{W}{N_i \ln 2} \sum_{j=1}^{N_i} \left(\frac{\bar{\gamma}_j^i}{1+\bar{\gamma}_j^i}\right)^2 \frac{1}{P_i^2}. \tag{4.32}$$

As such, the Newton step is $\Delta P_i = -\frac{\partial f(P_i)}{\partial P_i} / \frac{\partial^2 f(P_i)}{\partial P_i^2}$, and Newton decrement is $\Theta =$

Algorithm Newton's method

if $t = 0$, **then**

1: Initialise $P_i(t)$, $\forall i$.

else

2: Calculate the Newton's step through $\Delta P_i = -\frac{\partial f(P_i)}{\partial P_i} / \frac{\partial^2 f(P_i)}{\partial P_i^2}$ based on (4.31) and (4.32). Update $P_i(t+1)$ via $P_i(t+1) = \left[P_i(t) + \delta(t)\,\Delta P_i\right]_0^{P_i^{\max}}$, $\delta(t)$ is the step size determined by backtracking line search.

if convergence ($|\Theta|/2 \leq \epsilon$, ϵ is the tolerance)

break;

else

3: $t \leftarrow t+1$, and go to step 2.

end if

end if

$\left(\frac{\partial f(P_i)}{\partial P_i}\right)^2 / \frac{\partial^2 f(P_i)}{\partial P_i^2}$, which is used as the stopping criterion [BV04]. Hence the optimal solution of (4.28) can be obtained based on Newton's method. In addition, with the help of Lemma 2, the optimal solutions of (4.29) and (4.30) are

$$G_i(\nu_i) = 0, \;\; \mathcal{E}_{ii'}\left(\nu_i, \nu_{i'}\right) = 0, \; \forall i, i'. \tag{4.33}$$

By using the solutions of (4.28), (4.29) and (4.30), the dual function $g(\boldsymbol{\mu}, \boldsymbol{\nu}, \boldsymbol{\theta})$ in (4.26) can be obtained. To determine the optimal dual variables, first the dual problem $\mathbf{P3-D}$ is reformulated. Based on Lemma 2, the dual problem can be equivalently rewritten as

$$\begin{aligned} \mathbf{P3-D}: \min_{\boldsymbol{\mu}\geq 0, \boldsymbol{\nu}\geq 0, \boldsymbol{\theta}\geq 0} & g(\boldsymbol{\mu}, \boldsymbol{\nu}, \boldsymbol{\theta}), \\ \text{s.t.} \;\; & \nu_i \leq \eta, \; \forall i, \\ & \beta_{\mathcal{E}} \nu_{i'} \leq \nu_i, \; \forall i, i', i' \neq i. \end{aligned} \tag{4.34}$$

The above problem is concave which can be solved by the subgradient method [BM08],

and $\boldsymbol{\mu}$, $\boldsymbol{\nu}$, and $\boldsymbol{\theta}$ are updated such that

$$\mu_j^i(t+1) = \left[\mu_j^i(t) - \chi(t)\left(\bar{\gamma}_j^i - \Gamma_j^i\right)\right]^+, \tag{4.35}$$

$$\begin{aligned}\nu_i(t+1) &= \left[\nu_i(t) - \chi(t)\left(G_i + E_i + \beta_{\mathcal{E}}\sum_{i'=0}^{M}\mathcal{E}_{i'i}^k - \mathcal{J}_i - \sum_{i'=0}^{M}\mathcal{E}_{ii'}\right)\right]^+ \\ &\overset{(a)}{=} \left[\nu_i(t) - \chi(t)\left(E_i - \frac{P_i^*\left(\boldsymbol{\mu}(t),\boldsymbol{\nu}(t),\boldsymbol{\theta}(t)\right)}{\rho_i} - \mathcal{J}_{i,o}\right)\right]^+, \end{aligned}\tag{4.36}$$

$$\theta_j^i(t+1) = \left[\theta_j^i(t) - \chi(t)\left(\mathcal{I} - \sum_{i'=0,i'\neq i}^{M} P_{i'}^*\left(\boldsymbol{\mu}(t),\boldsymbol{\nu}(t),\boldsymbol{\theta}(t)\right)h_{i,j}^{i'}\right)\right]^+, \forall i, \forall j, \tag{4.37}$$

where $[x]^+ = \max\{x, 0\}$, t is the iteration index, and $\chi(t)$ is the step size of the iteration t.[3] In (4.36), step (a) is obtained by considering $\mathcal{J}_i$ given in (4.18) and $G_i, \mathcal{E}_{ii'}$ given in (4.33). Note that the updated ν_i needs to satisfy the constraints of (4.34).

After obtaining the optimal $\boldsymbol{\mu}^*$, $\boldsymbol{\nu}^*$, and $\boldsymbol{\theta}^*$ of $\mathbf{P3}-\mathbf{D}$, the corresponding solution $P_i\left(\boldsymbol{\mu}^*,\boldsymbol{\nu}^*,\boldsymbol{\theta}^*\right)$ of (4.28) is the optimal power solution of the primal problem **P3**. When the optimal BS transmit power is determined, the optimal G_i and $\mathcal{E}_{ii'}$ of **P3** can be obtained by equivalently solving the following simple linear program (LP):

$$\begin{aligned}&\mathbf{P4}: \min_{\mathcal{E},\mathbf{G}} \sum_{i=0}^{M} G_i, \\ &\text{s.t.} \quad \text{C2, C4, C5.}\end{aligned}\tag{4.38}$$

The problem **P4** can be efficiently solved by using CVX [GB]. Then, **P3** is completely solved.

Based on the previous analysis to solve the problem **P2**, the proposed algorithm is summarised in Algorithm 4.

[3]There are many step size selections such as constant step size and diminishing step size. In this chapter, the nonsummable diminishing step length is used, as shown in [BM08].

Algorithm 4 Algorithm for Solving Problem **P2**

if $t = 0$
  Initialise $\mu_j^i(t)$, $v_i(t)$, $\theta_j^i(t)$, $\forall i, \forall j$, which are feasible for dual problem in (4.34). Initialise the step size $\chi(t)$ and the maximum iteration number $t_{\max}$.
else
  Calculate $P_i(t)$ through Newton's method.
  Update $\mu_j^i(t+1)$, $v_i(t+1)$, $\theta_j^i(t+1)$ according to (4.35)-(4.37), subject to the constraints of (4.34).
  if convergence or exceed the maximum iteration number
    $P_i^* = P_i(t)$.
    break
  else
    $t \leftarrow t + 1$.
  end if
end if
Calculate problem **P4** through CVX, and acquire the optimal $\mathcal{E}_{ii'}^*$ and G_i^* based on P_i^*. Thus, the optimal resource allocation policy $(\mathbf{P}^*, \mathcal{E}^*, \mathbf{G}^*)$ is obtained.

4.7.3 Other Scenarios

In this subsection, another three scenarios are given, namely the implementation of power control or energy cooperation solely, or neither of them is utilised in the HetNet. These scenarios are considered as baselines for the proposed algorithm, and the comparisons are shown in the simulation results of Section 4.8.

4.7.3.1 No Energy Cooperation, Power Control Solely

In this scenario, the energy transfer efficiency $\beta_{\mathcal{E}}$ is set as 0, which means that the energy cooperation is infeasible. Then, the proposed Algorithm 3 is applied to solve this problem.

4.7.3.2 No Power Control, Energy Cooperation Solely

In this scenario, each BS is assumed to use the maximum transmit power. Then, the new problem is as follows:

$$\mathbf{P5}: \quad \max_{\mathcal{E},\mathbf{G}} \frac{\sum_{i=0}^{M}\sum_{j=1}^{N_i} R_j^i}{\sum_{i=0}^{M} G_i}, \tag{4.39}$$
$$\text{s.t.} \quad \text{C2}, \text{C4}, \text{C5}.$$

Since the numerator of the objective function is independent of $\mathcal{E}$ and $\mathbf{G}$, **P5** can be equivalently transformed as

$$\mathbf{P5-1}: \min_{\mathcal{E},\mathbf{G}} \sum_{i=0}^{M} G_i, \tag{4.40}$$
$$\text{s.t.C2}, \text{C4}, \text{C5}.$$

The optimisation problem **P5-1** is a LP problem, which can be solved by CVX. Thus, the optimal grid energy consumption $\mathbf{G}^*$ and optimal transferred energy $\mathcal{E}^*$ can be obtained for maximising energy efficiency.

4.7.3.3 No Energy Cooperation nor Power Control

In this scenario, the transmit power of BS_i is $P_i^{\max}$, and there is no energy cooperation in the network. The optimal grid energy consumption G_i^* consumed by BS_i is directly calculated as $G_i^* = \left[\frac{P_i^{\max}}{\rho_i} + \mathcal{J}_{i,o} - E_i\right]^+$, and therefore the energy efficiency is directly calculated as $\sum_{i=0}^{M}\sum_{j=1}^{N_i} R_j^i / \sum_{i=0}^{M} G_i^*$.

Table 4-B: Simulation Parameters

Parameter	**Value**
Cell radius	500 m
Macro cell bandwidth W	20 MHz
Noise power density σ^2	-174 dBm/Hz
Static power consumption of MBS $\mathcal{J}_{0,o}$	780 W
Static power consumption of PBS $\mathcal{J}_{i,o}$	13.6 W
Path loss of MBS h_j^0	$128.1 + 37.6\log_{10}d(\text{km})$
Path loss of PBS h_j^i	$140.7 + 36.7\log_{10}d(\text{km})$
Min harvested energy of MBS a_0	575 W
Max harvested energy of MBS b_0	660 W
Min harvested energy of PBS a_i	15 W
Max harvested energy of PBS b_i	25 W
Min SINR requirement Γ_j^i	0 dB
Max transmit power of MBS $P_0^{\max}$	46 dBm
Max transmit power of PBS $P_0^{\max}$	30 dBm
Efficiency of power amplifier ρ_i	0.3 [BSHD14]

4.8 Simulation Results

In this section, numerical results are presented to demonstrate the performance of the proposed power control algorithm with and without energy cooperation. In the simulations, PBSs and UEs are uniformly distributed. The energy harvesting process E_i at BS_i is modeled as a stationary stochastic process with pdf $f_i(z_i) = 1/(b_i - a_i), \forall z_i \in [a_i, b_i]$ where a_i and b_i is the minimum and maximum harvested energy of BS_i respectively [ZPSY13a]. For the first three figures, the ratio of the maximum interference temperature to noise $\frac{\mathcal{I}}{\sigma^2 W}$ is 25 dB, and the last figure shows the impact of the maximum interference temperature. Iteration number is 500. The basic simulation parameters are shown in Table 4-B.

Figure 4.5 shows the energy efficiency versus the number of UEs UE_{num}. The number of PBSs and the energy transfer efficiency factor $\beta_{\mathcal{E}}$ are set as 5 and 0.7, respectively. It is found that the proposed algorithm consisting of energy cooperation and power control achieves higher energy efficiency than the other three scenarios. The implementation of power control can significantly improve the energy efficiency, compared with the non

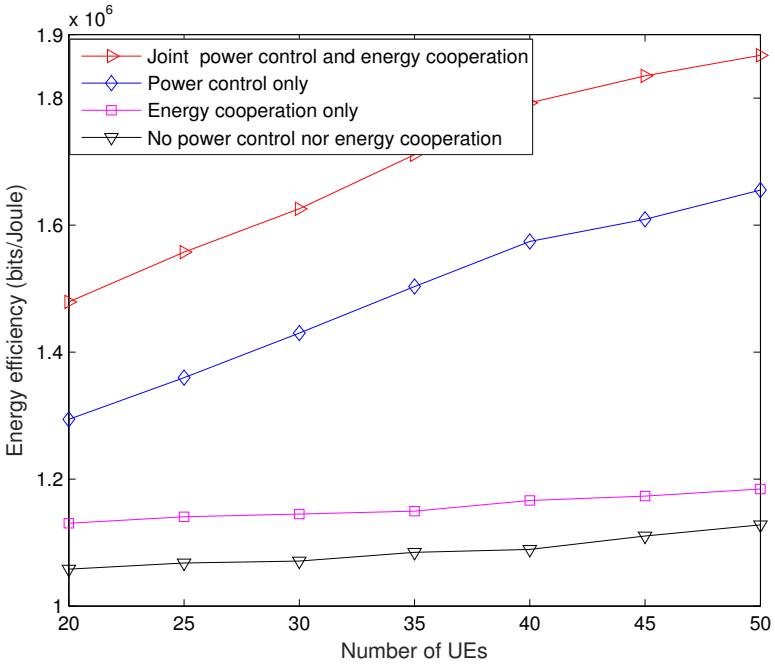

Figure 4.5: Energy efficiency versus the number of UEs.

power-control cases. In addition, by using the proposed joint power control and energy cooperation algorithm, there is a big improvement in energy efficiency when more UEs demand services in the network, due to the fact that the proposed algorithm is capable of exploiting the multiuser diversity (i.e., different UEs experience different path loss, and more UEs with lower path loss help enhance energy efficiency.) [TV05].

Figure 4.6 investigates the energy efficiency versus the number of PBSs. The energy transfer efficiency $\beta_{\mathcal{E}}$ and the number of UEs $\mathrm{UE}_{\mathrm{num}}$ are set as 0.7 and 30, respectively. The proposed joint energy cooperation and power control algorithm outperforms the other cases. As more PBSs are deployed in the HetNet, the advantage of the proposed algorithm becomes more significant. This can be explained by the fact that more renewable energy harvested by PBSs can be transferred between BSs through energy cooperation, to reduce the consumption of grid energy.

Figure 4.7 depicts the energy efficiency versus the energy transfer efficiency factor $\beta_{\mathcal{E}}$. The number of PBSs is set as 5. In this figure, the non energy cooperation scenario

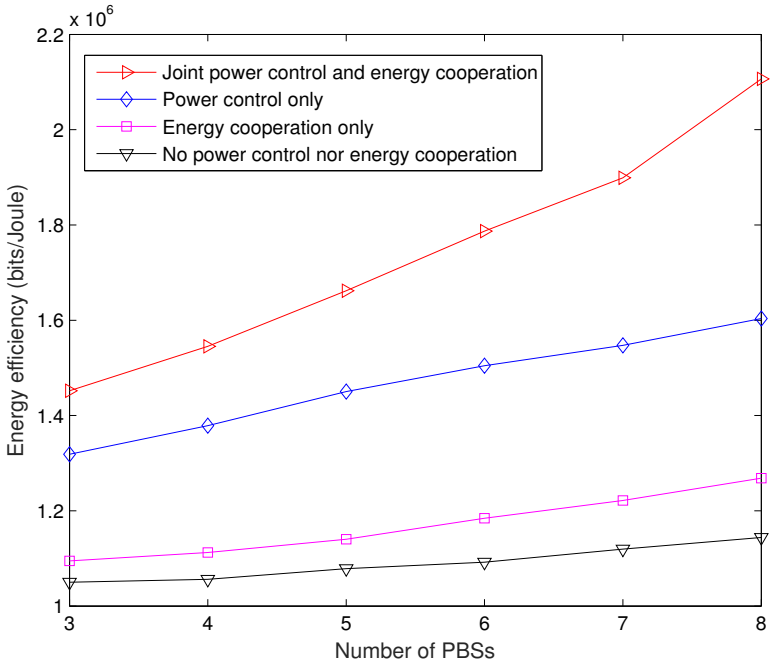

Figure 4.6: Energy efficiency versus the number of PBSs.

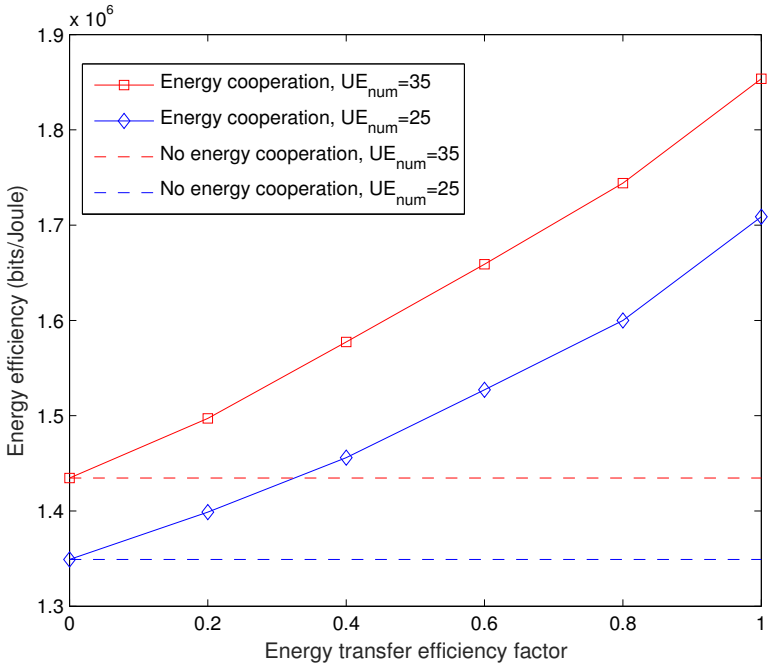

Figure 4.7: Energy efficiency versus the energy transfer efficiency factor $\beta_{\mathcal{E}}$.

is considered as a baseline for comparison. It can be observed that there is a substantial increase in energy efficiency when improving the energy transfer efficiency, since the harvested renewable energy can be efficiently transferred between BSs for reducing the grid energy consumption. Moreover, the performance gap between the energy cooperation and non energy cooperation expands when improving the energy transfer efficiency, which indicates that energy cooperation plays a pivotal role in improving the energy efficiency of the HetNet with hybrid energy supplies. Again, energy efficiency is enhanced by increasing the number of UEs due to the achievable multiuser diversity gain [TV05].

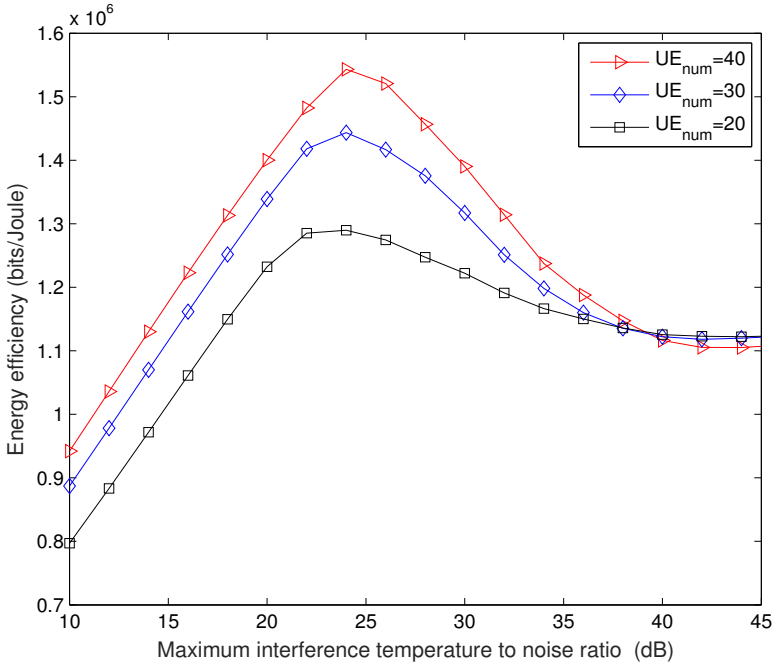

Figure 4.8: Energy efficiency versus the ratio of the maximum interference temperature to noise $\mathcal{I}/\sigma^2 W$ (dB).

Figure 4.8 shows the energy efficiency versus the ratio of the maximum interference temperature to noise $\frac{\mathcal{I}}{\sigma^2 W}$ (dB) for different numbers of UEs. I set the number of PBSs as 5 and the energy transfer efficiency factor as 0.7. The maximum interference temperature $\mathcal{I}$ represents the upper bound of the interference, which puts a limit on the BS's transmit power. It can be seen that energy efficiency first increases with $\frac{\mathcal{I}}{\sigma^2 W}$. When the ratio is beyond the optimal value, it decreases with increasing $\frac{\mathcal{I}}{\sigma^2 W}$. The reason is

that increasing $\frac{\mathcal{I}}{\sigma^2 W}$ allows the BS to use larger transmit power, so as to improve the lower-bound date rate in (4.23) and maximise the objective function of the transformed problem **P3**, however, larger BS transmit power results in more grid energy consumption, which deteriorates energy efficiency, and becomes a comparably inefficient solution for **P2**. When $\frac{\mathcal{I}}{\sigma^2 W}$ is set as larger than a critical value (35 dB in this figure), the energy efficiency converges to a constant value, because of the maximum BS transmit power constraint. In practice, optimal value of $\mathcal{I}$ is found in an off-line manner [NLS12]. As suggested before, energy efficiency grows with the number of UEs.

4.9 Summary

In this chapter, first, the user association optimisation problem in energy cooperation enabled HetNets is studied without power control. A user association algorithm is proposed aiming to optimise the energy efficiency and the number of accepted UEs. Simulation results show that the application of the proposed algorithm with energy cooperation achieves larger energy efficiency and number of accepted UEs than non energy cooperation case. Meanwhile, the advantage of the proposed algorithm with energy cooperation is more obvious when more PBSs and UEs are located in a macro geographical area, due to its capability of exploiting multiuser diversity. Then, under conventional user association scheme, the power control problem in energy cooperation enabled HetNets with hybrid energy supplies is taken into account. An efficient power control algorithm is proposed to maximise energy efficiency of the overall network. Simulation results have demonstrated that the proposed algorithm with energy cooperation and power control achieves better performance than other cases, namely, applying energy cooperation or power control solely, or neither of them.

Chapter 5

Resource Allocation in Energy Cooperation Enabled NOMA HetNets

5.1 Overview

This chapter focuses on resource allocation in energy cooperation enabled two-tier heterogeneous networks (HetNets) with non-orthogonal multiple access (NOMA), where BSs are powered by both renewable energy sources and the conventional grid. A problem is formulated to find the optimum user association and power control schemes for maximising the energy efficiency of the overall network, under quality of service constraints. First a distributed algorithm is proposed to provide the optimal user association solution for the fixed transmit power. Then, a joint user association and power control optimisation algorithm is developed to determine the traffic load in energy cooperation enabled NOMA HetNets, which achieves much higher energy efficiency performance than existing schemes. Simulation results demonstrate the effectiveness of the proposed algorithm, and show that NOMA can achieve higher energy efficiency performance than orthogonal

multiple access (OMA) in the considered networks.

5.2 System Model and Problem Formulation

In this section, the system model for energy cooperation in two-tier NOMA HetNets is presented, and the corresponding joint user association and power control problem is formulated.

5.2.1 Downlink NOMA Transmission

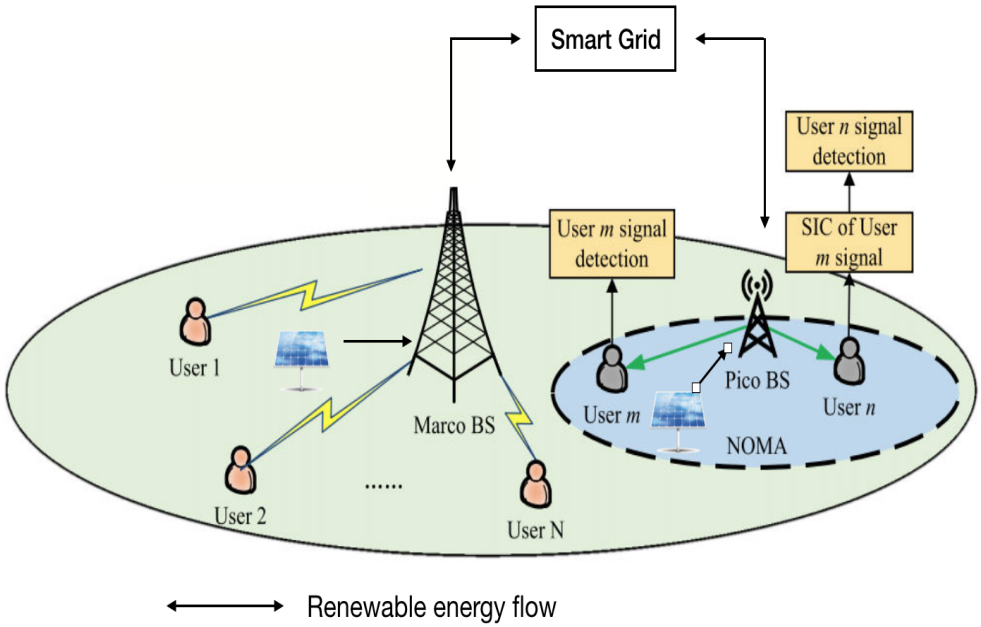

Figure 5.1: An example of an energy cooperation enabled two-tier NOMA HetNet powered by both solar panels and the conventional grid.

As shown in Figure 5.1, a two-tier energy cooperation enabled HetNet consisting of one macro BS (MBS) and M pico BSs (PBSs) is considered, where NOMA-based downlink transmission is utilised, and all BSs are assumed to share the same frequency band. In such a network, BSs are powered by both the conventional power grid and renewable energy sources, and energy can be shared between BSs through the smart

grid. Let $m \in \{1, 2, 3, ..., M+1\}$ be the m-th BS, in which $m = 1$ denotes the MBS, and the other values denote PBSs. There are N randomly located user equipments (UEs) in this network, and each UE is associated with only one BS. All BSs and UEs are single-antenna nodes. In this chapter, it is assumed that the global perfect channel state information (CSI) is available. Let $j \in \{1, 2, 3, ..., N\}$ index the j-th UE. According to the NOMA scheme [SKB+13, DAP16], the superimposed signal transmitted by the BS m is $s_m = \sum_{j=1}^{N} x_{jm}\sqrt{P_{jm}}s_{jm}$ with $\mathrm{E}\left[s_{jm}(s_{jm})^H\right]=1$, $\forall m, j$, where $x_{jm} \in \{0, 1\}$ is the binary user association indicator, i.e., $x_{jm} = 1$ when the j-th UE is associated with the m-th BS and otherwise it is zero, s_{jm} is the j-th user-stream and P_{jm} is the corresponding allocated transmit power. When the j-th UE is associated with the m-th BS, its received signal can be expressed as

$$\begin{aligned} y_{jm} =& h_{jm}\sqrt{P_{jm}}s_{jm} + \underbrace{h_{jm}\sum_{j^{'}=1,j^{'}\neq j}^{N} x_{j^{'}m}\sqrt{P_{j^{'}m}}s_{j^{'}m}}_{\text{Intra-cell interference}} \\ &+ \underbrace{\sum_{m^{'}=1,m^{'}\neq m}^{M+1} h_{jm}^{m^{'}}\left(\sum_{j^{'}=1}^{N} x_{j^{'}m^{'}}\sqrt{P_{j^{'}m^{'}}}s_{j^{'}m^{'}}\right)}_{\text{Inter-cell interference}} + \varpi_o, \end{aligned} \tag{5.1}$$

where $x_{j^{'}m}, x_{j^{'}m^{'}} \in \{0, 1\}$, h_{jm} is the channel coefficient from the associated BS m, $h_{jm}^{m^{'}}$ is the interfering channel coefficient from the BS $m^{'}$, and ϖ_o is the additive white Gaussian noise. The power density of ϖ_o is σ^2. In NOMA systems, successive interference cancelation (SIC) is employed at UEs, to cancel the intra-cell interference from the stronger UEs' data signals. Without loss of generality, assuming that there are k_m ($k_m \leq N$) UEs constituting a group that is served by the m-th BS at the same time and frequency band, the corresponding channel to inter-cell interference plus noise ratios (CINRs) are ordered as

$$\frac{|h_{1m}|^2}{I_{1m}^{(2)} + \sigma^2} \geq \cdots \geq \frac{|h_{jm}|^2}{I_{jm}^{(2)} + \sigma^2} \geq \cdots \geq \frac{|h_{k_m m}|^2}{I_{k_m m}^{(2)} + \sigma^2}, \tag{5.2}$$

where $I_{jm}^{(2)}$ is the inter-cell interference power at the j-th UE and σ^2 is the noise power. Based on the principle of multi-cell NOMA [SKB+13], the power allocation of the UEs' data signals in the m-th cell needs to satisfy

$$0 \leq P_{1m} \leq \cdots \leq P_{jm} \leq \cdots \leq P_{k_m m}, \sum_{j=1}^{k_m} P_{jm} = P_m, \tag{5.3}$$

where P_m is the total transmit power of the m-th BS. Such order is optimal for decoding and guaranteeing the user fairness [SKB+13], namely the data signals of UEs with weaker downlink channels and larger interference need to be allocated more transmit power to achieve the desired quality of service (QoS). For the special case of single-cell, i.e., $I_{jm}^{(2)} = 0$, (5.3) reduces to the order based on the channel power gains, as seen in [DAP16]. Therefore, based on (5.1), the data rate after SIC at the j-th UE is given by

$$\tau_{jm} = W \log_2 \left(1 + \gamma_{jm}\right), \tag{5.4}$$

where W is the system bandwidth, and γ_{jm} is the signal-to-interference-plus-noise ratio (SINR) given by

$$\begin{aligned} \gamma_{jm} &= \frac{P_{jm} \left|h_{jm}\right|^2}{\underbrace{\left|h_{jm}\right|^2 \sum_{j'=1}^{j-1} P_{j'm}}_{I_{jm}^{(1)}} + \underbrace{\sum_{m'=1, m' \neq m}^{M+1} \left|h_{jm}^{m'}\right|^2 P_{m'}}_{I_{jm}^{(2)}} + \sigma^2} \\ &= \frac{P_{jm}}{\sum_{j'=1}^{j-1} P_{j'm} + (I_{jm}^{(2)} + \sigma^2) / \left|h_{jm}\right|^2}, \quad j \leq k_m \end{aligned} \tag{5.5}$$

in which $I_{jm}^{(1)}$ is the remaining intra-cell interference after SIC, and $P_{m'} = \sum_{j'=1}^{N} x_{j'm'} P_{j'm'}$ is the total transmit power of the m'-th BS. Although this chapter focuses on the single-carrier system, it can be straightforwardly extended to the multi-carrier system by letting W be the subcarrier bandwidth and τ_{jm} multiply the subcarrier indicator to be the data rate of a subcarrier. Thus, the optimal solution over all subcarriers in the multi-carrier

case can be iteratively obtained by following the decomposition approach of this chapter.

5.2.2 Energy Model

Each BS is powered by both the conventional grid and renewable energy sources. The energy drawn by the m-th BS from the conventional grid is denoted as G_m. The energy harvested by the m-th BS from renewable energy sources is denoted by E_m. The energy transferred from BS m to BS $m^{'}$ is denoted as $\mathcal{E}_{mm'}$, and the energy transfer efficiency factor between two BSs is denoted as $\beta_{\mathcal{E}} \in [0, 1]$. Hence $(1 - \beta_{\mathcal{E}})$ specifies the level of energy loss during the energy transmission process. In addition, It is assumed that there is no battery to avoid the time-consuming and expensive energy waste during the charging/discharging process, and the energy cooperation problem in each time slot is independent. The time slot length is normalised as one to simplify the power-to-energy conversion. Therefore, the transmit energy consumption at the m-th BS should satisfy

$$P_m \leq G_m + E_m + \underbrace{\beta_{\mathcal{E}} \sum_{m'=1, m' \neq m}^{M+1} \mathcal{E}_{m'm}}_{\text{Energy received from other BSs}} - \underbrace{\sum_{m'=1, m' \neq m}^{M+1} \mathcal{E}_{mm'}}_{\text{Energy transferred to other BSs}}, \tag{5.6}$$

where $P_m = \sum_{j=1}^{N} x_{jm} P_{jm}$ is the total transmit power of the m-th BS.

From (5.6), it can be seen that in energy cooperation enabled networks, the grid energy consumption of a BS depends on its harvested renewable energy, transferred energy and transmit power. Given a BS's transmit power, its grid energy consumption needs to be formulated as a random variable, since the amount of harvested renewable energy and transferred energy is uncertain, which is different from the conventional network without energy cooperation.

5.2.3 Problem Formulation

Our aim is to maximise the energy efficiency of such networks. The energy efficiency (bits/Joule) is defined as the ratio of the overall network throughput to the overall grid energy consumption, i.e., the network energy efficiency is

$$\mathcal{U}\left(\mathbf{x},\mathbf{P},\boldsymbol{\mathcal{E}},\mathbf{G}\right)=\Big(\sum_{m=1}^{M+1}\sum_{j=1}^{N}x_{jm}\tau_{jm}\Big)/\sum_{m=1}^{M+1}G_m. \tag{5.7}$$

In this way, the harvested renewable energy can be maximally utilised to reduce the grid energy consumption [HA14]. Therefore, our problem can be formulated as

$$\begin{aligned}
\mathbf{P1}: \max_{\mathbf{x},\mathbf{P},\boldsymbol{\mathcal{E}},\mathbf{G}} \quad & \mathcal{U}\left(\mathbf{x},\mathbf{P},\boldsymbol{\mathcal{E}},\mathbf{G}\right), \\
\text{s.t.} \quad & \text{C1}: \sum_{m=1}^{M+1}x_{jm}\tau_{jm}\geq\overline{\tau}_{\min},\ \forall j, \\
& \text{C2}: \sum_{m=1}^{M+1}x_{jm}=1,\ \forall j, \\
& \text{C3}: P_m+\sum_{m'=1,m'\neq m}^{M+1}\mathcal{E}_{mm'}\leq G_m+ \\
& \qquad E_m+\beta_{\mathcal{E}}\sum_{m'=1,m'\neq m}^{M+1}\mathcal{E}_{m'm},\ \forall m, \\
& \text{C4}: \sum_{j=1}^{N}x_{jm}P_{jm}=P_m,\ \forall m, \\
& \text{C5}: x_{jm}\in\{0,1\},\forall j,\forall m, \\
& \text{C6}: G_m\geq 0,\mathcal{E}_{mm'}\geq 0,\forall j,\forall m, \\
& \text{C7}: 0\leq P_m\leq P_{\max}^{m},P_{jm}\geq 0,\forall j,\forall m,
\end{aligned} \tag{5.8}$$

where $\mathbf{x}=[x_{jm}]$, $\mathbf{P}=[P_{jm}]$, $\boldsymbol{\mathcal{E}}=\left[\mathcal{E}_{mm'}\right]$, $\mathbf{G}=[G_m]$, $\overline{\tau}_{\min}$ denotes the required minimum data rate for a UE, $P_{\max}^{m}$ is the maximum transmit power of the BS m. Constraint C1 guarantees the data rate performance of UEs. C2 and C5 ensure that each UE cannot be associated with multiple BSs. C3 is the energy consumption constraint and C4 is the

power allocation under NOMA principle in a cell. C6 indicates that the consumed grid energy and transferred energy are non-negative values, and C7 is the maximum transmit power constraint.

From the objective of **P1** and its constraint C3, It is shown that when more renewable energy is harvested and shared between BSs, the total grid energy consumption of the network can be reduced, which boosts the energy efficiency.

5.3 User Association under Fixed Transmit Powers

P1 is a mixed integer non-linear programming (MINLP) problem, and constitutes a challenging problem. In this section, It is assumed that the transmit power is fixed, and accordingly the original problem **P1** can be simplified as

$$\begin{aligned} \mathbf{P2}: \max_{\mathbf{x},\boldsymbol{\mathcal{E}},\mathbf{G}} \quad & \mathcal{U}\left(\mathbf{x},\boldsymbol{\mathcal{E}},\mathbf{G}\right) \\ \text{s.t.} \quad & \text{C1, C2, C3, C4, C5, C6.} \end{aligned} \tag{5.9}$$

The problem **P2** is still a combinatorial problem due to its discrete nature. To efficiently solve it, a decomposition approach is adopted. For a given $\mathbf{G}$ and $\boldsymbol{\mathcal{E}}$, the above problem can be rewritten as

$$\begin{aligned} \mathbf{P2.1}: \max_{\mathbf{x}} \quad & \mathcal{U}\left(\mathbf{x}\right) \\ \text{s.t.} \quad & \text{C1, C2, C4, C5.} \end{aligned} \tag{5.10}$$

5.3.1 Lagrangian Dual Analysis

Based on **P2.1**, the Lagrangian function can be written as

$$L\left(\mathbf{x},\boldsymbol{\lambda},\boldsymbol{\theta}\right)=\mathcal{U}\left(\mathbf{x}\right)-\sum_{j=1}^{N}\lambda_j\left(\overline{\tau}_{\min}-\sum_{m=1}^{M+1}x_{jm}\tau_{jm}\right)-\sum_{m=1}^{M+1}\theta_m\left(\sum_{j=1}^{N}x_{jm}P_{jm}-P_m\right), \tag{5.11}$$

where λ_j and θ_m are the non-negative Lagrange multipliers. Then, the dual function is given by

$$g\left(\boldsymbol{\lambda},\boldsymbol{\theta}\right)=\begin{cases}\max\limits_{\mathbf{x}} L\left(\mathbf{x},\boldsymbol{\lambda},\boldsymbol{\theta}\right)\\ \text{s.t. C2, C5}\end{cases}, \tag{5.12}$$

and the dual problem of **P2.1** is expressed as

$$\min_{\boldsymbol{\lambda},\boldsymbol{\theta}} g\left(\boldsymbol{\lambda},\boldsymbol{\theta}\right). \tag{5.13}$$

Given the dual variables λ_j and θ_m, the optimal solution for maximising the Lagrangian w.r.t. $\mathbf{x}$ is

$$x_{jm}^{*}=\begin{cases}1, & \text{if} \quad m=m^{*}\\ 0, & \text{otherwise}\end{cases}, \tag{5.14}$$

where $m^{*}=\underset{m}{\operatorname{argmax}}\left(\mu_{jm}\right)$ with

$$\mu_{jm}=\tau_{jm}/\sum_{m=1}^{M+1}G_m+\lambda_j\tau_{jm}-\theta_m P_{jm}. \tag{5.15}$$

The solution of (5.14) can be intuitively interpreted based on the fact that given the grid energy consumption, UEs select BSs which provide the maximum data rates. Since the objective of the dual problem is not differentiable, the subgradient method is utilised to

obtain the optimal solution $(\boldsymbol{\lambda}^*, \boldsymbol{\theta}^*)$ of the dual problem, which is given by

$$\lambda_j(t+1) = \left[\lambda_j(t) - \delta(t)\left(\sum_{m=1}^{M+1} x_{jm}\tau_{jm} - \overline{\tau}_{\min}\right)\right]^+, \tag{5.16}$$

$$\theta_m(t+1) = \left[\theta_m(t) - \delta(t)\left(P_m - \sum_{j=1}^{N} x_{jm}P_{jm}\right)\right]^+, \tag{5.17}$$

where $[a]^+ = \max\{a, 0\}$, t is the iteration index, and $\delta(t)$ is the step size. Note that there exist several step size selections such as constant step size and diminishing step size. Here, the nonsummable diminishing step length is used [BM08].

After obtaining the optimal $(\boldsymbol{\lambda}^*, \boldsymbol{\theta}^*)$ based on (5.16) and (5.17), the corresponding $\mathbf{x}$ is the solution of the primal problem **P2.1**. Therefore, based on the Lagrangian dual analysis, user association can be determined in a centralised or distributed way. The centralised user association is intuitive, and requires a central controller, which has the global CSI and determines which UE is connected to a BS in this network. In this chapter, A distributed user association algorithm is proposed which does not require any centralized coordination, as summarised in Algorithm 5. Since our problem satisfies the conditions of the convergence proof in [BM08], the convergence of the proposed algorithm is guaranteed. The complexity of the proposed algorithm is $\mathcal{O}((M+1)N)$ for each iteration and the convergence is fast (less than 40 iterations in the simulation), which is much lower than the brute force algorithm $\mathcal{O}\left((M+1)^N\right)$. Note that the broadcast operations have negligible effect on computational complexity.

5.3.2 Genetic Algorithm

In this subsection, a genetic algorithm (GA)-based user association is developed to solve the problem **P2.1**. Such algorithm will be compared with the proposed Algorithm 5. GA can achieve good performance when the population of candidate solutions is sufficient [YHY05]. Specifically, each feasible chromosome represents a possible solution

Algorithm 5 Distributed User Association

Step 1: At UE side

if $t = 0$
  Initialise $\lambda_j(t)$, $\forall j$. Each UE measures its received inter-cell interference via pilot signal from all BSs, and feedbacks the CINR values to the corresponding BSs. Meanwhile, each UE selects the BS with the largest CINR value.
else
  UE j receives the values of μ_{jm} and τ_{jm} from BSs.
  Determines the serving BS m according to $m^* = \underset{m}{\operatorname{argmax}} (\mu_{jm})$.
  Update $\lambda_j(t)$ according to (6.16).
end if
$t \leftarrow t + 1$.
Each UE feedbacks the user association request to the chosen BS, and broadcasts the value of $\lambda_j(t)$.

Step 2: At BS side

if $t = 0$
  Initialise $\theta_m(t)$, $\forall m$.
else
  Receives the updated user association matrix $\mathbf{x}$.
  Updates $\theta_m(t)$ according to (6.17), respectively.
  Each BS calculates μ_{jm} and τ_{jm} under NOMA principle.
end if
$t \leftarrow t + 1$.
Each BS broadcasts the values of μ_{jm} and τ_{jm}.

that satisfies the constraints of problem **P2.1**, which is defined as

$$\mathcal{D}_i = \{[m_{1i}], [m_{2i}], \ldots, [m_{Ni}]\}, \; i \in \{1, \ldots, K\}, \tag{5.18}$$

where m_{ji} is the gene representing the index of the BS that the j-th UE is associated with, and it has an integer value varying from 1 to $M + 1$, and K is the population size. During each generation, the fitness of each chromosome is evaluated, to select high fitness chromosomes and produce higher fitness offsprings. Based on the objective of problem **P2.1**, the fitness value of the chromosome $\mathcal{D}_i$ is calculated as

$$\Phi_i (\mathcal{D}_i) = \mathcal{U} (\mathcal{D}_i). \tag{5.19}$$

Then, all chromosomes are ranked from the best to the worst with ranking r, based on their fitness values. The probability that a chromosome is selected as a parent to produce offspring is given by $\rho_s(r) = \frac{q(1-q)^{r-1}}{1-(1-q)^K}$ with a predefined value q [YHY05]. In each generation process, a uniform crossover operation with the probability ρ_c is utilised to produce offspring by swapping and recombining genes based on the parental chromosomes. In addition, a uniform mutation operation with the probability ρ_m is employed. Such generation procedure is repeated until reaching the maximum number of generations, and is summarised in Algorithm 6. Given the maximum number of generations Ω and fixed population size K, the complexity of the proposed algorithm is $\mathcal{O}(\Omega K \log(K))$ [GD91]. The performance of the GA-based user association algorithm heavily depends on the population size and number of generations, due to the inherent nature of GA [YHY05]. In the simulation results of Section V, it will be demonstrated that overall, the proposed Algorithm 5 outperforms GA-based Algorithm 6 when the population size of GA is not very large, and thus has lower complexity.

Algorithm 6 GA-based User Association

if $t = 0$
  Initialise a set of feasible chromosomes $\{\mathcal{D}_i\}$ with population size K, and the maximum number of generations $t_{\max}$.
else
  Rank $\{\mathcal{D}_i\}$ based on the fitness values given by (5.19).
  Based on the selection probability $\rho_s(r)$, chromosomes are selected to produce offspring via uniform crossover and mutation operations.
  if exceed the maximum number of generations
    $x^*_{jm} := \{\mathcal{D}^*_i\}$, where $\{\mathcal{D}^*_i\}$ is the feasible chromosome with the highest fitness value.
    break
  else
    $t \leftarrow t + 1$.
  end if
end if

The aforementioned approach provides user association solutions for problem **P2.1**. After obtaining the user association solution $\mathbf{x} = \left[x^*_{jm}\right]$, the corresponding pair $(\mathbf{G}, \boldsymbol{\mathcal{E}})$

is obtained by solving the following simple linear programming (LP):

$$\mathbf{P2.2}: \min_{\boldsymbol{\mathcal{E}},\mathbf{G}} \quad \sum_{m=1}^{M+1} G_m \tag{5.20}$$
$$\text{s.t.} \quad \text{C3}, \text{C6}.$$

The problem **P2.2** can be efficiently solved by using existing software, e.g. CVX [GB].

When no energy cooperation is allowed, i.e., $\mathcal{E}_{mm'} = 0, \forall j, \forall m$, the optimal grid energy consumption $\mathbf{G}$ of problem **P2.2** under the user association solution $\mathbf{x} = \left[x^*_{jm}\right]$ is directly obtained as

$$G^*_m = \left[P_m - E_m\right]^+, \tag{5.21}$$

where $P_m = \sum_{j=1}^{N} x^*_{jm} P_{jm}$.

Based on the solutions of subproblems **P2.1** and **P2.2**, an iterative algorithm is proposed to solve the problem **P2**, which is summarised in Algorithm 7.

Algorithm 7 Resource Allocation Algorithm under Fixed Transmit Power

if $t = 0$
  For a fixed $\mathbf{P}$, initialise $G_m, \forall j, m$.
else
  Determine $x_{jm}(t)$ under fixed $(\boldsymbol{\mathcal{E}}, \mathbf{G})$ by selecting the UE association algorithm from Algorithm 5 or Algorithm 6.
  Given $x_{jm}(t)$, update the energy allocation policy $(\boldsymbol{\mathcal{E}}, \mathbf{G})$ by solving the LP **P2.2** via CVX.
  if convergence
    Obtain optimal resource allocation policy $(\mathbf{x}^*, \boldsymbol{\mathcal{E}}^*, \mathbf{G}^*)$.
    break
  else
    $t \leftarrow t + 1$.
  end if
end if

5.4 Joint User Association and Power Control Scheme

In this section, the joint resource allocation and power control design is considered. Specifically, an algorithm to solve the MINLP problem **P1** is developed through the decomposition approach. As discussed in the previous section, first the user association indicators are determined given the resource allocation policy $(\mathbf{P}, \boldsymbol{\mathcal{E}}, \mathbf{G})$, which can be obtained by solving problem **P2.1** via Algorithm 5 or Algorithm 6. Then, under a fixed user association $\{x_{jm}\}$, the problem for optimising $(\mathbf{P}, \boldsymbol{\mathcal{E}}, \mathbf{G})$ is written as

$$\begin{aligned} \mathbf{P3}: \max_{\mathbf{P},\boldsymbol{\mathcal{E}},\mathbf{G}} \quad & \mathcal{U}\left(\mathbf{P}, \boldsymbol{\mathcal{E}}, \mathbf{G}\right) \\ \text{s.t.} \quad & \text{C1}, \text{C3}, \text{C4}, \text{C6}, \text{C7}. \end{aligned} \tag{5.22}$$

From the energy efficiency function, it can be found that the power allocation vectors $\mathbf{P}$ and $\mathbf{G}$ are coupled in the objective of problem **P3**. Thus, given $\mathbf{G}$ and $\boldsymbol{\mathcal{E}}$, the above problem can be decomposed into

$$\begin{aligned} \mathbf{P3.1}: \max_{\mathbf{P}} \quad & \sum_{m=1}^{M+1} \sum_{j=1}^{N} x_{jm} \tau_{jm} \\ \text{s.t.} \quad & \text{C1}, \text{C3}, \text{C4}, \text{C7}. \end{aligned} \tag{5.23}$$

Problem **P3.1** is non-convex. Hence a tractable suboptimal solution based on the Karush-Kuhn-Tucker (KKT) conditions is provided. The Lagrangian function of problem **P3.1** is

$$\begin{aligned} L\left(\mathbf{P}, \boldsymbol{\nu}, \boldsymbol{\chi}\right) = & \sum_{m=1}^{M+1} \sum_{j=1}^{N} x_{jm} \tau_{jm} - \sum_{j=1}^{N+1} \chi_j \Big(\overline{\tau}_{\min} - \sum_{m=1}^{M+1} x_{jm} \tau_{jm} \Big) \\ & - \sum_{m=1}^{M+1} \nu_m \Big(\sum_{j=1}^{N} x_{jm} P_{jm} - \varphi_m \Big), \end{aligned} \tag{5.24}$$

where $\varphi_m = \min \Big\{ G_m + E_m + \beta \mathcal{E} \sum\limits_{m'=1, m' \neq m}^{M+1} \mathcal{E}_{m'm} - \sum\limits_{m'=1, m' \neq m}^{M+1} \mathcal{E}_{mm'}, P_{\max}^{m} \Big\}$ according to constraints C3 and C7, and χ_j and ν_m are the non-negative Lagrange multipliers.

Without loss of generality, assuming that the j-th UE is associated with the BS m, i.e., $x_{jm} = 1$, based on the KKT conditions, I have

$$\frac{\partial L}{\partial P_{jm}} = (1+\chi_j)\left(\frac{W\Lambda_{jm}}{1+P_{jm}\Lambda_{jm}}\right) - \Theta_{jm}^{(1)} - \Theta_{jm}^{(2)} - \nu_m \log(2) = 0, \tag{5.25}$$

where $\Lambda_{jm} = \frac{|h_{jm}|^2}{I_{jm}^{(1)}+I_{jm}^{(2)}+\sigma^2}$ is referred to as the channel to interference plus noise ratio at the j-th UE. Based on (5.3) and (5.5), $\Theta_{jm}^{(1)}$ resulting from the intra-cell interference is given by

$$\Theta_{jm}^{(1)} = \sum_{\ell>j}^{k_m} (1+\chi_\ell)\frac{W\gamma_{\ell m}}{1+\gamma_{\ell m}}\Lambda_{lm}, \tag{5.26}$$

and $\Theta_{jm}^{(2)}$ resulting from the inter-cell interference is given by

$$\Theta_{jm}^{(2)} = \sum_{m'=1,m'\neq m}^{M+1}\sum_{j'=1}^{N} \frac{\left(1+\chi_{j'}\right)x_{j'm'}W\gamma_{j'm'}\left|h_{j'm'}^{m}\right|^2}{\left(1+\gamma_{j'm'}\right)\left(I_{j'm'}^{(1)}+I_{j'm'}^{(2)}+\sigma^2\right)}. \tag{5.27}$$

Based on (5.25), the transmit power allocated to the j-th user-stream in the m-th cell is obtained as

$$P_{jm}^{*} = \Big[\frac{(1+\chi_j)W}{\Theta_{jm}^{(1)}+\Theta_{jm}^{(2)}+\nu_m\log(2)} - \frac{1}{\Lambda_{jm}}\Big]^{+}. \tag{5.28}$$

In (5.28), the allocated transmit power is a monotonic function of ν_m. As such, given $\{\chi_j\}$, a one-dimension search scheme is adopted over the Lagrange multipliers $\{\nu_m\}$, which can efficiently obtain the optimal $\boldsymbol{\nu}^*$ that satisfies constraints C3 and C7. According to (5.28), it can be easily found that ν_m^* needs to satisfy $0 \leq \nu_m^* \leq \nu_m^{\max}$, where $\nu_m^{\max} = \max_j \Big\{ \left((1+\chi_j)W\Lambda_{jm} - \Theta_{jm}^{(1)} - \Theta_{jm}^{(2)}\right)/\log(2)\Big\}$. Here, $\nu_m^* = 0$ represents that there is no limitation about the transmit power of the j-th user-stream and $\nu_m^* = \nu_m^{\max}$ corresponds to the case that no transmit power is allocated to the j-th user-stream. Thus, by fixing $\{\chi_j\}$, $\boldsymbol{\nu}^*$ can be obtained by using Algorithm 8. For achieving a specific accuracy ς, the complexity of Algorithm 8 is $\mathcal{O}\left(\log\left(1/\varsigma\right)\right)$. After obtaining $\boldsymbol{\nu}^*$, the

Lagrange multiplier χ_j can be updated by using the subgradient method, which is similar to (5.16).

Algorithm 8 One-dimension Search Algorithm

if $t = 0$
  Given χ_j, initialise $\nu_m^l = 0, \nu_m^h = \nu_m^{\max}$, $\forall m$,
  and calculate $F_l = \sum_{j=1}^{N} x_{jm} P_{jm}^{*(l)}$ and $F_h = \sum_{j=1}^{N} x_{jm} P_{jm}^{*(h)}$,
  where $\left\{P_{jm}^{*(l)}\right\}$ and $\left\{P_{jm}^{*(h)}\right\}$ are the allocated transmit powers of
  the j-th UE's data stream for the cases of ν_m^l and ν_m^h respectively,
  which are calculated by using (5.28).
else
  while $F_l \neq \varphi_m$ and $F_h \neq \varphi_m$
    Let $\nu_m = \frac{\nu_m^l + \nu_m^h}{2}$, and compute F_m.
    if $F_m = \nu_m$
      The optimal dual variable ν_m^* is obtained.
      break
    elseif $F_m < \varphi_m$
      $\nu_m^h = \nu_m$.
    else $F_m > \varphi_m$
      $\nu_m^l = \nu_m$.
    end if
  end while
end if

To ensure the system stability, the Mann iterative method is utilised to update the transmit power in each iteration [HNS+12], which is given by

$$P_{jm}^{(\ell+1)} = (1 - \eta(\ell)) P_{jm}^{(\ell)} + \eta(\ell) P_{jm}^{*}, \tag{5.29}$$

where ℓ is the iteration index, $0 < \eta(\ell) < 1$ is the step size, which is usually chosen as $\eta(\ell) = \frac{\ell}{2\ell+1}$. After obtaining the optimal solution of problem **P3.1**, the corresponding $(\mathbf{G}, \boldsymbol{\mathcal{E}})$ can be updated by solving the LP problem **P2.2** via CVX. As such, the solution of problem **P3** can be iteratively obtained. Note that the convergence of KKT-based algorithm is usually faster than the gradient-based designs [KC06].

Based on the previous analysis, the proposed joint user association and power control scheme in energy cooperation enabled NOMA HetNets is summarised in Algorithm 9.

Algorithm 9 Joint User Association and Power Control

if $t = 0$
  Initialise $P_m, G_m, E_m, \forall m$
else
  Determine $x_{jm}(t)$ under $(\mathbf{P}, \mathbf{G}, \boldsymbol{\mathcal{E}})$ by selecting the UE association algorithm from Algorithm 1 or Algorithm 2.
  Given $x_{jm}(t)$ and the corresponding $(\mathbf{G}, \boldsymbol{\mathcal{E}})$, update the transmit power $\mathbf{P}$ based on the following rule:
    Loop:
    a) Given $\Theta_{jm}^{(2)}$, loop over UE j:
      i): Obtain $\{\nu_m^*\}$ using Algorithm 4 given $\{\chi_j\}$
      ii): Obtain P_{jm} according to (5.28) with $\{\nu_m^*, \chi_j\}$.
      iii): Update $\{\chi_j\}$ using subgradient method.
      iv): Update P_{jm} using (5.29).
      Until convergence.
    b) Update $\Theta_{jm}^{(2)}$ using (5.27).
    Until convergence.
  Based on the updated $\mathbf{P}$, update G_m and $\mathcal{E}_{mm'}$ by solving LP problem **P2.2** via CVX.
  if convergence
    Obtain optimal resource allocation policy $(\mathbf{x}^*, \mathbf{P}^*, \boldsymbol{\mathcal{E}}^*, \mathbf{G}^*)$.
    break
  else
    $t \leftarrow t + 1$.
  end if
end if

5.4.1 Comparison with FTPA

In 4G networks, fractional transmission power allocation (FTPA) scheme is adopted [SKB+13]. The rule of FTPA is that the transmit power will be allocated based on the UEs' channel conditions, i.e., the data signals of UEs with weaker downlink channels will own more transmit power. Based on the CINR order in (5.2), the transmit power allocated to the j-th UE's data stream in the m-th cell under FTPA protocol is expressed as [SKB+13]

$$P_{jm} = P_m \left(\frac{|h_{jm}|^2}{I_{jm}^{(2)} + \sigma^2} \right)^{-\alpha} / \sum_{l=1}^{N} x_{lm} \left(\frac{|h_{lm}|^2}{I_{lm}^{(2)} + \sigma^2} \right)^{-\alpha}, \tag{5.30}$$

where $0 \leq \alpha \leq 1$ is the decay factor. Here, $\alpha = 0$ represents equal power allocation. For larger α, the transmit power allocated to the data-stream of the UE with largest

CINR becomes lower, and more power will be allocated to the data-stream of the UE with the lowest CINR, in order to achieve the user-fairness and the optimal decoding. However, the detrimental effect of using such simple power allocation scheme is that distant UEs may receive worse inter-cell interference without power control among BSs, due to the fact that each BS has to assign larger transmit power to the far-away UEs. Therefore, compared to the single-cell NOMA case [DAP16], the inter-cell interference has a significant impact on the power allocation of multi-tier NOMA HetNets.

5.4.2 Comparison with No Renewable Energy

When there is no renewable energy harvesting (i.e., $E_m = 0,\ \forall m$), no renewable energy can be shared between BSs (i.e., $\mathcal{E}_{mm'} = \mathcal{E}_{m'm} = 0,\ \forall m, m^{'}$), and thus the required energy can only be supplied by the conventional grid. In this case, $P_m = G_m,\ \forall m$, and the original problem **P1** reduces to

$$\mathbf{P4}: \max_{\mathbf{x},\mathbf{P}} \quad \frac{\sum_{m=1}^{M+1}\sum_{j=1}^{N} x_{jm}\tau_{jm}}{\sum_{m=1}^{M+1}\sum_{j=1}^{N} x_{jm}P_{jm}} \tag{5.31}$$

$$\text{s.t.} \quad \text{C1}, \text{C2}, \text{C4}, \text{C5}, \text{C7}.$$

The above problem is non-linear fractional programming and non-deterministic polynomial (NP)-hard, which can be solved by using the proposed Algorithm 5 with $E_m = 0$ and $\mathcal{E}_{mm'} = \mathcal{E}_{m'm} = 0$.

5.4.3 Comparison with No Energy Cooperation

In this case, the energy transfer efficiency $\beta_{\mathcal{E}}$ is set to 0, which means that the harvested renewable energy cannot be transferred between BSs. Each BS is powered by the conventional grid and its harvested renewable energy, i.e., the transmit energy consumption at a BS needs to satisfy $P_m \leq G_m + E_m,\ \forall m$. Then, the proposed Algorithm 5 can still

Table 5-A: Simulation Parameters

Parameter	**Value**
Cell radius	500 m
System bandwidth W	10 MHz
Noise power density σ^2	-174 dBm/Hz
Path loss of MBS $\|h_{j1}\|^2$	$128.1 + 37.6\log_{10}d(\text{km})$
Path loss of PBS $\|h_{jm}\|^2$	$140.7 + 36.7\log_{10}d(\text{km})$
Max transmit power of MBS P_1	46 dBm [GMR+12]
Max transmit power of PBS P_m	30 dBm [GMR+12]

be applied to solve this problem, and during each iteration, the grid energy consumption is updated as $G_m = [P_m - E_m]^+$ based on the updated P_m.

5.5 Simulation Platform and Results

In this section, numerical results are presented to demonstrate the effectiveness of the proposed algorithm compared with other schemes as well as the conventional counterpart. Since the renewable energy arrival rate changes slowly in practice and is stationary at each information transmission time slot [ZZZ+16], the amounts of harvested energy at the MBS and PBSs are considered to be constant and each PBS has the same level of renewable energy during each transmission time slot for the sake of simplicity. Our analysis and proposed algorithm are independent of the specific renewable energy distribution. If there is no special circumstance, then the energy harvesting models of PBSs and MBSs are the same as Table 4-B in chapter 4. In the simulation, I focus on the large-scale channel fading condition in low mobility environment, due to the fact that user association is carried out in a large time scale and the small-scale fading can be averaged out [KSK11, LCC+15]. In addition, PBSs and UEs are uniformly distributed in a macrocell geographical area. Iteration number is 500. The basic simulation parameters are shown in Table 5-A.

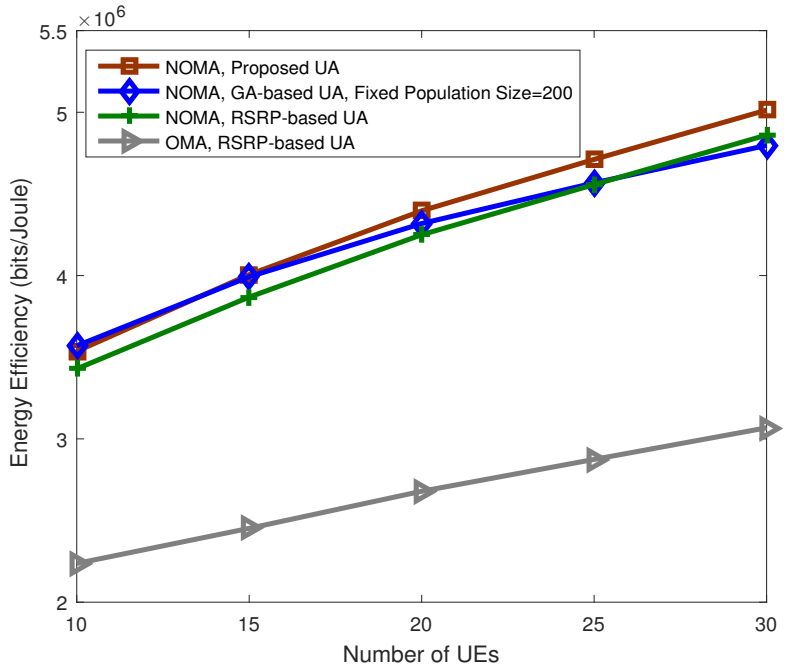

Figure 5.2: Energy efficiency versus the number of UEs for different user association algorithms.

5.5.1 User Association under Fixed Transmit Power

In this subsection, different user association algorithms under fixed transmit power are studied, i.e., power control is unavailable at BSs. Based on the NOMA power allocation condition in (5.3), it is defined that the total transmit power at each BS is $P_m = P_{\max}^m$, and adopt an arithmetic progression power allocation approach for the sake of simplicity, namely the transmit power of the j-th UE's data signal is $P_{jm} = \frac{2j}{k_m(1+k_m)} P_m, j \in \{1, 2, 3, ..., k_m\}$ when k_m UEs are multiplexed in the power domain of the m-th cell. Also the comparison with the conventional Reference Signal Received Power (RSRP) based user association is provided. The aim of this subsection is to show the performance for different user association algorithms under the same fixed power allocation condition.

Figure 5.2 shows the energy efficiency versus the number of UEs with the number of PBSs $M = 6$ and the energy transfer efficiency factor $\beta_{\mathcal{E}} = 0.9$. The minimum QoS is set as $\overline{\tau}_{\min} = 0.1$ bits/s/Hz and the amount of energy harvested by MBS and PBS as 37

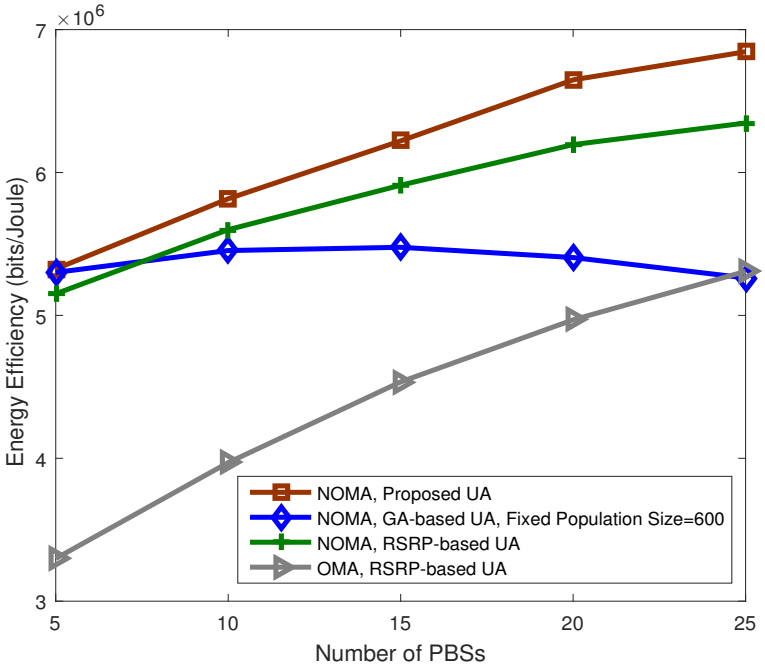

Figure 5.3: Energy efficiency versus the number of PBSs for different user association algorithms.

dBm and 27 dBm, respectively[1]. The maximum number of generations for the GA-based user association is 10, $q = 0.1$, and $\rho_c = \rho_m = 0.4$. The proposed user association scheme with NOMA achieves better energy efficiency than the other cases. The energy efficiency increases with the number of UEs because of the multiuser diversity gain (i.e., different UEs experience different path loss, and more UEs with lower path loss help enhance the overall energy efficiency.) [TV05]. The use of NOMA outperforms OMA. By using the GA-based user association, the energy efficiency slowly increases with the number of UEs, due to the fact that the efficiency of the GA-based algorithm depends on the population size [YHY05]. In other words, given the population size (e.g., $K = 200$ in this figure), the GA algorithm may not obtain good solutions when the number of UEs grows large, which indicates that larger populations of candidate solutions is needed [YHY05].

Figure 5.3 shows the energy efficiency versus the number of PBSs with the number

[1]In real networks, the renewable energy generation rate is constant during a certain period, and the time scale of the user association and power control process is much shorter, typically less than several minutes [KSK11, LCC+15]. In addition, the amount of energy harvested by a MBS is usually larger than that at a PBS, since MBS can fit larger solar panel [LCC+15, HA13a].

of UEs $N = 40$ and the energy transfer efficiency factor $\beta_{\mathcal{E}} = 0.9$. The minimum QoS is set as $\overline{\tau}_{\min} = 0.1$ bits/s/Hz and the amount of harvested energy at MBS and PBS as 37 dBm and 27 dBm, respectively. The maximum number of generations for GA is 10, $q = 0.1$, and $\rho_c = \rho_m = 0.4$. NOMA achieves higher energy efficiency than OMA, since NOMA can achieve higher spectral efficiency. The proposed user association algorithm outperforms the other cases, and the performance gap between the proposed user association and the conventional RSRP-based user association is larger when deploying more PBSs, due to the fact that the proposed user association can achieve more BS densification gains [ABC+14]. For the GA-based user association algorithm with the population size $K = 600$, solutions are inferior when the number of PBSs is large, as larger populations of candidate solutions are needed [YHY05].

5.5.2 Power Control under Fixed User Association

In this subsection, three power allocation schemes are considered, namely the power control method proposed in Section IV, FTPA and the conventional fixed transmit power, to confirm the advantages of our proposal. The conventional RSRP-based user association is adopted in the simulation, and all the considered cases experience the same user association condition. In addition, BSs use their maximum transmit powers in the OMA scenario, and the total transmit power of each BS for FTPA is set as $P_m = P_{\max}^m$, $m \in \{1, 2, 3, ..., M + 1\}$.

Figure 5.4 shows the energy efficiency versus the number of PBSs with the number of UEs $N = 50$ and the energy transfer efficiency factor $\beta_{\mathcal{E}} = 0.9$. The minimum QoS is set as $\overline{\tau}_{\min} = 1$ bits/s/Hz and the amount of energy harvested by MBS and PBS as 37 dBm and 27 dBm, respectively. It can be seen that by using NOMA with the proposed power control, energy efficiency rapidly increases with the number of PBS. The proposed algorithm achieves better performance than the other cases. When deploying more PBSs, the performance gap between the proposed solution and the other cases is larger, which indicates that the proposed power control algorithm can achieve more BS densification

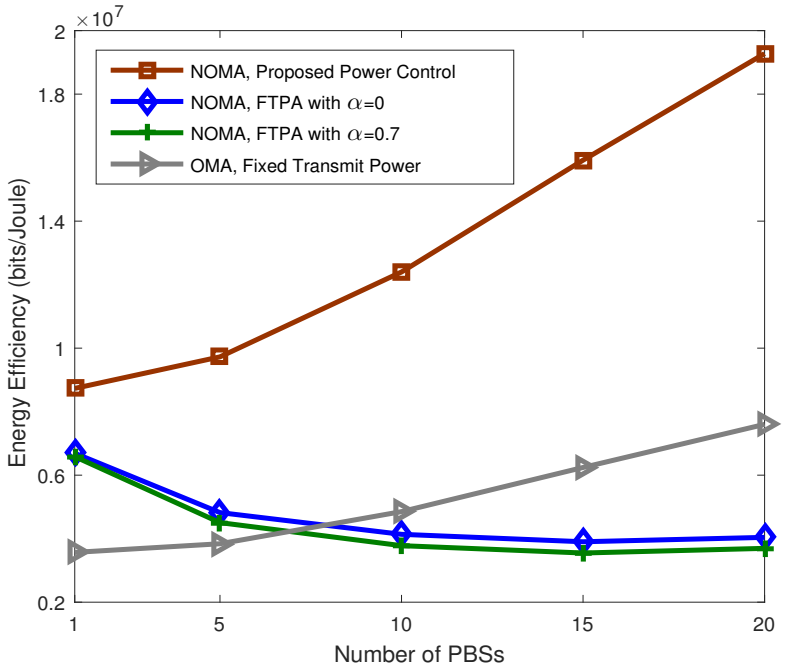

Figure 5.4: Energy efficiency versus the number of PBSs for different power allocation policies.

gains and efficiently coordinate the inter-cell interference. When the number of PBSs is not large, NOMA with FTPA can outperform the conventional OMA case, since NOMA can achieve better spectral efficiency than OMA [DAP16]. However, when adding more PBSs, NOMA with FTPA may not provide higher energy efficiency. The reason is that more UEs will be offloaded to picocells, and the inter-cell interference will become worse, which means that the transmit power of each user-stream needs to be larger to combat the inter-cell interference. As suggested in Section 5.4.1, FTPA with $\alpha = 0$ achieves higher energy efficiency of the network than the $\alpha = 0.7$ case, since the data-streams for UEs with poorer channel condition (i.e., lower CINR) have to be allocated more power in the case of FTPA with $\alpha = 0.7$, which reduces the total throughput of the network under the same energy consumption.

Figure 5.5 shows the energy efficiency versus the energy transfer efficiency factor $\beta_{\mathcal{E}}$ with the number of PBSs $M = 3$ and the number of UEs $N = 40$. The minimum QoS is set as $\overline{\tau}_{\min} = 1$ bits/s/Hz and the amount of harvested energy at MBS and

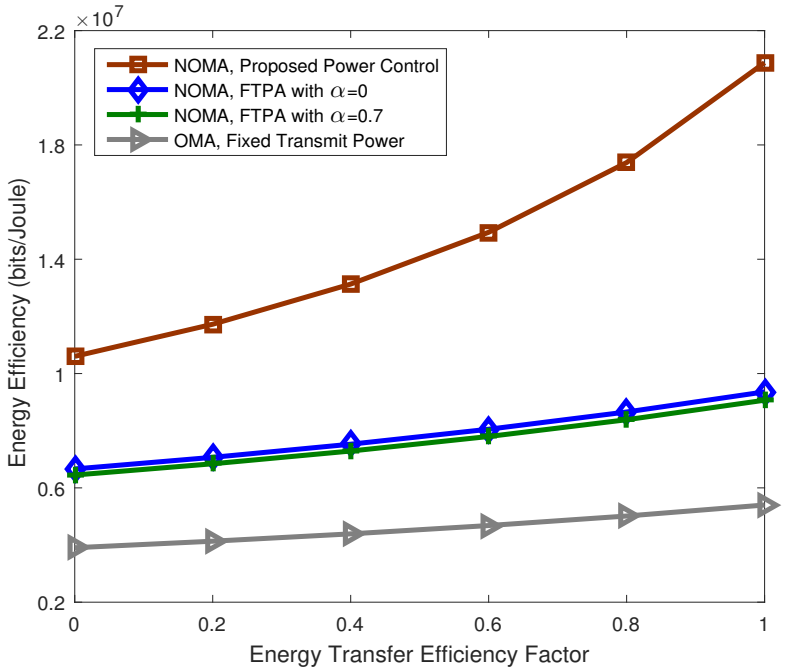

Figure 5.5: Energy efficiency versus energy transfer efficiency factor for different power allocation policies.

PBS to 40 dBm and 35 dBm, respectively. Compared to the no energy cooperation case (i.e., $\beta_{\mathcal{E}} = 0$), the use of energy cooperation can enhance the energy efficiency, particularly when the energy transfer efficiency factor is large. The implementation of NOMA can achieve higher energy efficiency than the conventional OMA system because of higher spectral efficiency, and the proposed power control algorithm outperforms the other cases. Moreover, the energy efficiency grows at a much higher speed when applying the proposed algorithm. For a specified $\beta_{\mathcal{E}}$, FTPA with $\alpha = 0$ achieves higher energy efficiency of the network than the $\alpha = 0.7$ case, as suggested in Figure 5.4.

Figure 5.6 shows the tradeoff between the energy efficiency and the minimum QoS with the number of PBSs $M = 3$ and the number of UEs $N = 30$. The energy transfer efficiency factor is set to $\beta_{\mathcal{E}} = 0.9$ and the amount of energy harvested by MBS and PBS to 37 dBm and 27 dBm, respectively. For a given minimum QoS, the proposed power control under NOMA achieves higher energy efficiency than conventional OMA. When better QoS is required by the UE, energy efficiency of both NOMA and OMA cases

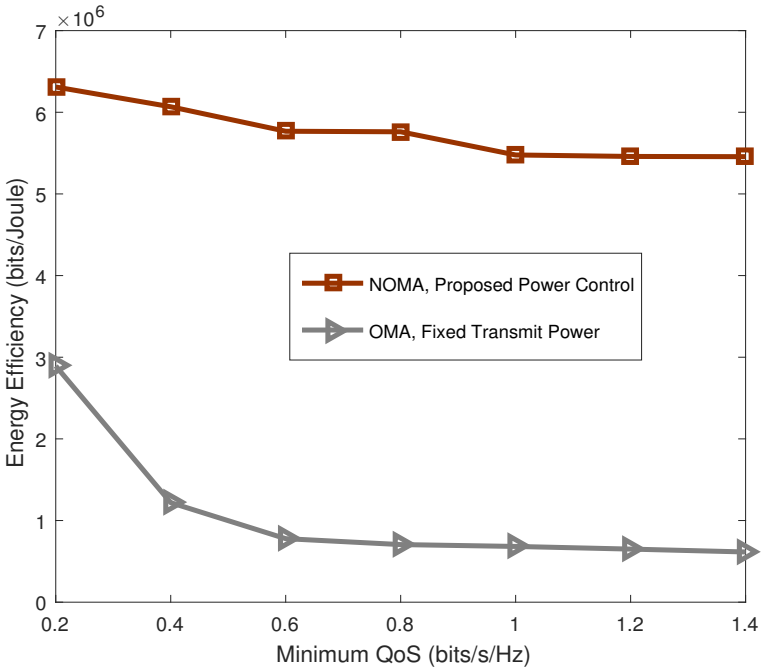

Figure 5.6: Tradeoff between the energy efficiency and the minimum QoS for NOMA and OMA.

decreases. The reason is that for the proposed solution, more transmit power will be allocated to the UEs with lower CINRs to achieve such minimum QoS, which results in more energy consumption; for conventional OMA, it means that more UEs cannot obtain the desired QoS and have to experience outage. It can be seen that energy efficiency decreases significantly in the low minimum QoS regime, because many UEs receive low QoS and increasing the level of the minimum QoS means that these UEs cannot be served. In practice, the minimum QoS can be found in an off-line manner [NLS12].

5.5.3 Joint User Association and Power Control

In this subsection, the benefits of joint user association and power control design in energy cooperation enabled NOMA HetNets are examined. Also comparisons by considering different power allocation schemes with the conventional RSRP-based user association are presented. In the OMA scenario, transmit power at the BS is set to $P_m = P_{\max}^m$ in the OMA scenario.

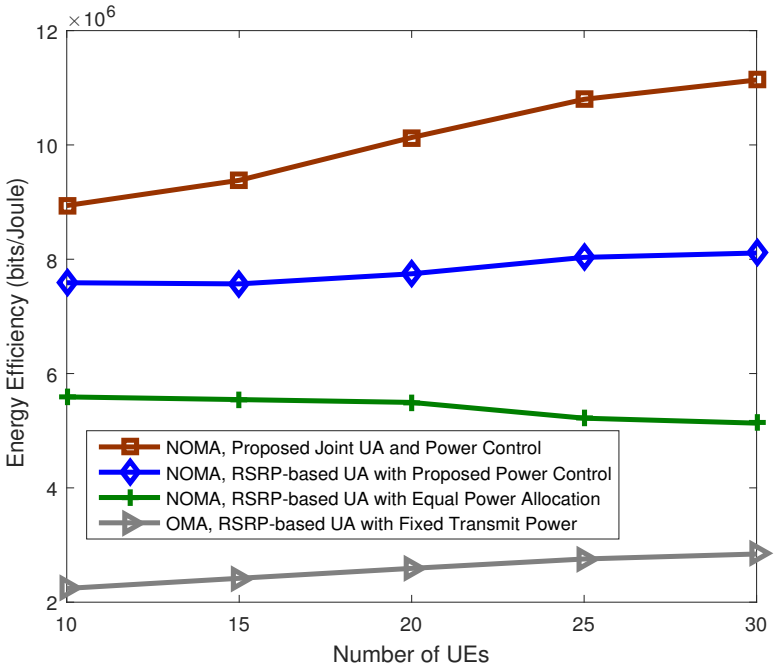

Figure 5.7: Energy efficiency versus the number of UEs for different joint user association and power allocation designs.

Figure 5.7 shows the energy efficiency versus the number of UEs with the number of PBSs $M = 5$ and the energy transfer efficiency factor $\beta_{\mathcal{E}} = 0.9$. The minimum QoS is set as $\overline{\tau}_{\min} = 0.5$ bits/s/Hz and the amount of harvested energy at MBS and PBS as 32 dBm and 22 dBm, respectively. It can be seen that the proposed joint user association and power control algorithm achieves higher energy efficiency than the other cases, and significantly improves the performance when more UEs are served in the network. The reason is that the proposed algorithm is capable of obtaining larger multiuser diversity gains. The use of NOMA can obtain higher energy efficiency than the OMA case, due to NOMA's capability of achieving higher spectral efficiency. Additionally, when equal power allocation is adopted in NOMA HetNets with the conventional RSRP-based user association, energy efficiency decreases with increasing the number of UEs of the network, which can be explained by the fact that given the total transmit power of a BS, the transmit power allocated to the data-streams of the UEs with better channel condition reduces when more UEs are served simultaneously.

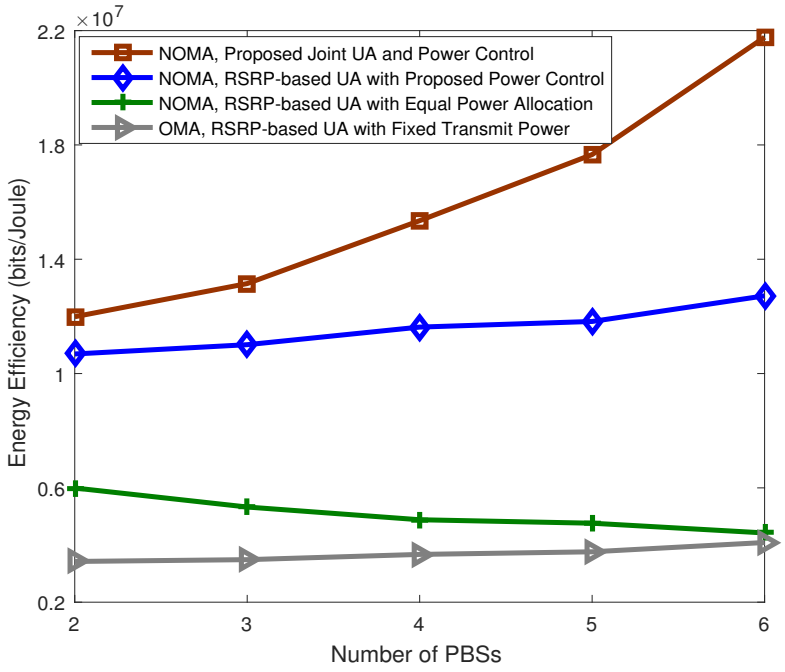

Figure 5.8: Energy efficiency versus the number of PBSs for different joint user association and power allocation designs.

Figure 5.8 shows the energy efficiency versus the number of PBSs with the number of UEs $N = 50$ and the energy transfer efficiency factor $\beta_{\mathcal{E}} = 0.9$. The minimum QoS is set as $\overline{\tau}_{\min} = 0.1$ bits/s/Hz and the amount of energy harvested by MBS and PBS as 37 dBm and 27 dBm, respectively. The proposed design outperforms the other cases. By using the proposed joint user association and power control with NOMA, the energy efficiency significantly increases with the PBS number, since the proposed design can obtain more BS densification gains. Again, the use of NOMA achieves better performance than OMA. For the case of RSRP-based user association with NOMA and equal power allocation, energy efficiency decreases with increasing the number of PBSs, because the inter-cell interference has a big adverse effect on the NOMA transmission [SVL+17].

5.6 Summary

This chapter studies user association and power control in energy cooperation aided two-tier HetNets with NOMA. A distributed user association algorithm is proposed based on the Lagrangian dual analysis, which does not require a central controller. Then, a joint user association and power control algorithm is proposed which achieves higher energy efficiency performance than the existing schemes. Simulation results show that the proposed algorithm can efficiently coordinate the intra-cell and inter-cell interference and has the capability of exploiting the multiuser diversity and BS densification. The application of NOMA can achieve larger energy efficiency than OMA due to the higher spectral efficiency of NOMA.

Chapter 6

Resource Allocation in Energy Cooperation Enabled Caching HetNets

6.1 Overview

In this chapter an optimisation problem for joint user association and power control in cache-enabled heterogeneous networks (HetNets) with energy cooperation is formulated, which aims at maximising the network throughput while minimising the conventional grid energy consumption. Simulation results demonstrate that the proposed joint user association and power control algorithm can significantly enhance the sum data rate and the energy efficiency of the whole network.

6.2 System Model and Problem Formulation

A cache-enabled energy-cooperative HetNet is considered consisting of macro base stations (MBSs) and pico BSs (PBSs), where each BS equips with a cache to store content files. Let $\mathcal{B}$ and $\mathcal{U}$ denote the set of BSs and the set of user equipment (UEs), respectively. The cache size of each MBS and PBS are L_{M} and L_{S} respectively. In such networks, each BS is powered by both the conventional grid and renewable energy sources, and energy can be shared between BSs via the smart grid.

6.2.1 Caching Strategy

It is assumed that there is a finite content library denoted as $\boldsymbol{\mathcal{F}} = \{\mathcal{F}_1, \ldots, \mathcal{F}_f, \ldots, \mathcal{F}_F\}$, where $\mathcal{F}_f$ is the f-th content and the number of contents is F. Each content has unit size and the number of contents that can be cached locally by a BS is usually lower than F in practice [CLQK17]. The probability that a content f is requested by a UE is denoted as $p_f\,(0 \leq p_f \leq 1)$, and $\sum_{f=1}^{F} p_f = 1$.

The probabilistic caching strategy is considered, i.e., the probability that a specific content f is cached by BS i is $0 \leq q_{f_i} \leq 1$. Let L_i denote the cache size of BS i. In this caching strategy, $\{q_{f_i}\}$ for BS i needs to satisfy the following conditions[BG15]:

$$\sum_{f=1}^{F} q_{f_i} \leq L_i,\ \forall i \in \mathcal{B}, f \in \boldsymbol{\mathcal{F}}, \tag{6.1}$$

where $L_i = L_{\mathrm{M}}$ if the serving BS i is MBS, and otherwise $L_i = L_{\mathrm{S}}$. According to the law of total probability, the hit probability that BS i stores the content requested by a UE is $\sum_{f=1}^{F} p_f q_{f_i}$.

6.2.2 Energy Model

Similar to the previous chapter, here, each BS draws energy from both the conventional grid and renewable energy sources. Also, for simplicity, the implicit multiplication by 1 time slot is omitted when converting between power and energy [RCZ18]. During each transmission time slot, the transmit power of BS i is P_i ($i \in \mathcal{B}$), the conventional grid energy consumed by BS i is G_i, and the energy harvested by BS i from renewable energy sources is E_i. The energy transferred from BS i to BS $i^{'}$ is $\mathcal{E}_{ii'}$, and the energy transfer efficiency factor between BSs is $\beta \in [0, 1]$. In addition, it is assumed that there is no energy storage [XZ15b], and the energy cooperation problem in each time slot is independent. As such, the transmit power at the i-th BS should satisfy

$$P_i < G_i + E_i + \beta \sum_{i' \in \mathcal{B}, i' \neq i} \mathcal{E}_{i'i} - \sum_{i' \in \mathcal{B}, i' \neq i} \mathcal{E}_{ii'}. \tag{6.2}$$

6.2.3 Problem Formulation

Since the maximisation of the network throughput will give rise to severe data rate imbalance among UEs [GSSBH11], a proportionally fair network throughput is considered, which is the sum of the logarithmic throughput over all UEs, to alleviate the data rate imbalance problem. Let $x_{ij} (i \in \mathcal{B}, j \in \mathcal{U})$ denote the binary user association indicator, i.e. $x_{ij} = 1$ when UE j is associated with BS i and otherwise it is zero. Then, $k_i = \sum_{j \in \mathcal{U}} x_{ij}$ denotes the number of UEs served by the BS i, and $\left(\sum_{f=1}^{F} p_f q_{f_i} \right)^{k_i}$ is the probability that k_i associated UEs can be served by BS i that caches their requested contents[1]. When $x_{ij} = 1$, the data rate of the j-th UE can be defined as $\mu_{ij} = \log (R_{ij})$

[1]Note that when some UEs request the same content, they may still have different demand on SINR and data rates. For simplicity, it is assumed that user-streams are independent.

with the data rate R_{ij}. Here, the date rate R_{ij} (in bits/s) of the j-th UE is given by

$$R_{ij} = \left(\sum_{f=1}^{F} p_f q_{f_i} \right)^{k_i} \frac{B}{\sum\limits_{j \in \mathcal{U}} x_{ij}} \log\left(1 + \gamma_{ij}\right) \tag{6.3}$$

with the signal-to-interference-plus-noise ratio (SINR)

$$\gamma_{ij} = \frac{P_i h_{ij}}{\sum\limits_{i' \in \mathcal{B}, i' \neq i} P_{i'} h_{i'j} + \sigma^2}, \tag{6.4}$$

where B is the system bandwidth, h_{ij} is the channel gain between UE j and its associated BS i, $h_{i'j}$ is the interfering channel gain between UE j and BS $i^{'}$, and σ^2 is the noise power. It is seen that the level of data rate depends on both channel conditions and hit probability, and the hit probability has a big impact on the throughput in cache-enabled cellular networks, as indicated by (6.3).

Our aim is to maximise the network throughput while minimising the overall grid

energy consumption, which is formulated as

$$\begin{aligned}
\mathbf{P1}: \quad & \max_{\mathbf{q},\mathbf{x},\mathbf{P},\boldsymbol{\mathcal{E}},\mathbf{G}} \sum_{i\in\mathcal{B}}\sum_{j\in\mathcal{U}} x_{ij}\mu_{ij} - \eta\sum_{i\in\mathcal{B}} G_i, \qquad (6.5)\\
& \text{s.t. C1}: \sum_{i\in\mathcal{B}} x_{ij}\gamma_{ij} \geq \gamma_{\min},\ \forall j\in\mathcal{U},\\
& \quad \text{C2}: \sum_{i\in\mathcal{B}} x_{jm} = 1,\ \forall j\in\mathcal{U},\\
& \quad \text{C3}: P_i < G_i + \beta \sum_{i'\in\mathcal{B},i'\neq i} \mathcal{E}_{i'i}\\
& \qquad\qquad - \sum_{i'\in\mathcal{B},i'\neq i} \mathcal{E}_{ii'} + E_i, \forall i\in\mathcal{B},\\
& \quad \text{C4}: \sum_{f=1}^{F} q_{f_i} \leq L_i, \forall i\in\mathcal{B}, f\in\boldsymbol{\mathcal{F}},\\
& \quad \text{C5}: 0\leq q_{f_i}\leq 1,\ \forall f\in\boldsymbol{\mathcal{F}}, \forall i\in\mathcal{B},\\
& \quad \text{C6}: x_{ij}\in\{0,1\}, \forall i, \forall j\in\mathcal{U},\\
& \quad \text{C7}: G_i\geq 0, \mathcal{E}_{ii'}\geq 0, \forall i\in\mathcal{B},\\
& \quad \text{C8}: 0\leq P_i\leq P_{\max}^{i}, \forall i\in\mathcal{B},
\end{aligned}$$

where $\mathbf{q}=[q_{f_i}]$, $\mathbf{x}=[x_{ij}]$, $\mathbf{P}=[P_i]$, $\boldsymbol{\mathcal{E}}=\left[\mathcal{E}_{ii'}\right]$, $\mathbf{G}=[G_i]$. According to (6.2), grid energy consumption depends on harvested energy, transferred energy and the transmit powers of BSs. η is a weighted parameter that provides a tradeoff between the network throughput and the grid energy consumption, and $\gamma_{\min}$ denotes the minimum SINR required by a UE. Constraint C1 guarantees the data rate requirement; C2 and C6 ensure that each UE cannot be associated with multiple BSs; C3 is the energy consumption constraint; C4 and C5 are the probabilistic caching constraints, as mentioned in (6.1); C7 indicates that the consumed grid energy and transferred energy are non-negative values, and C8 is the maximum transmit power constraint.

6.3 Joint User Association and Power Control Scheme

In this section, an algorithm is proposed to solve problem **P1**. By setting $k_i = \sum_{j\in\mathcal{U}} x_{ij}$, problem **P1** can be equivalently expressed as

$$\begin{aligned}\mathbf{P2}: \max_{\mathbf{q},\mathbf{x},\mathbf{P},\boldsymbol{\mathcal{E}},\mathbf{G}} & \sum_{i\in\mathcal{B}}\sum_{j\in\mathcal{U}} x_{ij}\log\left(c_{ij}\right) + \sum_{i\in\mathcal{B}} k_i^2 \log\left(\sum_{f=1}^{F} p_f q_{f_i}\right) \\ & - \sum_{i\in\mathcal{B}} k_i \log\left(k_i\right) - \eta\sum_{i\in\mathcal{B}} G_i, \qquad (6.6)\\ \text{s.t.} \quad & \text{C1, C2, C3, C4, C5, C6, C7, C8,} \\ & \text{C9}: \sum_{j\in\mathcal{U}} x_{ij} = k_i, \forall i,\end{aligned}$$

where $c_{ij} = B\log\left(1+\gamma_{ij}\right)$.

6.3.1 Content Placement and User Association

Problem **P2** is a mixed integer non-linear programming (MINLP) problem and non-convex. To solve it, a decomposition approach is adopted. Given $\{\mathbf{P}, \boldsymbol{\mathcal{E}}, \mathbf{G}\}$ in problem **P2**, first the following joint content placement and user association problem is addressed,

$$\begin{aligned}\mathbf{P2.1}: \quad & \max_{\mathbf{q},\mathbf{x}} \sum_{i\in\mathcal{B}}\sum_{j\in\mathcal{U}} x_{ij}\log\left(c_{ij}\right) + \sum_{i\in\mathcal{B}} k_i^2 \log\left(\sum_{f=1}^{F} p_f q_{f_i}\right) \\ & - \sum_{i\in\mathcal{B}} k_i \log\left(k_i\right), \qquad (6.7)\\ & \text{s.t.} \quad \text{C1, C2, C4, C5, C6, C9.}\end{aligned}$$

To solve problem **P2.1**, the following lemma is needed:

Lemma 3. *Let $p_{(1)} \geq \cdots \geq p_{(f)} \geq \cdots \geq p_{(F)}$ represent the ordered probability that the content (f) is requested by a UE, the optimal content placement solution of problem*

P2.1 *is*

$$q_{f_i}^* = \begin{cases} 1, & f_i = (1), \ldots, (L_i) \\ 0, & otherwise \end{cases}, \forall i \in \mathcal{B}. \tag{6.8}$$

Proof. It can be found that the objective of problem **P2.1** is an increasing function of the hit probability $\sum_{f=1}^{F} p_f q_{f_i}$ under arbitrary user association $\mathbf{x}$. Based on the constraints C4 and C5, the contents can be divided into L_i groups $\mathcal{F}_l\,(l = 1, \ldots, L_i)$ at BS i, and the contents in $\mathcal{F}_l$ have greater request probability than $\mathcal{F}_{l+1}$, such that $\sum_{(f)\in\mathcal{F}_l} q^l_{(f)_i} = 1$, $\sum_{l=1}^{L_i} q^l_{(f)_i} = q_{(f)_i}$ and $\bigcup_{l=L_i} \mathcal{F}_l = \boldsymbol{\mathcal{F}}$. Then, I have $\sum_{f=1}^{F} p_f q_{f_i} = \sum_{l=1}^{L_i} \sum_{(f)\in\mathcal{F}_l} p_{(f)} q^l_{(f)_i} \leq \sum_{l=1}^{L_i} p_{(l)} \left(\sum_{(f)\in\mathcal{F}_l} q^l_{(f)_i} \right) \Rightarrow \sum_{f=1}^{F} p_f q_{f_i} \leq \sum_{l=1}^{L_i} p_{(l)}$, and the equality satisfies under (6.8). □

With the help of Lemma 3, problem **P2.1** can be equivalently rewritten as

$$\begin{aligned} \widetilde{\mathbf{P}}\mathbf{2.1}: \quad & \max_{\mathbf{x}} \sum_{i\in\mathcal{B}} \sum_{j\in\mathcal{U}} x_{ij} \log\left(c_{ij}\right) + \sum_{i\in\mathcal{B}} k_i^2 \log\left(\sum_{f=1}^{L_i} p_{(f)} \right) \\ & - \sum_{i\in\mathcal{B}} k_i \log\left(k_i\right), \\ & \text{s.t.} \quad \text{C1, C2, C6, C9.} \end{aligned} \tag{6.9}$$

The problem $\widetilde{\mathbf{P}}\mathbf{2.1}$ is combinatorial. To solve it, first its dual problem is analysed.

The Lagrangian function of problem $\widetilde{\mathbf{P}}\mathbf{2.1}$ is written as

$$\begin{aligned} \mathcal{L}\left(\mathbf{x}, \mathbf{k}, \boldsymbol{\mu}, \boldsymbol{\nu}\right) = & \sum_{i\in\mathcal{B}} \sum_{j\in\mathcal{U}} x_{ij} \log\left(c_{ij}\right) + \sum_{i\in\mathcal{B}} k_i^2 \log\left(\sum_{f=1}^{L_i} p_{(f)} \right) - \\ & \sum_{i\in\mathcal{B}} k_i \log\left(k_i\right) - \sum_{j\in\mathcal{U}} \mu_j \left(\gamma_{\min} - \sum_{i\in\mathcal{B}} x_{ij}\gamma_{ij} \right) - \\ & \sum_{i\in\mathcal{B}} \nu_i \left(\sum_{j\in\mathcal{U}} x_{ij} - k_i \right), \end{aligned} \tag{6.10}$$

where $\mathbf{k} = [\mathbf{k_i}]$, $\boldsymbol{\mu} = [\mu_j]$, $\boldsymbol{\nu} = [\nu_i]$, μ_j and ν_i are non-negative Lagrange multipliers.

Accordingly, the dual function $\mathcal{D}(\cdot)$ is

$$\mathcal{D}(\boldsymbol{\mu},\boldsymbol{\nu}) = \begin{cases} \max\limits_{\mathbf{x},\mathbf{k}} \mathcal{L}(\mathbf{x},\mathbf{k},\boldsymbol{\mu},\boldsymbol{\nu}) \\ \text{s.t. C2, C6.} \end{cases} \tag{6.11}$$

Thus, the dual problem of (6.9) is given by

$$\min_{\boldsymbol{\mu}\geq 0,\boldsymbol{\nu}\geq 0} \mathcal{D}(\boldsymbol{\mu},\boldsymbol{\nu}). \tag{6.12}$$

Given the dual variables μ_j and ν_i, the solution of maximising the Lagrangian with respect to (w.r.t.) $\mathbf{x}$ can be explicitly obtained as

$$x_{ij}^* = \begin{cases} 1, & \text{if} \quad i = i^* \\ 0, & \text{otherwise} \end{cases}, \tag{6.13}$$

where $i^* = \arg\max\limits_{i} (\log(c_{ij}) + \mu_j \gamma_{ij} - \nu_i)$. Taking the second-order derivative of the Lagrangian w.r.t. k_i yields

$$\frac{\partial^2 \mathcal{L}}{\partial k_i^2} = 2\log\left(\sum_{f=1}^{L_i} p_{(f)}\right) - \frac{1}{k_i}. \tag{6.14}$$

Since $\sum\limits_{f=1}^{L_i} p_{(f)} \leq 1$, I have $\frac{\partial^2 \mathcal{L}}{\partial k_i^2} < 0$, which means that the Lagrangian is a concave function of k_i. By setting $\frac{\partial \mathcal{L}}{\partial k_i} = 0$, the optimal k_i^* is given by

$$k_i^* = -\frac{W\left(-2\log\left(\sum\limits_{f=1}^{L_i} p_{(f)}\right) e^{\nu_i - 1}\right)}{2\log\left(\sum\limits_{f=1}^{L_i} p_{(f)}\right)}, \tag{6.15}$$

where $W(z)$ is the Lambert-W function representing the solution of $z = we^w$.

Based on (6.13), It can be found that $\mathcal{D}(\boldsymbol{\mu},\boldsymbol{\nu})$ is not a differentiable function of μ_j and ν_i, and the closed-form optimal solution $(\boldsymbol{\mu}^*,\boldsymbol{\nu}^*)$ does not exist. Thus, the subgradient

method is utilised to obtain $(\boldsymbol{\mu}^*, \boldsymbol{\nu}^*)$, which is given by

$$\mu_j(t+1) = \left[\mu_j(t) - \delta(t)\left(\sum_{i\in\mathcal{B}} x_{ij}(t)\gamma_{ij} - \gamma_{\min}\right)\right]^+, \tag{6.16}$$

$$\nu_i(t+1) = \left[\nu_i(t) - \delta(t)\left(k_i(t) - \sum_{j\in\mathcal{U}} x_{ij}(t)\right)\right]^+, \tag{6.17}$$

where $[a]^+ = \max\{a, 0\}$, t is the iteration index, and $\delta(t)$ is the step size. Note that in (6.16) and (6.17), $x_{ij}(t)$ and $k_i(t)$ are updated according to (6.13) and (6.15).

Based on the previous analysis, a distributed cache-enabled user association algorithm is developed, which is summarised in Algorithm 10. Since our problem satisfies the convergence conditions shown in [BM08], the convergence of the proposed algorithm is guaranteed and the convergence proof of the proposed algorithm is provided in Appendix A.

6.3.2 Power Allocation

In this subsection, the power allocation optimisation problem is studied. After obtaining the content placement and user association solution $\{\mathbf{q}, \mathbf{x}\}$ via the proposed approach in subsection 6.3.1, problem **P2** is expressed as

$$\begin{aligned} \mathbf{P2.2}: \quad & \max_{\mathbf{P},\boldsymbol{\mathcal{E}},\mathbf{G}} \sum_{i\in\mathcal{B}}\sum_{j\in\mathcal{U}} x_{ij}\log(c_{ij}) - \eta\sum_{i\in\mathcal{B}} G_i, \\ & \text{s.t.} \quad \text{C1, C3, C7, C8.} \end{aligned} \tag{6.18}$$

Problem **P2.2** is a non deterministic polynomial (NP)-hard problem w.r.t. $\{P_i\}$. To solve this problem, a decomposition approach is adopted. Firstly, given $\boldsymbol{\mathcal{E}}$ and $\mathbf{G}$, P_i is

Algorithm 10 Proposed User Association under Fixed Transmit Powers

Step 1: At UE side

1. **if** $t = 0$, **then**
2. Initialise $\mu_j(t)$, $\forall j$. Each UE measures its receive SINR via pilot signal from all BSs to calculate c_{ij}.
3. **else**
4. UE j receives the values of $\nu_i(t)$ via BS broadcast.
5 Determines the serving BS i according to $i^* = \arg\max_i \left(\log\left(c_{ij}\right) + \mu_j \gamma_{ij} - \nu_i\right)$.
6. Update $\mu_j(t)$ according to (6.16).
7. **end if**
8. $t \leftarrow t + 1$.
9. Each UE feedbacks the user association request to the chosen BS,

Step 2: At BS side

1. **if** $t = 0$, **then**
2. Initialise $\nu_i(t)$, $\forall i$.
3. **else**
4. Each BS calculates the value of $k_i\left(t\right)$ according to (6.15), in which the hit probability is calculated by using Lemma 3.
5. Receives the updated user association matrix $\mathbf{x}$.
6. Updates $\nu_i(t)$ according to (6.17), respectively.
7. **end if**
8. $t \leftarrow t + 1$.
9. Each BS broadcasts the values of $\nu_i\left(t\right)$.

optimised by solving the following problem:

$$\mathbf{P2.2-1}: \quad \max_{\mathbf{P}} \sum_{i\in\mathcal{B}} \sum_{j\in\mathcal{U}} x_{ij} \log\left(c_{ij}\right), \tag{6.19}$$

$$\text{s.t.} \quad \text{C1, C3, C8.}$$

Considering the fact that finding the global optimal solution of problem $\mathbf{P2.2-1}$ is challenging, a tractable suboptimal solution based on the Newton's direction is provided. As illustrated in [YKS13], such efficient approach has fast convergence, and can lead to good solutions. By dualising w.r.t. data rate constraint C1, first the problem is

transformed $\mathbf{P2.2-1}$ as

$$\begin{aligned}\widetilde{\mathbf{P}}\mathbf{2.2-1}: \ \max_{\mathbf{P}} & \sum_{i\in\mathcal{B}}\sum_{j\in\mathcal{U}} x_{ij}\log\left(c_{ij}\right) \\ & -\sum_{j\in\mathcal{U}}\theta_j\left(\gamma_{\min}-\sum_{i\in\mathcal{B}}x_{ij}\gamma_{ij}\right), \qquad (6.20)\\ \text{s.t.} \quad & 0\le P_i\le\varphi_i,\forall i,\end{aligned}$$

where $\{\theta_j\}$ are non-negative dual variables, and $\varphi_i=\min\Big\{P^i_{\max}, G_i+\beta\sum\limits_{i'\in\mathcal{B},i'\neq i}\mathcal{E}_{i'i}-\sum\limits_{i'\in\mathcal{B},i'\neq i}\mathcal{E}_{ii'}+E_i\Big\}$ based on constraints C3 and C8. Note that the appropriate θ_j can be obtained by using the subgradient method, similar to (6.16). For fixed θ_j, a power control solution based on the Newton's direction is provided. Let $f\left(P_i\right)$ denote the the object function of problem $\widetilde{\mathbf{P}}\mathbf{2.2-1}$. The first-order and the second-order partial derivatives of $f\left(P_i\right)$ w.r.t. P_i are calculated as

$$\begin{aligned}\frac{\partial f\left(P_i\right)}{\partial P_i}=&\sum_{j\in\mathcal{U}}\frac{\gamma_{ij}}{a_{ij}\left(1+\gamma_{ij}\right)}\frac{x_{ij}}{P_i}-\sum_{i'\in\mathcal{B},i'\neq i}\sum_{j\in\mathcal{U}}\frac{h_{ij}\gamma^2_{i'j}}{a_{i'j}\left(1+\gamma_{i'j}\right)h_{i'j}}\frac{x_{i'j}}{P_{i'}}+\\ &\sum_{j\in\mathcal{U}}\theta_j\gamma_{ij}\frac{x_{ij}}{P_i}-\sum_{i'\in\mathcal{B},i'\neq i}\sum_{j\in\mathcal{U}}\theta_j\frac{h_{ij}\gamma^2_{i'j}x_{i'j}}{h_{i'j}P_{i'}}, \qquad (6.21)\end{aligned}$$

and

$$\begin{aligned}\frac{\partial^2 f\left(P_i\right)}{\partial P_i^2}=&-\sum_{j\in\mathcal{U}}\frac{1+a_{ij}}{a^2_{ij}(1+\gamma_{ij})^2}\left(\frac{\gamma_{ij}}{P_i}\right)^2x_{ij}+\sum_{i'\in\mathcal{B},i'\neq i}\sum_{j\in\mathcal{U}}\frac{h^2_{ij}\gamma^3_{i'j}\left(2a_{i'j}+\gamma_{i'j}\left(a_{i'j}-1\right)\right)}{h^2_{i'j}P^2_{i'}a^2_{i'j}\left(1+\gamma_{i'j}\right)^2}x_{i'j}+\\ &\sum_{i'\in\mathcal{B},i'\neq i}\sum_{j\in\mathcal{U}}2\theta_j\frac{h^2_{ij}\gamma^3_{i'j}}{h^2_{i'j}P^2_{i'}}x_{i'j}, \qquad (6.22)\end{aligned}$$

respectively, where $a_{ij}=\log\left(1+\gamma_{ij}\right)$.

To guarantee the increment direction, the modified Newton's search direction is used given by $\Delta P_i=\frac{\partial f(P_i)}{\partial P_i}/\left|\frac{\partial^2 f(P_i)}{\partial P_i^2}\right|$. Then, the power control solution is updated according

to

$$P_i\left(\varrho+1\right)=\left[P_i\left(\varrho\right)+\delta\left(\varrho\right)\Delta P_i\right]_0^{\varphi_i}, \tag{6.23}$$

where ϱ denotes the iteration index, $\delta\left(\varrho\right)$ is the step size that can be determined by backtracking line search [BV04]. The optimal P_i^* can be obtained when reaching convergence. After obtaining the solution of problem $\mathbf{P2.2-1}$, the corresponding $(\boldsymbol{\mathcal{E}},\mathbf{G})$ can be updated by solving the linear program

$$\begin{aligned}\mathbf{P2.2-2}:\ &\min_{\boldsymbol{\mathcal{E}},\mathbf{G}}\sum_{i\in\mathcal{B}}G_i,\\ &\text{s.t. C3, C7.}\end{aligned} \tag{6.24}$$

The problem $\mathbf{P2.2-2}$ can be solved by using the existing convex softwares such as CVX [GB]. Thus, the solution of problem $\mathbf{P2.2}$ can be iteratively obtained.

6.3.3 Joint User Association and Power Allocation Scheme

Based on the analysis in subsections 6.3.1 and 6.3.2, a joint user association and power control algorithm is developed to maximise the network throughput while minimising the grid energy consumption of the network, which is shown in Algorithm 11. Note that as long as both user association and power control aim to the same objective function in every iteration, the overall algorithm is guaranteed to converge [YKS13].

6.4 Simulation Platform and Results

In this section, simulation results are presented to demonstrate the effectiveness of the proposed joint user association and power control algorithm. It is considered that the renewable energy of each BS is constant in each transmission time slot for simplicity. Our analysis and proposed algorithm are independent of the specific renewable energy

Algorithm 11 Joint User Association and Power Control

1: **if** $t = 0$
2: Initialise $P_i, G_i, E_i, \forall i$
3: **else**
4: Determine q_{f_i} and $x_{ij}(t)$ under $(\mathbf{P}, \mathbf{G}, \boldsymbol{\mathcal{E}})$ by using Algorithm 10.
5: Given $x_{ij}(t)$ and the corresponding $(\mathbf{G}, \boldsymbol{\mathcal{E}})$, update transmit power $\mathbf{P}$ based on the following rule:
Loop:
a) Given θ_j, loop over $i \in \mathcal{B}$:
ii): Update P_i according to (6.23). Until convergence.
b) Update θ_j via subgradient method. Until convergence.
6. Based on the updated $\mathbf{P}$, update G_i and $\mathcal{E}_{ii'}$ by solving the convex problem $\mathbf{P2.2-2}$ via CVX.
7: **if** convergence
8: Obtain optimal resource allocation policy $(\mathbf{q}^*, \mathbf{x}^*, \mathbf{P}^*, \boldsymbol{\mathcal{E}}^*, \mathbf{G}^*)$.
9: **break**
10: **else**
11: $t \leftarrow t + 1$.
12: **end if**
13: **end if**

distribution. The energy harvesting process at each BS is modeled as a stationary stochastic process followed by [ZPSY13b]. More details about the values of maximum and minimum harvested energy is mentioned in Table 4-B in chapter 4. In addition, It is assumed that the content popularity follows the Zipf distribution [LBS99], and the contents in the library $\boldsymbol{\mathcal{F}}$ are ordered based on popularity. Thus, the request probability that the f-th most popular content is $p_f = f^{-\alpha} / \sum_{f=1}^{F} f^{-\alpha}$ [LBS99], where α is the Zipf exponent to represent the popularity skewness. The performance of our proposed user association and power control scheme is compared with conventional reference signal received power (RSRP)-based user association and fixed transmit powers respectively. In the simulation, PBSs and UEs are uniformly distributed in a macrocell geographical area. Iteration number is 500 and basic simulation parameters are shown in Table 6-A.

First the impact of cache size for the proposed joint user association and power control algorithm is evaluated. In the simulation, the Zipf exponent is $\alpha = 0.9$, and the energy transfer efficiency factor is $\beta = 0.9$. For the case of RSRP-based user association with fixed transmit power, each BS uses its maximum transmit power to obtain higher

Table 6-A: Simulation Parameters

Parameter	**Value**
Cell radius	500 m
System bandwidth B	10 MHz
Noise power density σ^2	-174 dBm/Hz
Path loss of MBS i h_{ij}	$128.1 + 37.6\log_{10}d(\text{km})$
Path loss of PBS i h_{ij}	$140.7 + 36.7\log_{10}d(\text{km})$
Min SINR requirement $\gamma_{\min}$	0 dB
Max transmit power of MBS ${P^i}_{\max}$, i is MBS	46 dBm
Max transmit power of PBS ${P^i}_{\max}$, i is PBS	30 dBm
Content library size F	10^5

throughput. Figure 6.1 and 6.2 show the sum data rate and the corresponding energy efficiency versus cache size for different resource allocation schemes respectively. The UE number is $|\mathcal{U}| = 30$, PBS number is 7, and the MBS's cache size is $L_{\text{M}} = 8000$. The weighted parameter is set as $\eta = 1$. Figure 6.1 confirms that the use of proposed joint user association and power control algorithm can significantly enhance the throughput of the whole network, compared to the RSRP-based user association with/without power control cases, and the sum date rate increases with cache size. Figure 6.2 shows that the proposed joint user association and power control algorithm's energy efficiency is lower than the RSRP-based user association with proposed power control scheme. That's because in the formulated problem the relative importance of the throughput is much higher than the grid energy consumption due to the magnitude order. Hence, the high throughput performance lead to a higher grid energy consumption which is followed by lower energy efficiency. Meanwhile it can be seen that expand the cache capacity has negligible effect on the grid energy consumption, as indicated from (6.18). In addition, it is confirmed from Figure 6.1 and 6.2 that when experiencing the identical RSRP-based user association condition, our proposed power control algorithm can curtail the total grid energy consumption without sacrificing throughput, compared to the fixed transmit power case.

Figure 6.3 shows the energy efficiency versus PBS number for the joint user association and power control design and the RSRP-based user association with fixed transmit

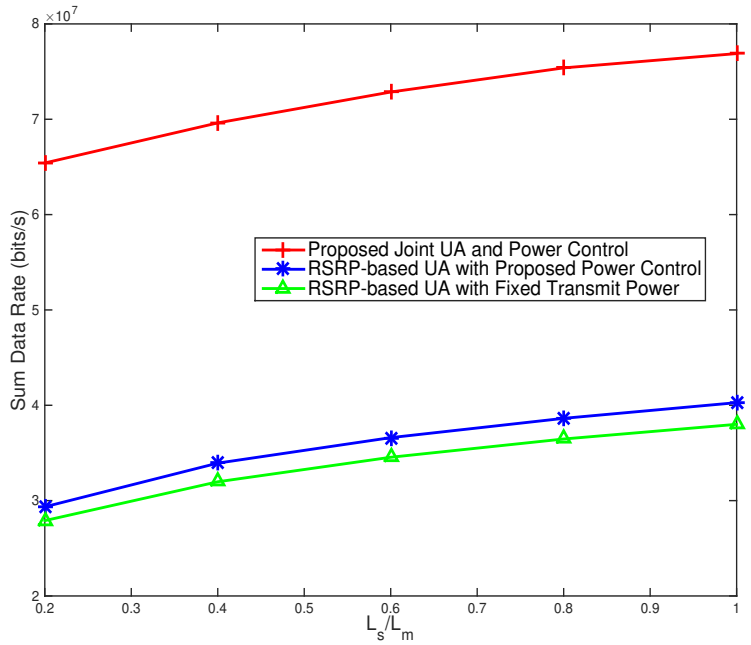

Figure 6.1: Sum data rate versus cache size for different resource allocation designs.

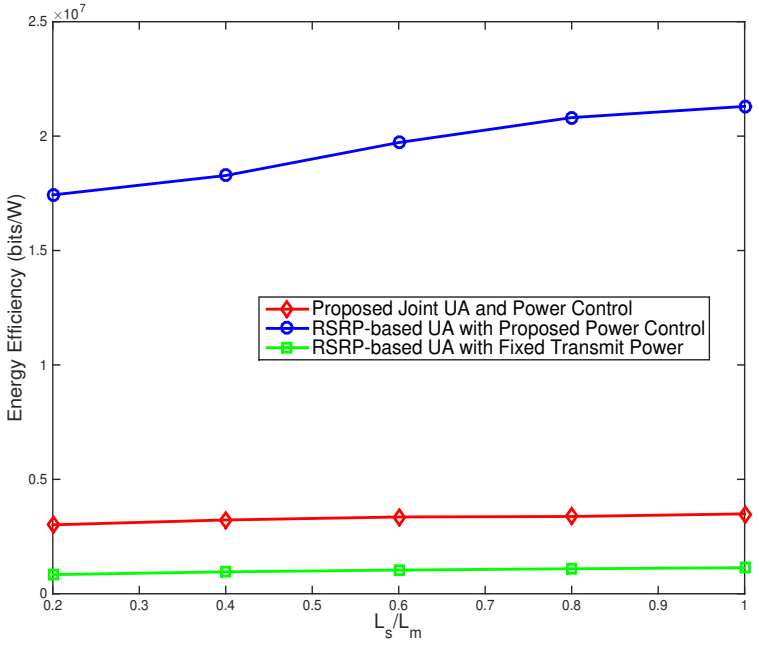

Figure 6.2: Energy efficiency versus cache size for different resource allocation designs.

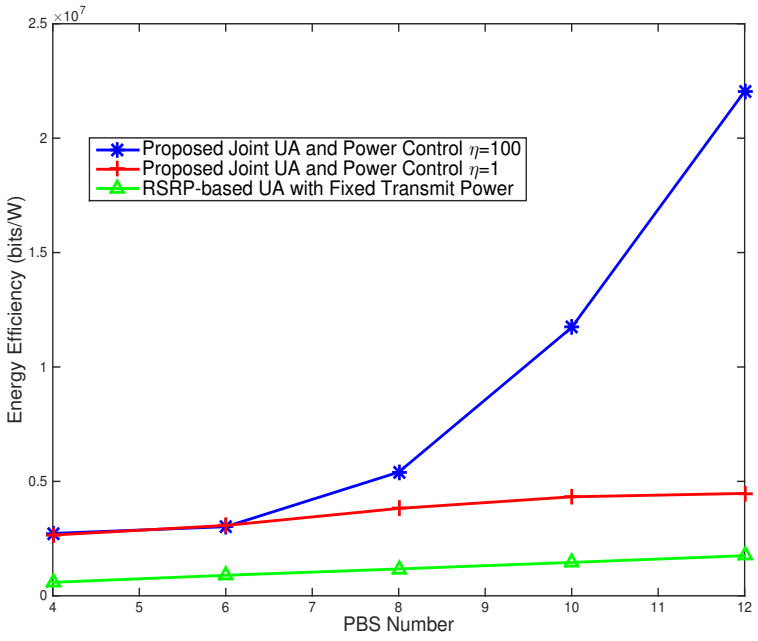

Figure 6.3: Energy efficiency versus PBS number for different resource allocation designs.

powers. The UE number is $|\mathcal{U}| = 30$, and the MBS and PBS's cache size are $L_{\mathrm{M}} = 7000$ and $L_{\mathrm{S}} = 5000$, respectively. It is also confirmed that the proposed algorithm outperforms the conventional design in the perspectives of energy efficiency. Meanwhile, Figure 6.3 confirms that deploying more PBSs can improve the energy efficiency, due to more closer caches and higher BS densification gains. Meanwhile, It can be seen that by using the proposed algorithm, the higher weighted parameter η provides a better performance in energy efficeincy.

Figure 6.4 shows the sum data rate versus energy transfer efficiency factor for different resource allocation designs. The UE number is $|\mathcal{U}| = 40$, PBS number is 5, the MBS and PBS's cache size are $L_{\mathrm{M}} = 8000$ and $L_{\mathrm{S}} = 5000$ respectively. The Zipf exponent is $\alpha = 0.9$, and the weighted parameter is set as $\eta = 1$. It is implied from Figure 6.4 that the variation of energy transfer efficiency factor has negligible effect on the sum data rate in such network, compared to other system parameters such as PBS number and cache size.

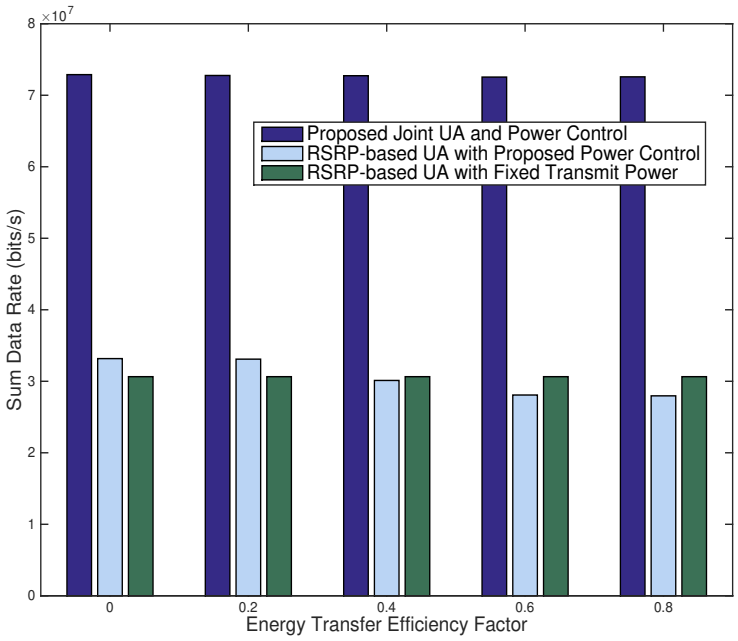

Figure 6.4: Sum data rate versus energy transfer efficiency factor for different resource allocation designs.

6.5 Summary

This chapter studies resource allocation in cache-enabled HetNets with energy cooperation. A joint user association and power control algorithm is proposed to maximise the throughput of the network while minimising the grid energy consumption. The results confirm the effectiveness of the proposed algorithm in network throughput compared with conventional resource allocation schemes. Meanwhile, the energy efficiency of the joint user association and power control scheme is lower than the resouce allocation scheme with RSRP-based user association and proposed power control, which attribute to the relative importance of network throughput and grid energy consumption. Also, the impact of PBS numbers and cache sizes are investigated.

Appendix A: Convergence Analysis

The first-order derivatives of the dual function $\mathcal{D}(\cdot)$ w.r.t. μ_j and ν_i are given by

$$\frac{\partial \mathcal{D}(\boldsymbol{\mu}, \boldsymbol{\nu})}{\partial \mu_j} = \sum_{i \in \mathcal{B}} x_{ij}(\mu_j, \nu_i)\, \gamma_{ij} - \gamma_{\min}, \tag{A.1}$$

and

$$\frac{\partial \mathcal{D}(\boldsymbol{\mu}, \boldsymbol{\nu})}{\partial \nu_i} = k_i(\nu_i) - \sum_{i \in \mathcal{B}} x_{ij}(\mu_j, \nu_i), \tag{A.2}$$

respectively. Since $x_{ij} \in \{0, 1\}$, $\sum\limits_{i \in \mathcal{B}} x_{ij}(\mu_j, \nu_i)\, \gamma_{ij}$ is bounded. In the considered problem, $k_i = \sum\limits_{i \in \mathcal{B}} x_{ij}(\mu_j, \nu_i) \leq |\mathcal{U}|$, and thus $k_i(\nu_i)$ is bounded. Hence there exists a scalar value ξ such that in each iteration, the subgradients of the dual function in (6.11) are bounded as

$$\sup_t \left\{ \left| \frac{\partial \mathcal{D}(\boldsymbol{\mu}, \boldsymbol{\nu})}{\partial \mu_j} \right| \right\} \leq \xi, \tag{A.3}$$

$$\sup_t \left\{ \left| \frac{\partial \mathcal{D}(\boldsymbol{\mu}, \boldsymbol{\nu})}{\partial \nu_i} \right| \right\} \leq \xi. \tag{A.4}$$

Therefore, the condition of convergence proof in [BM08] is satisfied, and the proposed subgradient method will converge to the optimum of dual problem in (6.12).

Chapter 7

Conclusions and Future Work

7.1 Conclusions

This research work optimised resource allocation schemes in energy cooperation enabled green networks under different scenarios.

The research in Chapter 3 was the first work on power control in energy cooperation enabled millimeter wave (mmWave) networks. It formulated the problem to maximise the time average network throughput while keeping the network stable. Based on the Lyapunov optimisation technique, an online Dynamic Energy-aware Power Allocation (DEPA) algorithm was proposed to optimise the transmit powers of base stations (BSs) and transferred energy among BSs. The simulation results showed that with energy cooperation, the required storage capacity was much lower compared with the scenarios without energy cooperation.

Then in Chapter 4, resource allocation in energy cooperation enabled heterogeneous networks (HetNets) was investigated. First, user association was formulated as an optimisation problem, aiming at maximising the number of accepted UEs by taking advantage of energy cooperation while minimising the energy transfer loss between BSs. An

energy efficient user association algorithm was proposed based on the primal-dual interior point method. Simulation results showed that the proposed algorithm can greatly increase the energy efficiency and the number of accepted UEs of the whole network. Then, power control in energy cooperation enabled heterogeneous networks (HetNets) was considered. Transmit power, grid energy consumption, and transferred energy were optimised for maximising the energy efficiency of the whole network. An energy efficient algorithm was proposed, in which the optimal resource allocation policy was obtained by using the lagrangian duality method. Simulation results demonstrated that energy efficiency is substantially improved by using the proposed power control algorithm with energy cooperation, compared with the cases where either power control or energy cooperation were considered.

After that, joint user association and power control in energy cooperation enabled two-tier HetNets with non-orthogonal multiple access (NOMA) was studied, where BSs were powered by both renewable energy sources and the conventional grid. The resource allocation problem for maximising the energy efficiency of the overall network was formulated, under quality of service constraints. First a distributed algorithm was proposed to provide the optimal user association solution for the fixed transmit power. Then, a joint user association and power control optimisation algorithm was developed to determine the traffic load in energy cooperation enabled NOMA HetNets, which achieved much higher energy efficiency performance than existing schemes. Simulation results demonstrated the effectiveness of the proposed algorithm, and show that NOMA can achieve higher energy efficiency performance than OMA in the considered networks.

An optimisation problem for joint user association and power control in cache-enabled HetNets with energy cooperation was investigated, which aimed at maximising the network throughput while minimising the conventional grid energy consumption. Simulation results demonstrated that the proposed joint user association and power control algorithm can significantly enhance the sum data rate and the energy efficiency of the whole network.

All algorithms proposed in this thesis focused on resource allocation in energy cooperation enabled networks. The proposed algorithms provide useful guidelines and potential solutions for the user association and power control mechanisms in energy cooperation enabled networks.

7.2 Future work

In this section, extensions to current work and some future research directions are proposed.

7.2.1 Performance Indicators for Energy Cooperation Enabled Networks

5G wireless networks are expected to be more energy efficient and support higher throughput. Instead of these two main performance indicators, lower delay is also urgently needed. Especially, in energy cooperation enabled networks, except the data transmission delay, the energy transferred time related to the distance also need to be considered which will impact the of UEs. However, until now, the existing models and parameters may not be sufficient to address the energy transfer delay problem for energy cooperation networks. Hence, how to quantify the delay metric and optimise it in energy cooperation enabled 5G cellular networks are waited to be conducted.

7.2.2 Resource Allocation in Joint Energy Cooperation and CoMP Enabled Networks

To mitigate the intercell interference in cellular networks, the concept of coordinated multipoint (CoMP) is proposed. In CoMP enabled networks, BSs can share their channel state information with all the other BSs in the same cluster and serve one UE with the same time-frequency resource or use beamforming to avoid strong interference from each

others. Nowadays, CoMP transmission has been extensively investigated [IDM+11].

With CoMP in energy cooperation enabled networks, when the energy of some BSs is not enough, in addition to use the transferred energy from other BSs who have abundant energy, several BSs could jointly serve the same UE with less transmit powers. CoMP and energy cooperation could be seen as the complementation for each other to fulfill the QoS requirement of UEs. Under this scenario, resource allocation such as user association and power control need to be redesigned carefully to balance the tradeoff between CoMP and energy cooperation.

References

[5GP] 5G-ppp 5g vision.

[ABC+14] J. G. Andrews, S. Buzzi, W. Choi, S. V. Hanly, A. Lozano, A. C. Soong, and J. C. Zhang. What will 5G be? *IEEE J. Sel. Areas Commun.*, 32(6):1065–1082, Jun. 2014.

[ABK+17] J. G. Andrews, T. Bai, M. N. Kulkarni, A. Alkhateeb, A. K. Gupta, and R. W. Heath. Modeling and analyzing millimeter wave cellular systems. *IEEE Trans. Commun.*, 65(1):403–430, Jan. 2017.

[AGD+11] G. Auer, V. Giannini, C. Desset, I. Godorand P. Skillermark, M. Olsson, M. A. Imran, D. Sabella, M. J. Gonzalez, O. Blume, and A. Fehske. How much energy is needed to run a wireless network? *IEEE Wireless Commun.*, 18(5):40–49, 2011.

[AH13] T. Aota and K. Higuchi. A simple downlink transmission power control method for worst user throughput maximization in heterogeneous networks. In *Proc. 7th International Conference on Signal Processing and Communication Systems (ICSPCS)*, pages 1–6, Dec. 2013.

[ALS+14] M. R. Akdeniz, Y. Liu, M. K. Samimi, S. Sun, S. Rangan, T. S. Rappaport, and E. Erkip. Millimeter wave channel modeling and cellular capacity evaluation. *IEEE J. Sel. Areas Commun.*, 32(6):1164–1179, Jun. 2014.

[BBPC16] D. Bethanabhotla, O. Y. Bursalioglu, H. C. Papadopoulos, and G. Caire. Optimal user-cell association for massive mimo wireless networks. *IEEE Trans. Wireless Commun.*, 15(3):1835–1850, Mar. 2016.

[BG15] B. Blaszczyszyn and A. Giovanidis. Optimal geographic caching in cellular networks. In *Proc. IEEE ICC*, pages 3358–3363, Jun. 2015.

[BM08] S. Boyd and A. Mutapcic. *Subgradient methods.* Stanford University, 2008.

[BSHD14] E. Björnson, L. Sanguinetti, J. Hoydis, and M. Debbah. Designing multi-user MIMO for energy efficiency: When is massive MIMO the answer? In *Proc. IEEE WCNC*, pages 242–247, Apr. 2014.

[BV04] S. Boyd and L. Vandenberghe. *Convex Optimization.* Cambridge Univer-

sity Press, 2004.

[CK17] D. Chen and V. Kuehn. Joint resource allocation and power control for maximizing the throughput of multicast c-ran. In *Proc. 11th International ITG Conference on Systems, Communications and Coding*, Feb. 2017.

[CLD+17] J. Cui, Y. Liu, Z. Ding, P. Fan, and A. Nallanathan. Optimal user scheduling and power allocation for millimeter wave noma systems. *IEEE Trans. Wireless Commun.*, PP(99):1–1, 2017.

[CLQK17] Z. Chen, J. Lee, T. Q. S. Quek, and M. Kountouris. Cooperative caching and transmission design in cluster-centric small cell networks. *IEEE Trans. Wireless Commun.*, 16(5):3401–3415, 2017.

[CLW12] Y. Cui, V. K. N. Lau, and Y. Wu. Delay-aware bs discontinuous transmission control and user scheduling for energy harvesting downlink coordinated mimo systems. *IEEE Trans. Sign. Proces.*, 60(7):3786–3795, Jul. 2012.

[CS16] V. Chamola and B. Sikdar. Solar powered cellular base stations: current scenario, issues and proposed solutions. *IEEE Commun. Mag.*, 54(5):108–114, May 2016.

[CSZ14a] Y. K. Chia, S. Sun, and R. Zhang. Energy cooperation in cellular networks with renewable powered base stations. *IEEE Trans. Wireless Commun.*, 13(12):6996–7010, Dec. 2014.

[CSZ14b] Y.K. Chia, S. Sun, and R. Zhang. Energy cooperation in cellular networks with renewable powered base stations. *IEEE Trans. Wireless Commun.*, 13(12):6996–7010, Dec. 2014.

[DAP16] Z. Ding, F. Adachi, and H. V. Poor. The application of mimo to non-orthogonal multiple access. *IEEE Trans. Wireless Commun.*, 15(1):537–552, Jan. 2016.

[Din67] W. Dinkelbach. On nonlinear fractional programming. *Management Science*, 13(7):492–498, 1967.

[DLN+14] H. S. Dhillon, Y. Li, P. Nuggehalli, Z. Pi, and J. G. Andrews. Fundamentals of heterogeneous cellular networks with energy harvesting. *IEEE Trans. Wireless Commun.*, 13(5):2782–2797, May 2014.

[DWY+15] L. Dai, B. Wang, Y. Yuan, S. Han, C. l. I, and Z. Wang. Non-orthogonal multiple access for 5g: solutions, challenges, opportunities, and future research trends. *IEEE Commun. Mag.*, 53(9):74–81, Sept. 2015.

[Elm] J. Elmirghani. Ict industry tackles growth in co2 emissions.

[Eva11] D. Evans. *The Internet of Things–How the Next Evolution of the Internet Is Changing Everything.* CISCO White Paper, 2011.

[FMJ17] M. Feng, S. Mao, and T. Jiang. Boost: Base station on-off switching strategy for green massive mimo hetnets. *IEEE Trans. Wireless Commun.*, 16(11):7319–7332, Nov. 2017.

[GB] M. Grant and S. Boyd. Cvx: Matlab software for disciplined convex programming.

[GD91] D. E. Goldberg and K. Deb. *A Comparative Analysis of Selection Schemes Used in Genetic Algorithms.* Morgan Kaufmann Publishers, Inc., 1991.

[GLM13] Z. Guo, T. J. Lim, and M. Motani. Base station energy cooperation in green cellular networks. In *Proc. IEEE Global Conference on Signal and Information Processing (GlobalSIP)*, pages 349–352, Dec. 2013.

[GMR+12] A. Ghosh, N. Mangalvedhe, R. Ratasuk, B. Mondal, M. Cudak, E. Visotsky, T. A. Thomas, J. G. Andrews, P. Xia, H. S. Jo, H. S. Dhillon, and T. D. Novlan. Heterogeneous cellular networks: From theory to practice. *IEEE Commun. Mag.*, 50(6):54–64, June 2012.

[GOYU12] B. Gurakan, O. Ozel, J. Yang, and S. Ulukus. Two-way and multiple-access energy harvesting systems with energy cooperation. In *Proc. IEEE Signals, Systems and Computers (ASILOMAR)*, pages 58–62, Nov. 2012.

[GOYU13a] B. Gurakan, O. Ozel, J. Yang, and S. Ulukus. Energy cooperation in energy harvesting communications. *IEEE Trans. Commun.*, 61(12):4884–4898, Dec. 2013.

[GOYU13b] B. Gurakan, O. Ozel, J. Yang, and S. Ulukus. Energy cooperation in energy harvesting two-way communications. In *Proc. IEEE ICC*, pages 3126–3130, Jun. 2013.

[GOYU13c] B. Gurakan, O. Ozel, Jing Yang, and S. Ulukus. Energy cooperation in

energy harvesting communications. *IEEE Trans. Commun.*, 61(12):4884–4898, Dec. 2013.

[GSSBH11] A. Garcia-Saavedra, P. Serrano, A. Banchs, and M. Hollick. Energy-efficient fair channel access for IEEE 802.11 WLANs. In *Proc. IEEE WoWMoM*, pages 1–9, Jun. 2011.

[GTZN14] J. Gong, J. S. Thompson, S. Zhou, and Z. Niu. Base station sleeping and resource allocation in renewable energy powered cellular networks. *IEEE Trans. Commun.*, 62(11):3801–3813, Nov. 2014.

[GXDZ14] Y. Guo, J. Xu, L. Duan, and R. Zhang. Joint energy and spectrum cooperation for cellular communication systems. *IEEE Trans. Commun.*, 62(10):3678–3691, Oct. 2014.

[HA13a] T. Han and N. Ansari. Green-energy aware and latency aware user associations in heterogeneous cellular networks. In *Proc. IEEE GLOBECOM*, pages 4946–4951, Dec. 2013.

[HA13b] T. Han and N. Ansari. On optimizing green energy utilization for cellular networks with hybrid energy supplies. *IEEE Trans. Wireless Commun.*, 12(8):3872–3882, Aug. 2013.

[HA14] T. Han and N. Ansari. Powering mobile networks with green energy. *IEEE Wireless Commun.*, 21(1):90–96, Feb. 2014.

[HBB11] Z. Hasan, H. Boostanimehr, and V. K. Bhargava. Green cellular networks: A survey, some research issues and challenges. *IEEE Commun. Surveys & Tuts.*, 13(4):524–540, Apr. 2011.

[HH15] E. Hossain and M. Hasan. 5G cellular: Key enabling technologies and research challenges. *IEEE Instrum. Meas. Mag.*, 18(3):11–21, Jun. 2015.

[HHA+11] C. Han, T. Harrold, S. Armour, I. Krikidis, S. Videv, P. M. Grant, H. Haas, J. S. Thompson, I. Ku, C. X. Wang, T. A. Le, M. R. Nakhai, J. Zhang, and L. Hanzo. Green radio: radio techniques to enable energy-efficient wireless networks. *IEEE Commun. Mag.*, 49(6):46–54, Jun. 2011.

[HN13] L. Huang and M. J. Neely. Utility optimal scheduling in energy-harvesting networks. *IEEE/ACM Trans. Netw.*, 21(4):1117–1130, Aug. 2013.

[HNS+12] Z. Han, D. Niyato, W. Saad, T. Başar, and A. Hjøungnes. *Game Theory in Wireless and Communication Networks: Theory, Models, and Applications.* Cambridge University Press, 2012.

[HYM+17] Q. Han, B. Yang, G. Miao, C. Chen, X. Wang, and X. Guan. Backhaul-aware user association and resource allocation for energy-constrained hetnets. *IEEE Trans. Veh. Technol.*, 66(1):580–593, Jan. 2017.

[HZZN13] C. Hu, X. Zhang, S. Zhou, and Z. Niu. Utility optimal scheduling in energy cooperation networks powered by renewable energy. In *Proc. 19th Asia-Pacific Conference on Communications (APCC)*, pages 403–408, Aug. 2013.

[IADK17] S. M. R. Islam, N. Avazov, O. A. Dobre, and K. S. Kwak. Power-domain non-orthogonal multiple access (noma) in 5g systems: Potentials and challenges. *IEEE Commun. Surveys & Tuts.*, 19(2):721–742, 2017.

[IDM+11] R. Irmer, H. Droste, P. Marsch, M. Grieger, G. Fettweis, S. Brueck, H. P. Mayer, L. Thiele, and V. Jungnickel. Coordinated multipoint: Concepts, performance, and field trial results. *IEEE Commun. Mag.*, 49(2):102–111, Feb. 2011.

[JWY05] A. Jamalipour, T. Wada, and T. Yamazato. A tutorial on multiple access technologies for beyond 3g mobile networks. *IEEE Commun. Mag.*, 43(2):110–117, Feb. 2005.

[JZLL15] S. Jangsher, H. Zhou, V. O. K. Li, and K. C. Leung. Joint allocation of resource blocks, power, and energy-harvesting relays in cellular networks. *IEEE J. Sel. Areas Commun.*, 33(3):482–495, Mar. 2015.

[JZLS16] D. Jiang, P. Zhang, Z. Lv, and H. Song. Energy-efficient multi-constraint routing algorithm with load balancing for smart city applications. *IEEE Internet Things J.*, 3(6):1437–1447, 2016.

[KC06] M. Kobayashi and G. Caire. An iterative water-filling algorithm for maximum weighted sum-rate of gaussian mimo-bc. *IEEE J. Sel. Areas Commun.*, 24(8):1640–1646, Aug. 2006.

[KSK11] Y. Yi K. Son, H. Kim and B. Krishnamachari. Base station operation and

user association mechanisms for energy−delay tradeoffs in green cellular networks. *IEEE J. Sel. Areas Commun.*, 29(8):1525–1536, Sept. 2011.

[LBS99] L. Fan G. Phillips L. Breslau, P. Cao and S. Shenker. Web caching and zipf-like distributions: evidence and implications. In *Proc. IEEE INFOCOM*, pages 126–134, Mar. 1999.

[LCC+14] D. Liu, Y. Chen, K. K. Chai, T. Zhang, and M. Elkashlan. Opportunistic user association for multi-service hetnets using nash bargaining solution. *IEEE Commun. Lett.*, 18(3):463–466, Mar. 2014.

[LCC+15] D. Liu, Y. Chen, K. K. Chai, T. Zhang, and M. Elkashlan. Two dimensional optimization on user association and green energy allocation for HetNets with hybrid energy sources. *IEEE Trans. Commun.*, 63(11):4111–4124, 2015.

[LH12] T. H. Lee and Y. W. Huang. Resource allocation achieving high system throughput with qos support in ofdma-based system. *IEEE Trans. Commun.*, 60(3):851–861, Mar. 2012.

[LHSX17] Y. Luo, P. Hong, R. Su, and K. Xue. Resource allocation for energy harvesting-powered d2d communication underlaying cellular networks. *IEEE Trans. Veh. Technol.*, 66(11):10486–10498, Nov. 2017.

[LKM+16] S. Lahoud, K. Khawam, S. Martin, G. Feng, Z. Liang, and J. Nasreddine. Energy efficient joint scheduling and power control in multi-cell wireless networks. *IEEE J. Sel. Areas Commun.*, 34(12):3409–3426, 2016.

[LQE+17] Y. Liu, Z. Qin, M. Elkashlan, Z. Ding, A. Nallanathan, and L. Hanzo. Nonorthogonal multiple access for 5g and beyond. *Proc. IEEE*, 105(12):2347–2381, Dec. 2017.

[LQP14] S. Lakshminarayana, T. Q. S. Quek, and H. V. Poor. Cooperation and storage tradeoffs in power grids with renewable energy resources. *IEEE J. Sel. Areas Commun.*, 32(7):1386–1397, Jul. 2014.

[LSH16] D. Li, W. Saad, and C. S. Hong. Decentralized renewable energy pricing and allocation for millimeter wave cellular backhaul. *IEEE J. Sel. Areas Commun.*, 34(5):1140–1159, May 2016.

[LY06] Z. Luo and W. Yu. An introduction to convex optimization for communications and signal processing. *IEEE J. Sel. Areas Commun.*, 24(8):1426–1438, Aug. 2006.

[MHP+16] H. Munir, S. A. Hassan, H. Pervaiz, Q. Ni, and L. Musavian. Energy efficient resource allocation in 5g hybrid heterogeneous networks: A game theoretic approach. In *Proc. VTC Fall*, pages 1–5, Sept. 2016.

[MZK17] A. Mesodiakaki, E. Zola, and A. Kassler. User association in 5g heterogeneous networks with mesh millimeter wave backhaul links. In *Proc. IEEE WoWMoM*, pages 1–6, Jun. 2017.

[Nee06] M. J. Neely. Energy optimal control for time-varying wireless networks. *IEEE Trans. Inform. Theory*, 52(7):2915–2934, July. 2006.

[Nee10] M. J. Neely. *Stochastic Network Optimization with Application to Communication and Queueing Systems*. Morgan & Claypool, 2010.

[NGL+17] Y. Niu, C. Gao, Y. Li, L. Su, D. Jin, Y. Zhu, and D. O. Wu. Energy-efficient scheduling for mmwave backhauling of small cells in heterogeneous cellular networks. *IEEE Trans. Veh. Technol.*, 66(3):2674–2687, Mar. 2017.

[NLS12] D. W. K. Ng, E. S. Lo, and R. Schober. Energy-efficient resource allocation in ofdma systems with large numbers of base station antennas. *IEEE Trans. Wireless Commun.*, 11(9):3292–3304, Sept. 2012.

[NLS13] D. W. K. Ng, E. S. Lo, and R. Schober. Energy-efficient resource allocation in ofdma systems with hybrid energy harvesting base station. *IEEE Trans. Wireless Commun.*, 12(7):3412–3427, July 2013.

[Nys] D. Nystedt. Ericsson, orange deploy solar base-stations in africa.

[PDDLN16] S. Parsaeefard, R. Dawadi, M. Derakhshani, and T. Le-Ngoc. Joint user-association and resource-allocation in virtualized wireless networks. *IEEE Access*, 4:2738–2750, 2016.

[RB16] R. Ramamonjison and V. K. Bhargava. Energy allocation and cooperation for energy-efficient wireless two-tier networks. *IEEE Trans. Wireless Commun.*, 15(9):6434–6448, Sept. 2016.

[RCZ18] K. Rahbar, C. C. Chai, and R. Zhang. Energy cooperation optimization in microgrids with renewable energy integration. *IEEE Trans. Smart Grid*, 9(2):1482–1493, Mar. 2018.

[RMSM+17] N. Reyhanian, B. Maham, V. Shah-Mansouri, W. Tushar, and C. Yuen. Game-theoretic approaches for energy cooperation in energy harvesting small cell networks. *IEEE Trans. Veh. Technol.*, 66(8):7178–7194, Aug. 2017.

[RPI14] J. Rubio and A. Pascual-Iserte. Energy-aware broadcast multiuser-mimo precoder design with imperfect channel and battery knowledge. *IEEE Trans. Wireless Commun.*, 13(6):3137–3152, Jun. 2014.

[SKB+13] Y. Saito, Y. Kishiyama, A. Benjebbour, T. Nakamura, A. Li, and K. Higuchi. Non-orthogonal multiple access (noma) for cellular future radio access. In *Proc. IEEE VTC Spring*, Jun. 2013.

[SLW+15] F. Shan, J. Luo, W. Wu, M. Li, and X. Shen. Discrete rate scheduling for packets with individual deadlines in energy harvesting systems. *IEEE J. Sel. Areas Commun.*, 33(3):438–451, Mar. 2015.

[SVL+17] W. Shin, M. Vaezi, B. Lee, D. J. Love, J. Lee, and H. V. Poor. Non-orthogonal multiple access in multi-cell networks: Theory, performance, and practical challenges. *IEEE Commun. Mag.*, 55(10):176–183, Oct. 2017.

[Ter13] Tamas Terlaky. *Interior Point Methods of Mathematical Programming.* Springer Science & Business Media, Sep. 2013.

[TGH+16] T. Touzri, M. Ben Ghorbel, B. Hamdaoui, M. Guizani, and B. Khalfi. Efficient usage of renewable energy in communication systems using dynamic spectrum allocation and collaborative hybrid powering. *IEEE Trans. Wireless Commun.*, 15(5):3327–3338, May 2016.

[TGUBL13] N. Tekbiyik, T. Girici, E. Uysal-Biyikoglu, and K. Leblebicioglu. Proportional fair resource allocation on an energy harvesting downlink. *IEEE Trans. Wireless Commun.*, 12(4):1699–1711, Apr. 2013.

[TV05] D. Tse and P. Viswanath. *Fundamentals of Wireless Communication.*

Cambridge University Press, Cambridge, U.K., 2005.

[TY13a] K. Tutuncuoglu and A. Yener. Cooperative energy harvesting communications with relaying and energy sharing. In *Proc. IEEE Information Theory Workshop (ITW)*, pages 1–5, Sept. 2013.

[TY13b] K. Tutuncuoglu and A. Yener. Multiple access and two-way channels with energy harvesting and bi-directional energy cooperation. In *Proc. Information Theory and Applications Workshop (ITA)*, pages 1–8, Feb. 2013.

[Van14] R. J. Vanderbei. *Linear Programming: Foundations and Extensions*. Springer; 4th ed. 2014 edition, 2014.

[VY16] B. Varan and A. Yener. Matching games for wireless networks with energy cooperation. In *Proc. 14th International Symposium on Modeling and Optimization in Mobile, Ad Hoc, and Wireless Networks (WiOpt)*, pages 1–7, May 2016.

[WFGW14] S. Wang, C. Feng, C. Guo, and G. Wang. Efficiency and fairness aware resource allocations for energy and spectrum in downlink ofdma systems. *Electronics Lett.*, 50(5):411–413, Feb. 2014.

[WRW+14] D. Wang, P. Ren, Y. Wang, Q. Du, and L. Sun. Energy cooperation for reciprocally-benefited spectrum access in cognitive radio networks. In *Proc. IEEE Global Conf. Signal and Inf. Process. (GlobalSIP)*, pages 1320–1324, Dec. 2014.

[XCC+17] B. Xu, Y. Chen, J. R. Carrion, J. Loo, and A. Vinel. Energy-aware power control in energy cooperation aided millimeter wave cellular networks with renewable energy resources. *IEEE Access*, pages 432–442, 2017.

[XZ15a] J. Xu and R. Zhang. Comp meets smart grid: A new communication and energy cooperation paradigm. *IEEE Trans. Veh. Technol.*, 64(6):2476–2488, Aug. 2015.

[XZ15b] J. Xu and R. Zhang. Comp meets smart grid: A new communication and energy cooperation paradigm. *IEEE Trans. Veh. Technol.*, 64(6):2476–2488, Jun. 2015.

[XZ16] J. Xu and R. Zhang. Cooperative energy trading in comp systems powered by smart grids. *IEEE Trans. Veh. Technol.*, 65(4):2142–2153, Apr. 2016.

[YHY05] K. Yasuda, L. Hu, and Y. Yin. A grouping genetic algorithm for the multi-objective cell formation problem. *Int. J. Production Research*, 43(4):829–953, 2005.

[YKS13] W. Yu, T. Kwon, and C. Shin. Multicell coordination via joint scheduling, beamforming, and power spectrum adaptation. *IEEE Trans. Wireless Commun.*, 12(7):1–14, Jul. 2013.

[YRC+13] Q. Ye, B. Rong, Y. Chen, M. Al-Shalash, C. Caramanis, and J. G. Andrews. User association for load balancing in heterogeneous cellular networks. *IEEE Trans. Wireless Commun.*, 12(6):2706–2716, Jun. 2013.

[YU12] J. Yang and S. Ulukus. Optimal packet scheduling in an energy harvesting communication system. *IEEE Trans. Commun.*, 60(1):220–230, Jan. 2012.

[YWWZ17] K. Yang, L. Wang, S. Wang, and X. Zhang. Optimization of resource allocation and user association for energy efficiency in future wireless networks. *IEEE Access*, 5:16469–16477, 2017.

[ZCC+16] D. Zhang, Z. Chen, L. X. Cai, H. Zhou, J. Ren, and X. Shen. Resource allocation for green cloud radio access networks powered by renewable energy. In *Proc. IEEE GLOBECOM*, pages 1–6, Dec. 2016.

[ZLC+17] J. Zhao, Y. Liu, K. K. Chai, A. Nallanathan, Y. Chen, and Z. Han. Spectrum allocation and power control for non-orthogonal multiple access in hetnets. *IEEE Trans. Wireless Commun.*, 16(9):5825–5837, Sept. 2017.

[ZPSY13a] M. Zheng, P. Pawelczak, S. Stanczak, and H. Yu. Planning of cellular networks enhanced by energy harvesting. *IEEE Commun. Lett.*, 17(6):1092–1095, Jun. 2013.

[ZPSY13b] M. Zheng, P. Pawelczak, S. Stanczak, and H. Yu. Planning of cellular networks enhanced by energy harvesting. *IEEE Commun. Lett.*, 17(6):1092–1095, June 2013.

[ZSD16] A. Zappone, L. Sanguinetti, and M. Debbah. Non-cooperative power control for energy-efficient and delay-aware wireless networks. In *Proc. WSA*

2016; 20th International ITG Workshop on Smart Antennas, pages 1–6, March 2016.

[ZXL+15] T. Zhang, H. Xu, D. Liu, N. C. Beaulieu, and Y. Zhu. User association for energy-load tradeoffs in hetnets with renewable energy supply. *IEEE Commun. Lett.*, 19(12):2214–2217, Dec. 2015.

[ZZZ+16] S. Zhang, N. Zhang, S. Zhou, J. Gong, Z. Niu, and X. S. Shen. Energy-aware traffic offloading for green heterogeneous networks. *IEEE J. Sel. Areas Commun.*, 34(5):1116–1129, 2016.